University of Brasília

Institute of Exact Sciences
Department of Computer Science

Core switching Paradigms in Multi-core Elastic Optical Networks

Paradigmas de Comutação de Núcleo em Redes Ópticas Elásticas Multi-nucleadas

Ítalo Barbosa Brasileiro

Thesis presented in partial fulfillment of the requirements for the degree of Doctor of Philosophy in Informatics

Advisor
Prof. Dr. André Costa Drummond

Brazil
2024

University of Brasília

Institute of Exact Sciences
Department of Computer Science

Core switching Paradigms in Multi-core Elastic Optical Networks

Paradigmas de Comutação de Núcleo em Redes Ópticas Elásticas Multi-nucleadas

Ítalo Barbosa Brasileiro

Thesis presented in partial fulfillment of the requirements for the degree of Doctor of Philosophy in Informatics

Prof. Dr. André Costa Drummond (Advisor)
CIC/UnB

Prof. Dr. Andre Castelo Branco Soares
DC/UFPI

Dr. Gustavo Bittencourt Figueiredo
DC/UFBA

Prof.a Dr.a Priscila America Solis Mendez Barreto
CIC/UnB

Prof. Dr. Rodrigo Bonifácio de Almeida
Coordinator of the Graduate Program in Informatics

Brazil, Brasília, June 27 2024

Dedication

Primeiramente, agradeço a Deus e meu anjo da guarda, por sempre prover, guiar meu caminho e me proteger.

Dedico este trabalho aos meus pais, pelo amor, educação e criação. Agradeço profundamente aos meus irmãos e primos, que são meus eternos companheiros, minha inspiração e meus melhores amigos. Dedico também a toda a minha família, em especial às minhas tias queridas: Dione, por me ensinar a logística; Diana, por me ensinar a sorte; e Deyne, por me ensinar a leveza.

Dedico ao amor da minha vida, Diego, e sou eternamente grato pelo respeito, carinho e por cuidar tão bem de mim.

Agradeço imensamente aos meus mestres ao longo da caminhada acadêmica, sempre fontes de inspiração, persistência e dedicação: André Soares, Ricardo Lira, Valdemir Junior, Admela Jukan e, em especial, ao meu orientador, Professor André Drummond, pela paciência, agudeza de mente e espírito, senso crítico e de humor (escrevi isso depois da aprovação da tese, então não é "puxa-saquismo"). Agradeço aos meus fiéis amigos da vida: Pedro, Sthefanny, Ylka, Ruhan e João Victor, agradeço por sempre me acolherem e provocarem boas risadas. Aos meus amigos do batidão: Zied, Marla, Manuela, Jasenka, Iuli e Vien, obrigado por tornarem o dia a dia mais leve e favorável.

A todos, meu sincero agradecimento.

Acknowledgements

Gostaria de expressar minha sincera gratidão a todas as instituições e pessoas que contribuíram para a realização desta tese. Primeiramente, agradeço à Universidade de Brasília (UnB), a instituição onde obtive essa graduação, fundamental para minha formação profissional e pessoal. A UnB proporcionou as bases sólidas de conhecimento e o ambiente de aprendizado que me permitiram chegar até aqui. Ao Programa de Pós-Graduação em Informática (PPGINF) da UnB, que não apenas me ofereceu a oportunidade de realizar o doutorado, mas também me forneceu um suporte inestimável ao longo de toda a jornada. Agradeço imensamente à Coordenação de Aperfeiçoamento de Pessoal de Nível Superior (Capes) por seu apoio contínuo e incentivo à pesquisa no Brasil. O financiamento e os recursos fornecidos pela Capes foram essenciais para a realização deste trabalho e para meu desenvolvimento como pesquisador. Gostaria também de expressar minha gratidão à Technische Universität Braunschweig (TUBS) por me acolher durante o doutorado sanduíche e também na reta final do meu doutorado. A TUBS ofereceu um ambiente acadêmico enriquecedor e acolhedor, o que foi crucial para o avanço e a conclusão da minha pesquisa.

A todos que direta ou indiretamente contribuíram para a realização desta tese: muito obrigado!

Abstract

Elastic Optical Networks (EONs) emerge as a technology for efficient spectral allocation in optical fibers. A single EON fiber supports multiple circuits in parallel, allocating distinct spectral channels with variable bandwidth requirements. Multi-core fibers (MCF) emerge to increase resource availability further by holding multiple cores. MCFs enable Spatial Division Multiplexing (SDM) in EON, which increases spectral resources by utilizing the different spatial channels (cores). The current SDM-EON literature branches into two main paradigms: core-constrained and Spatial Lane Change (SLC). The former defines architectures where a circuit must remain in the same core along its route. The latter, SLC architectures, allow the core switching along the route. The impact caused by the two architectures lies in the deployment and energy cost versus the degree of flexibility in the resource allocation procedure. This thesis proposes solutions to improve resource utilization efficiency in both paradigms. A resource allocation solution with dedicated cores for different circuit categories is proposed for architectures focused on the core-constrained paradigm. This solution aims to maintain circuits more resilient to physical interferences in the most affected cores, besides adopting techniques to reduce spectral fragmentation in allocation. For the SLC paradigm, this thesis presents a solution adapted to network defragmentation scenarios. The proposed solution combines a defragmentation heuristic with two techniques for spectral reorganization without service interruption or suspension. The goal is to reduce the fragmentation state whenever a trigger is activated, resulting in greater resource availability after spectral reorganization. Finally, a novel core switching paradigm, named sparse core switching, is introduced, which entails an architecture on which different nodes in the network possess distinct degrees of flexibility to perform core switching. The main objective is to reduce drastically the deployment cost while maintaining switching flexibility only in more advantageous nodes. This approach saves resources on multiple levels and performs efficiently compared to core-constrained and SLC approaches.

Keywords: multi-core fibers, elastic optical networks, core-switching, performance evaluation

Resumo Expandido

A quantidade de banda transmitida pela Internet apresenta uma média de crescimento próximo a 30% ao ano. Estimativas apontam que em 10 anos as redes de transporte óptico crescerão em torno de 14 vezes, comparado ao cenário atual. Por isso, inovações tecnológicas nas redes ópticas de núcleo são constantemente exploradas, na busca por soluções que suportem de maneira eficiente o aumento contínuo da demanda por largura de banda.

O aumento no número de conexões também é impactado pela introdução de novas gerações de redes móveis, que compreende o estabelecimento da atual geração 5G e expectativas em torno do 6G e as futuras gerações [1]. As novas arquiteturas de rede trazem requisitos ainda mais rigorosos para latência de transmissão e disponibilidade de largura de banda na infraestrutura de rede.

A infraestrutura atual da espinha dorsal das redes de comunicação é composta por fibras ópticas, opera predominantemente na banda C, utiliza detecção direta e transmissão *Wavelength-Division Multiplexing* (WDM) [2]. Embora esta tecnologia permita capacidades de transferência de até 1 Tbps por fibra, ela fica aquém se comparada aos requisitos de taxa por *base station* previstos para 5G (100 Gbps) e 6G (1 Tbps) [3] Portanto, é necessário adotar tecnologias inovadoras para aprimorar a infraestrutura e apoiar a expansão contínua da Internet.

Considerando a necessidade de maior capacidade de transmissão para as fibras, as *Elastic Optical Networks* (EON) ganham destaque como tecnologia capaz de tornar mais eficiente a utilização do espectro óptico [4]. Nas EON, multiplos circuitos podem ser estabelecidos em paralelo na mesma fibra, por meio da alocação de diferentes canais espectrais. Esses canais são compostos por *slots*, faixas de frequência de 12,5 GHz no espectro óptico que podem ser alocadas independentemente para circuitos em paralelo. Por fim, os *slots* podem ser agrupados, formando canais de transmissão de maior capacidade, que admitem circuitos com maiores requisitos de largura de banda.

Na maior parte dos trabalhos que discutem as EON, os enlaces de transmissão são compostos por fibras com um único núcleo, denominadas *Single Core Fibers* (SCF). Como forma de aumentar a disponibilidade de recursos, alguns trabalhos consideram a utilização

de um tipo diferente de fibra óptica, chamada *Multi-Core Fiber* (MCF) [5]. As MCFs possuem mais de um núcleo (geralmente 7 ou 12) e cada núcleo possui seu próprio conjunto de *slots*. Superficialmente, cada MCF é operada como um grupo de fibras com núcleo único.

Nos cenários com aplicação de SCF, o aumento da quantidade de fibras causa crescimento linear na quantidade de equipamentos, também causando aumento linear do consumo de energia. As MCFs ajudam a superar esta situação com soluções de equipamentos que operam em todos os núcleos simultaneamente (como amplificadores [6], [7]), ou soluções mecânicas para separar os núcleos (como *fan-in/fan-out* [8]) substituindo a utilização de *splitters* em fibras de único núcleo. Também há ganho na economia de material utilizado na produção das fibras. É importante destacar que o ganho econômico é justificado quando as MCF com n núcleos apresentam desempenho similar a um conjunto de n fibras de único núcleo.

O uso de MCFs habilita a *Spatial-Division Multiplexing* (SDM), o que aumenta os recursos espectrais pela utilização dos diferentes canais espaciais (núcleos) das MCF. A respeito da arquitetura para a comutação de circuitos entre os diferentes núcleos, a literatura atual sobre SDM-EON é dividida em dois paradigmas principais: *core constrained* e *Spatial Lane Change* (SLC). A primeira representa arquiteturas nas quais o processo de alocação de recursos deve sempre considerar a utilização do mesmo núcleo para um dado circuito ao longo de toda a sua rota. Por outro lado, no cenário com SLC, a alocação de recursos pode atribuir diferentes núcleos nos múltiplos enlaces que compõem a rota. O impacto causado pelas duas arquiteturas se dá no custo de implantação e energético, que crescem em juntamente com o grau de flexibilidade na alocação de recursos.

Neste trabalho, são propostas soluções para melhorar a eficiência de utilização dos recursos nos dois paradigmas. A primeira solução apresentada nesta tese, chamada *Allocation with Strengthened Medium Core* (ASMC), é uma solução de alocação de recursos para arquiteturas com paradigma *core-constrained*. Esta arquitetura requer reduzido investimento em termos de equipamento de comutação, em específico *Spectrum Selective Switch* (SSS). Entretanto, a restrição de continuidade espectral diminui a flexibilidade para alocação de recursos, limitando as oportunidades de uso eficiente do espectro. Essa arquitetura também gera maior grau de fragmentação espectral, na qual as faixas de frequência disponíveis para alocação estão distribuídas em pequenos canais de *slots* livres e dispersos no espectro óptico dos núcleos.

Para cenários com arquitetura voltada ao paradigma *core constrained*, essa tese propõe uma solução de alocação de recursos com núcleos dedicados para as diferentes taxas de transmissão e formatos de modulação aplicados no circuito. A heurística ASMC aloca no núcleo central das MCF os circuitos que utilizam modulações mais resistentes ao impacto

de camada física, em especial o *crosstalk*. Os circuitos com formato de modulação mais eficiente devem ser alocados nos núcleos periféricos, onde o efeito de *crosstalk* é menos intenso. Qualquer núcleo externo pode ser alocado por circuitos com qualquer formato de modulação classificado como eficiente, porém haverá divisão entre circuitos com número de *slots* ímpar ou par, que devem ser alocados apenas em núcleos com paridade correspondente. O objetivo desta solução é manter circuitos mais resistentes à interferências físicas nos núcleos que sofrem maior impacto deste fator, além de adotar técnicas para reduzir a fragmentação espectral durante a alocação.

Comparamos a solução ASMC com outras soluções encontradas na literatura [9], [10]. Simulações são utilizadas para gerar os resultados de desempenho avaliados neste trabalho, e a qualidade das soluções é medida em função da taxa de bloqueio de circuitos e de banda. A organização espectral promovida pelo ASMC viabiliza o atendimento de mais circuitos quando comparada com as outras soluções da literatura. O ASMC reduz o bloqueio de banda em uma faixa média de 43.64% quando comparado à segunda melhor solução no cenário avaliado.

Em cenários com o paradigma de comutação SLC habilitado, um circuito estabelecido pode transitar entre núcleos de índice diferentes ao longo da sua rota. A restrição de continuidade de núcleo é removida, possibilitando a escolha de núcleos diferentes em cada um dos enlaces da rota durante a definição dos recursos espectrais para alocar. O paradigma SLC também relaxa a restrição de continuidade espectral, pois a alocação de recursos dispõe de múltiplos núcleos contendo seu próprio conjunto independente de *slots*. É importante destacar que a restrição de continuidade exige a alocação da mesma faixa espectral em cada enlace da rota para o mesmo circuito, e o conjunto de recursos escolhidos não podem ser alterados, exceto em casos de falhas na rede.

No contexto de arquiteturas com SLC habilitado, essa tese propõe uma solução para a desfragmentação da SDM-EON, combinando as técnicas *push-pull* e *fast-switching* para reorganizar os circuitos alocados sem interrupção ou suspensão do serviço. Para realizar o *push-pull*, o transmissor muda progressivamente o intervalo de frequência alocado por um circuito, deslizando a frequência central até um destino escolhido previamente. Esse ajuste permite mover o circuito pelos *slots*, contanto que não exista nenhum outro circuito ativo entre os *slots* de origem e destino selecionados. Já o *fast-switching* permite a mudança de núcleos entre as opções disponíveis de alocação, sem alteração do intervalo de frequência ocupado pelo circuito e sem sua interrupção.

A solução proposta nesta tese aplica as duas técnicas mencionadas durante fases de desfragmentação da rede. A desfragmentação é acionada sempre que um circuito não pode ser alocado na rede, e com o *push-pull* e *fast-switching*, os circuitos são deslocados para os *slots* de índice mais baixo, promovendo uma política *first-fit* para o reposicionamento

do circuito.

O objetivo desta solução é reduzir o estado de fragmentação da rede sempre que um determinado gatilho é acionado, resultando em maior disponibilidade de recursos após a reorganização espectral.

Por fim, nós avançamos o estado da arte com a proposta de um terceiro paradigma, derivado da combinação dos dois paradigmas citados anteriormente. A comutação esparsa de núcleos consiste em uma arquitetura com a aplicação seletiva da capacidade de comutação de núcleos. Neste paradigma, o comportamento previsto para a rede em termos de tráfego é considerado no processo de escolha de nós que terão maior capacidade de comutação de núcleos. Dessa forma, os diferentes nós da rede contam com diferentes graus de flexibilidade para realizar comutação de núcleos.

O objetivo principal da comutação esparsa de núcleo é reduzir o custo de implantação para valores próximos ao cenário sem comutação (*core constrained*), mantendo a flexibilidade de comutação em nós que tragam maior impacto positivo para a rede.

Para distribuir a capacidade de comutação, uma avaliação de tráfego deve ser feita antes da fase operacional. Nessa avaliação, uma simulação é feita considerando as informações da rede, incluindo o perfil de tráfego suportado. Além disso, durante esse teste é considerado que todos os nós têm capacidade total de comutação, equivalente ao cenário com o paradigma SLC. O objetivo é habilitar todas as comutações de núcleo da rede, e medir quais nós e núcleos utilizam mais a capacidade de comutação. Após o teste, os pares de núcleos são ordenados de acordo com sua utilização, e a distribuição de portas comutadoras segue a ordem da lista até que se esgote o orçamento disponível ou um limite pré-estabelecido seja alcançado. Por fim, uma simulação é executada representando a fase operacional da rede, e a comutação é restrita aos núcleos conectados pelas portas distribuidas na etapa anterior.

A avaliação de desempenho compara a solução de comutação esparsa com os outros dois paradigmas. Além disso, também é utilizada a distribuição aleatória como referência. Os resultados mostram que a heurística utilizada para comutação esparsa permite alcançar o desempenho do paradigma SLC com apenas 20.14% do orçamento requisitado na topologia USA, e 14.4% na topologia COST239. Com maior investimento, o desempenho da solução supera o paradigma com SLC habilitado nas duas topologias.

Como conclusão, após apresentar os dois paradigmas de comutação da literatura e propor um terceiro paradigma, essa tese lista uma série de desafios e possibilidades de trabalhos futuros no escopo de comutação de núcleo e redes ópticas elaśticas.

Palavras-chave: fibras multi-nucleadas, redes ópticas elásticas, comutação de núcleo, avaliação de desempenho

Contents

List of Figures

List of Tables

List of Acronyms

16QAM 16 Quadrature Amplitude Modulation

ARSCA-SP Anycast Routing, Spectrum and Core Allocation with Shortest Path

ASMC Allocation with Strengthened Medium Core

BBR Bandwidth Blocking Rate

BPSK Binary Phase-Shift Keying

CaP Crosstalk-aware provisioning strategy with dedicated path protection

CASC Crosstalk-Aware Spectrum Compactness

CASD Crosstalk-Aware Spectrum Defragmentation

EON Elastic Optical Network

FA-RSSMA Fragmentation-Aware Routing, Spectrum, Spatial Mode and Modulation Format Assignment

FA-RSSMA-CA Fragmentation-Aware Routing, Spectrum, Spatial Mode and Modulation Format Assignment with Congestion Avoidance

FF First Fit

FF-CASC First Fit Crosstalk-Aware Spectrum Compactness

FF-MRC First Fit Multidimensional Resource Compactness

FIPPMC Failure-Independent Path Protecting for Multi-Core network

FMF Few-Mode Fiber

FWDM Flexible Wavelength-Division Multiplexing

GMPLS Generalized Multi-Protocol Label Switching

IoT Internet of Things

LCoS Liquid Crystal on Silicon

LF Last Fit

MCF Multi-Core Fiber

MFF Modulation Format Fixed

MFS Modulation Format Switching

MIFMC Minimum Interference and Failure-independent path protecting for MultiCore networks

OEO Optical-Electrical-Optical

ONS Optical Networks Simulator

PLM photonic-lantern multiplexer

PMP Phase-Matching Points

QoS Quality of Service

QoT Quality of Transmission

QPSK Quadrature Phase-Shift Keying

RF-CASC Random Fit Crosstalk-Aware Spectrum Compactness

RF-MRC Random Fit Multidimensional Resource Compactness

RMLSA Routing, Modulation Level and Spectrum Allocation

RMSCA Routing, Modulation, Spectrum and Core Allocation

RMSF Root Mean Square Factor

ROADM Reconfigurable Add-Drop Multiplexer

RSS Root of Sum of Squares

SC Spectrum Compactness

SCF Single-Core Fiber

SDM Spatial-Division Multiplexing

SDM-EON Spatial-Division Multiplexed Elastic Optical Network

SLC Spatial Lane Change

SMF Single Mode Fiber

SPSA Shortest Path with Cumulative Spectrum Availability

SSS Spectrum Selective Switch

WDM Wavelength-Division Multiplexing

WSS Wavelength-Selective Switch

XT Crosstalk

List of Symbols

α Maximum percentage of switching ports enabled in a node

B Required bandwidth

$B_i^{c,e}$ represent the *ith* connection in the core c of link e

b_r First slot index for request r

β Propagation constant

C Set of cores

c number of cores

C_b Budget of a point under evaluation

C_e Set of cores in link e

c_d Destination (output) core for a SSS port connection

c_r Core for request r

c_s Source (input) core for a SSS port connection

D message processing time

d Indicates a destination node

E Set of directional fiber links

e_r Last slot index for request r

F_{max} Maximum allocated slot index

$F(e, c)$ set of free slot blocks f on core c inside link e

$F(r, c)$ set of free slot blocks on core c inside each link of lightpath r

$G^{c,e}$ number of available spectrum segments in the core c of link e

$g_j^{c,e}$ pectral resources of the jth available spectrum segment in the core c of link e

h XT increment per unit length

hp number of hops in a route

K number of candidate paths for each node pair in the network

k fiber coupling coefficient

L Fiber length

M Set of modulation formats

n number of adjacent cores (neighbors)

n_T number of occupied slots in a link

n_C number of occupied slots that are also occupied at the same index in adjacent cores

O OXC configuration time

P Set of slots

$pair(s, d)$ a pair of nodes, s for source and d for destination

P_i Propagation delay for link i

p_r path for request r

ϕ number of slots in a set P

R Set of requests generated in the network

r Fiber bending radius

S Set of chosen slots

s Number of slots in a spectral dimension

sr Indicates a source node

S_{ec} set of slots s in core c inside link e

$s^{max_{ec}}$ highest allocated slot index on core c of link e

$s^{min_{ec}}$ smallest allocated slot index on core c of link e

t_r number of slots for request r

V Set of nodes

W_i weight of a given link i

w_{tr} core pitch

XT_{TH} Crosstalk threshold

Chapter 1

Introduction

The internet is experiencing an explosive annual growth rate of 30%, with optical transport networks projected to expand to 14 times in 10 years their current size [14]. Consequently, continuous technological innovations in optical core networks are pursued to efficiently meet the ever-increasing bandwidth requirements.

The increase in the count of connections also undergoes the emergence of new mobile generations, comprehending the current growth of 5G and future expectations around 6G [1]. These mobile architectures bring even more strict requirements for transmission latency and bandwidth availability in the network infrastructure.

The legacy infrastructure currently available for optical networks predominantly operates within the C-band and utilizes direct detection and *Wavelength-Division Multiplexing* (WDM) transmission [2]. While this technology enables throughput capabilities of up to 1 Tbps per fiber, it falls short if compared to the anticipated base station rate requirements for 5G (100 Gbps) and 6G (1 Tbps) [3]. Hence, there arises the necessity for innovative technologies to reshape the infrastructure and support the ongoing expansion of the Internet.

The *Elastic Optical Network* (EON) have gained prominence as new technology to enable greater transmission capacity [4]. The optical spectrum in EON links is divided into frequency ranges of 12.5 GHz, named slots. In EON, it allows the establishment of multiple circuits in a single fiber by allocating different slots. Moreover, the slots can be grouped, forming larger capacity transmission channels, which admit circuits with larger bandwidth requirements.

The optical fibers considered in most papers around EON have a single core and are referred to as *Single-Core Fiber* (SCF). In an attempt to increase resource availability, some authors have hypothesized the use of a different type of optical fiber, called *Multi-Core Fiber* (MCF) [5]. The MCF has more than one core (usually 7 or 12), and each core has its own optical spectrum, which is multiplexed in slots. Conceptually, each MCF

is operated as a pool of single-core fibers. The use of MCFs enables the occurrence of *Spatial-Division Multiplexing* (SDM), which increases available spectral resources. Fig. 1.1 shows the core layout of a 7-, 12- and 19-core fiber.

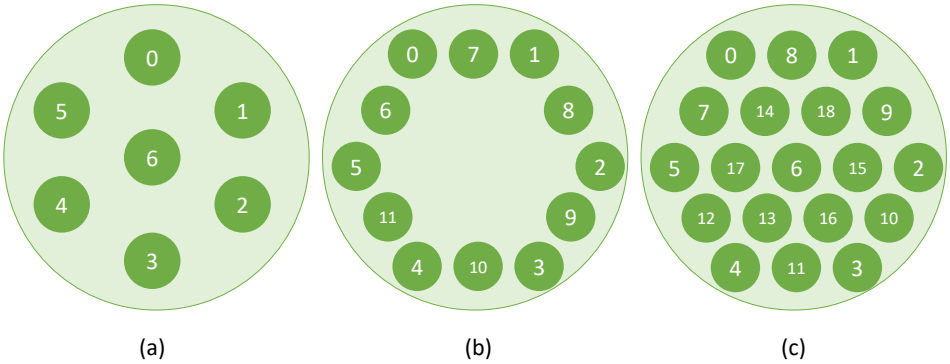

Figure (1.1) Multi core fiber, with (a) 7, (b) 12 and (c) 19 cores.

The multi-core fiber structure combined with the spatial multiplexing, brings a set of advantages. The most visible is the increase in spectral availability, which grows exponentially according to the number of cores. This allows the MCF to overcome the capacity limit and keep up with the increasing future Internet traffic [15]. Besides that, the linear increase in system equipment causes a linear increase in energy consumption. The MCF can help to overcome this situation with equipment solution that operates over all cores at once (as amplifiers [6]), or mechanical solutions to separate the cores (like fan-in/fan-out [8]) instead of the application of splitters in single core fibers.

An essential step for circuit allocation within the fiber cores is the resource selection phase. During this task, the resource allocator must choose and reserve the best resources for the upcoming circuit. It includes determining the most suitable modulation scheme for the signal, selecting the route to install the circuit, specifying the core (or core set) to be utilized, and defining the slot range for allocation. This intricate task catches considerable attention in the EON literature and is recognized as the *Routing, Modulation, Spectrum and Core Allocation* (RMSCA) problem [16].

One of the most outstanding problems prevalent in MCF is the *Crosstalk* (XT), a form of interference that can exert a meaningful impact on the performance if the RMSCA is not well-executed. XT predominantly occurs at specific locations along the fiber known as *Phase-Matching Points* (PMP). The occurrence of XT at these PMPs implies variations of phase shifts between neighboring cores. These phase-shift variations can fluctuate due to minor changes in fiber conditions, such as curvature and torsion [17].

Besides the XT, the slot allocation also must fulfill some constraints from the optical medium. During the signal propagation, to reduce the use of transceivers and avoid *Optical-Electrical-Optical* (OEO) conversion, it is preferable to keep the data transmission

in the optical domain. Therefore, it is necessary to satisfy the continuity and contiguity constraints. These constraints play an important role, especially in the resource selection phase, and must be accounted for as well in *Spatial-Division Multiplexed Elastic Optical Network* (SDM-EON) scenarios.

The current SDM-EON literature is divided into two main paradigms: core-constrained and *Spatial Lane Change* (SLC) enabled. The first one represents the scenarios in which the resource allocation process must consider a third restriction, the core continuity constraint. This constraint demands the allocation of an optical circuit in the same core along its whole route. On the other hand, in the second scenario, the circuit allocation process can pick different cores on different links of its route.

In this thesis, we advance the state of the art with a third paradigm, combining the core-constrained and the SLC-enabled paradigms. The sparse core switching distributes core switching power based on a predetermined heuristic, giving different nodes varying degrees of flexibility. The main goal is to reduce deployment costs close to the core-constrained scenario while maintaining flexibility at impactful nodes.

1.1 Objective

1.1.1 General objective

This thesis aims to study the core switching paradigms in multi-core elastic optical networks proposed in the literature, advance state-of-the-art methods regarding the efficiency of current solutions, and propose novel paradigms.

1.1.2 Specific objectives

This thesis fulfills the following specific objectives:

- Provides a broad literature review around multi-core fibers, spatial division multiplexing, core switching and elastic optical networks (Chapter 3).
- Classifies crosstalk evaluation models and access their impact in network operation (Chapter 4).
- Evaluates the core-constrained paradigm and propose a solution for resource allocation in this architecture (Chapter 5).
- Evaluates the SLC-enabled paradigm and propose a technique for defragmentation based on this architecture (Chapter 6).

- Propose the sparse core switching paradigm and evaluate novel solutions (Chapter 7).

1.2 Contributions

Through an extensive literature review, we elucidate the current state of the art related to MCF, encompassing both theoretical advancements and practical implementations. This literature review helps establishing a comprehensive foundation upon which to build our investigation.

A decisive aspect of MCF is the presence of crosstalk, which can significantly impact the efficacy of SDM-EON. This thesis presents a systematic classification and evaluation of the different manifestations of crosstalk within MCF and clarifies how distinct evaluations of crosstalk impact the SDM-EON performance.

Regarding the resource allocation in SDM-EON, this thesis proposes solutions tailored to different core-switching paradigms. In scenarios without SLC, we introduce a heuristic to efficiently allocate resources by allocating the circuits in reserved areas of the spectrum. The solution allocates circuits strategically in the different cores, enhancing overall network performance while minimizing fragmentation of resources.

In scenarios with the SLC paradigm, this thesis proposes a defragmentation solution designed to reallocate network resources seamlessly. By employing two techniques for spectrum displacement, our approach minimizes disruptions to ongoing circuits while improving resource utilization.

Furthermore, we explore the concept of sparse core switching, which represents a middle-ground solution between scenarios with core-constrained and SLC. By deploying the *Spectrum Selective Switch* (SSS) equipment in nodes where it yields the most substantial benefits, the sparse core switching optimizes network deployment costs and reduces power consumption. This strategic allocation of core-switching power enhances the efficiency and sustainability of future communication networks.

1.3 Publications

1.3.1 Publications related to this thesis

- BRASILEIRO, Ítalo Barbosa et al. Empowering hitless spectral defragmentation in elastic optical networks with spatial multiplexing. In: 2020 22nd International Conference on Transparent Optical Networks (ICTON). IEEE, 2020. p. 1-4.

- BRASILEIRO, Ítalo Barbosa; COSTA, Lucas R.; DRUMMOND, André C. Circuit allocation with strengthened medium core in spatially-multiplexed elastic optical networks. In: 2020 22nd International Conference on Transparent Optical Networks (ICTON). IEEE, 2020. p. 1-4.
- BRASILEIRO, Ítalo; COSTA, Lucas; DRUMMOND, André. A survey on challenges of spatial division multiplexing enabled elastic optical networks. Optical Switching and Networking, v. 38, p. 100584, 2020.
- BRASILEIRO, Ítalo ; DRUMMOND, André ; JUKAN, Admela. Sparse Spatial Lane Change Increases SDM Network Efficiency. In: European Conference on Optical Communications (ECOC), 2023.
- BRASILEIRO, Ítalo ; DRUMMOND, André ; JUKAN, Admela. Performance Analysis of Crosstalk-Aware Sparse Core-Switching Optical Networks. In: IEEE Global Communications Conference (Globecom), 2023.

1.3.2 Other publications

- DA SILVA, Kaio Alexandre et al. Estudo Sobre o Uso de Métricas de Fragmentaçao de Espectro no Projeto de Algoritmos RSA. In: Anais do XXXVI Simpósio Brasileiro de Redes de Computadores e Sistemas Distribuídos. SBC, 2018. p. 1089-1102.
- BENSALEM, Mounir et al. Embedding jamming attacks into physical layer models in optical networks. In: 2020 International Conference on Optical Network Design and Modeling (ONDM). IEEE, 2020. p. 1-6.
- COSTA, Lucas Rodrigues; BRASILEIRO, Ítalo Barbosa; DRUMMOND, André Costa. Novo RMLSA com Tonificação de Circuito e ciente da Qualidade de Transmissão com Baixa Margem em Redes Ópticas Elásticas. In: Anais do XXXVIII Simpósio Brasileiro de Redes de Computadores e Sistemas Distribuídos. SBC, 2020. p. 197-210.
- COSTA, Lucas R.; BRASILEIRO, Ítalo B.; DRUMMOND, André C. Low margin QoT-aware RMLSA with circuit invigoration in elastic optical networks. In: GLOBECOM 2020-2020 IEEE Global Communications Conference. IEEE, 2020. p. 1-6.
- COSTA, Lucas R.; BRASILEIRO, Ítalo B.; DRUMMOND, André C. Energy efficiency in sliceable-transponder enabled elastic optical networks. IEEE Transactions on Green Communications and Networking, v. 5, n. 2, p. 789-802, 2021.

1.4 Thesis organization

The organization of this thesis aims to cover the main topics related to the core switching literature in elastic optical networks.

Chapter 2 introduces the key concepts and main definitions to understand the elastic optical networks, the spatial division multiplexing, and the core switching problem. Around these main topics, some other valuable concepts are presented, such as the resource allocation problem, optical constraints, and crosstalk. Furthermore, in this chapter the two main paradigms related to core switching are illustrated.

Chapter 3 brings pertinent information related to the current state of the art. The chapter analyzes the scientific contributions within the literature relevant to our research and systematically arranges the key findings from these works to indicate the main themes and critical insights. Besides that, the chapter points to the equipment, technologies, and architectural components linked to core switching in the spatial domain.

Chapter 4 brings an evaluation of the impacts brought by the crosstalk effect. We measure the crosstalk thresholds and compare them with the values stated in the literature for the different modulation formats. Besides that, we compare different approaches to measuring crosstalk and show how significant is the difference in the blocking rate between a more simple and a more realistic approach.

Chapter 5 explores the first of three paradigms of core switching: the core-constrained SDM-EON. This chapter presents a novel resource allocation solution tailored to scenarios with core continuity constraints. We evaluate this solution in a comparative analysis against different resource allocation approaches from the literature described in Chapter 1.

Chapter 6 focuses on the second switching paradigm, namely the SLC-enabled SDM-EON. Also, in this chapter, we mention two innovative techniques sourced from the literature and show the potential of these two techniques associated with core switching to facilitate hit-less defragmentation.

Chapter 7 formulates the scattered distribution of core switching capacity. This solution is specifically designed for network planning scenarios and involves the distribution of switching ports among various SSS. It is constrained by an initial budget value, and the solution aims to facilitate efficient resource allocation. This chapter also assesses the complexity and feasibility of this solution. The resource-constrained port distribution enables the implementation of the Sparse Core Switching method, a novel third switching paradigm proposed within the work developed in this thesis. Our findings reveal that a well-designed heuristic solution can achieve performance equivalent to those of the SLC-enabled scenario while requiring significantly reduced monetary investments. Addi-

tionally, this chapter discusses the implications of crosstalk and spectral fragmentation within these paradigms, shedding light on their potential impact.

Chapter 8 serves as the concluding chapter of this thesis, offering a comprehensive overview of our research findings and contributions. It also provides insights into potential directions for future research endeavors and opportunities in the field.

Chapter 2

Multi-core elastic optical networks

2.1 Fundamental concepts and switching paradigms

The necessity of more available bandwidth grows for transport networks as the volume of data transmitted by optical links increases year after year. The advent of the *Internet of Things* (IoT) and mobile devices are the fastest growing category, exponentially increasing the number of active connections. Currently, numerous efforts are applied to develop new technologies for higher transmission capacities in large transport networks. In this context, the optical networks [4], [18], [19], [20], [21] gain prominence due to the use of light as data vector, enabling high transmission rates. Also, the optical transmission technology allows establishing multiple circuits in a single fiber through the allocation of different light frequency ranges.

The EON is characterized by the circuit allocation in multiple channels named *slots*, which are standardized frequency ranges of 12.5 GHz [15]. The slots can be grouped, forming channels with higher transmission capacity and allowing the establishment of circuits with larger bandwidth requirements [22], thus providing further flexibility and network elasticity. Currently, most of the works in the literature consider a 4 THz C-band capacity for each link [23], divided into 12.5 GHz frequency intervals, which results in 320 slots in each fiber [24], [16]. Fig. 2.1 represents a simplified view of the spectral components inside an optical link.

The Fig. 2.1 illustrates an optical fiber with 30 slots. Each slot represents a spectral range of 12.5 GHz, which supports a bit rate up to 12.5 Gbps in the BPSK modulation format [25]. The blocks painted in green, blue, and red represent circuits with same bandwidth allocated on that same link with different modulation formats. The elasticity is evident when establishing circuits with bandwidth requirements higher than a single slot capacity. In those cases, the resource allocation solution defines a group of slots to create a larger channel, which should fit the requested data rate most accurately. Fig 2.1

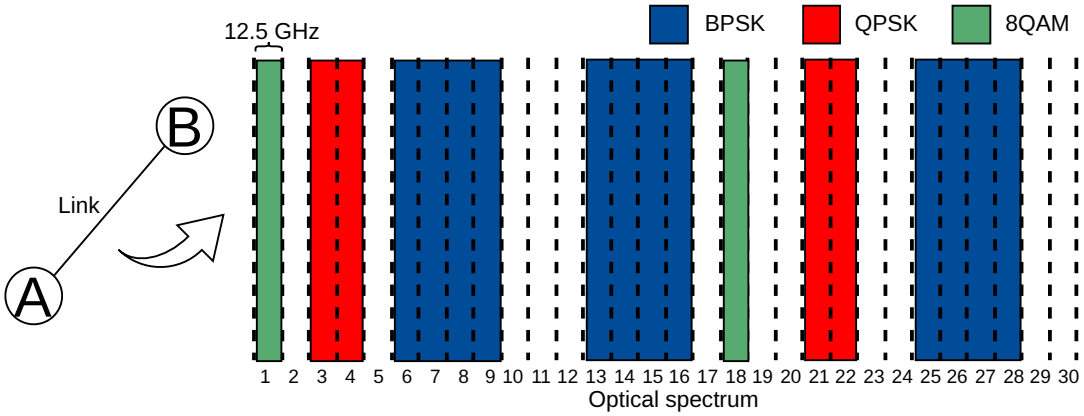

Figure (2.1) Spectrum inside optical fiber.

also depicts the guard band, a spectral gap usually with 1 slot between circuits to avoid high interference impact.

Until now, optical fiber transmission and advancements have provided enough resources to meet traffic demands. However, adopting single mode/core fibers provides little opportunity for expansion and a lack of resources for near-future traffic prediction. Optical networks that operate at Peta bps levels are expected in the upcoming mobile generations, and the single-core fibers are easily outperformed by this traffic of high proportions [26]. Recent experiments have demonstrated Pbps transmission capacity over a 37-core fiber [27].

The majority of EON papers consider fiber with just one core, known as SCF. Besides this approach, some authors apply another type of fiber, called MCF [5]. Unlike traditional single-core fibers, the MCFs have extra cores in the fiber, and each core has its own set of slots. Thus, MCF has additional spatial domain channels, increasing the transmission capacity [28]. This characteristic provided by the MCF is called spatial-division multiplexing, and the elastic optical networks constituted by MCF are called SDM-EON. Combining spectral flexibility and high core availability makes SDM-EON a strong candidate to support future Internet traffic [29] [30].

The concept of SDM relies on placing numerous spatial channels in a given fiber structure or fiber arrangement [31]. The type of channel depends on the technology employed. Different types of SDM-enabling technologies besides MCF are: Single-Mode Fiber Bundle, which is an arrangement of single spatial dimension fibers packed together to create a fiber bundle; Multi-Mode Fibers (and Few-Mode Fiber), which are fibers that support tens of transverse guided modes for a given optical frequency and polarization; Few-Mode Multi-Core Fibers, which are the combination of multi-core fibers and few-mode fibers; Vortex Fiber for Orbital Angular Momentum multiplexing, which uses light beams to carry orbital angular momentum; Hollow-Core Photonic Band Gap Fiber, which

is hollow fibers and wave-guiding is achieved via photonic bandgap mechanism; and Multi-Element Fiber, which consists of multiple fiber elements drawn and coated together. Authors in [31] present further detail and some references to these different fiber types. The scope of this thesis is delimited to MCF-related literature.

To ensure low application cost, the performance of a MCF with c cores should be the same (or very close) when compared to a pool of c SCF. Thus, the benefits come as a reduction in fabrication cost. At first sight, using MCFs with more cores is advantageous due to higher resource availability. However, the main factor of signal interference in the MCF is the leakage of a fraction of the signal power from a given core to its neighboring cores. This phenomenon, called XT (discussed further in this chapter), turns impracticable the allocation of some spectral ranges due to high interference caused by the active circuits in its neighboring cores.

One of the main challenges for MCF scenarios [11] is to achieve low crosstalk and high core density. The main variables that influence the XT intensity are the symbol rate, the modulation used, and especially the physical characteristics of the fiber [32]. Thus, to enable the application of MCFs with a large number of cores, the development of fibers that provide smaller crosstalk between neighboring cores is required [33], [34].

In most papers found in the literature, 7-core fibers (Fig. 1.1 (a)) are used, arranged in a hexagonal array [35], [36]. In this configuration, the central core presents 6 neighbors and consequently suffers higher *crosstalk* impact. The peripheral cores (0, 1, 2, 3, 4, and 5 of Fig. 1.1 (a)) have only 3 neighbors each. 12-core fibers present cores ring-like arrangement (Fig. 1.1 (b)). Each core has only 2 neighbors in this scenario, and all cores have the same *crosstalk* mean value. Fibers with 19 cores (Fig. 1.1 (c)) have up to 6 neighbors per core, resulting in a higher incidence of XT. Still, MCF with more cores can be used over smaller distances. For example, a MCF with 19 cores and a diameter of $200\mu m$ has high crosstalk but can be applied when fiber length is limited to values close to 10 km without significant XT interference [5].

Under the SDM-EON umbrella, the literature encompasses two main paradigms regarding the flexibility of core allocation: core-constrained and SLC-enabled switching. The choice of the paradigm to apply in a network impacts the node architecture, especially regarding the *Reconfigurable Add-Drop Multiplexer* (ROADM) design. Besides that, the chosen paradigm brings different degrees of freedom to the resource allocation procedure, which is discussed further in this thesis.

Fig. 2.2 presents two distinct ROADM architectures for SDM-EON, each with unique characteristics and cost implications. Fig. 2.2 (a) illustrates the core-constrained architecture, which generates the core continuity constraint. In this setup, lightpaths on each core, switch only to cores with the same index in the destination link. For example, circuit

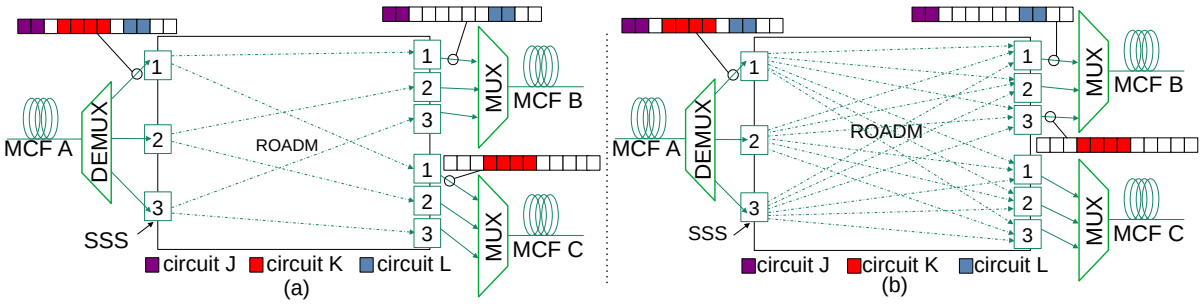

Figure (2.2) Potential architectures for SDM with (a) core-constrained and (b) SLC-enabled switching.

J in core 1 of fiber A can only switch to cores with index 1 of either fiber B or C. This architecture is advantageous for cost savings, reducing the need for complex SSS with higher port count. Since the switching is limited to circuits with matching indexes, the SSS requires fewer ports.

Fig. 2.2 (b) depicts the SLC-enabled ROADM architecture. This design offers greater flexibility in circuit allocation by allowing a lightpath to switch to any core in the destination links, regardless of its core index. For example, the circuit K on core 1 of MCF A in Fig. 2.2 (b) switches to core 3 (different index) in fiber B. This flexibility facilitates more efficient use of network resources and can improve network performance. However, this architecture generates increased costs due to the need for more complex SSS. These switches must be equipped with more ports to accommodate the unrestricted core switching, leading to higher implantation costs, energy consumption, and complexity in resource allocation.

When crossing a node, the input fiber crosses a spatial demultiplexer (SDM demux), which separates the spatial channels (cores). After the split, SCF are used for each core in the input fiber, and each SCF is addressed to a SSS. The main function of SSS is to switch in a lower granularity and redirect each circuit of the SCF independently. At this point, the complexity grows with the increase of output ports inside the SSS. After switching to the appropriate port, the circuit can be directed to the current node (drop) or follow the route to another node. In this case, it is directed to another SSS. This SSS adds the circuit to the SCF of the next appropriate core (not necessarily the same core of the input fiber when SLC-enabled). Then, the SCF will be multiplexed, and the other SCF composes the output MCF.

Various technologies can be used as SSS switching engines. Fig. 2.3 presents a more detailed view of an example of SSSs equipment installed in a given ROADM. After fanning out, an MCF with c cores becomes c SCFs. The light inside a given SCF crosses a diffraction grating and suffer dispersion in the spectral dimension, and each output wavelength focuses on different mirror positions according to the destination [37]. After reflection,

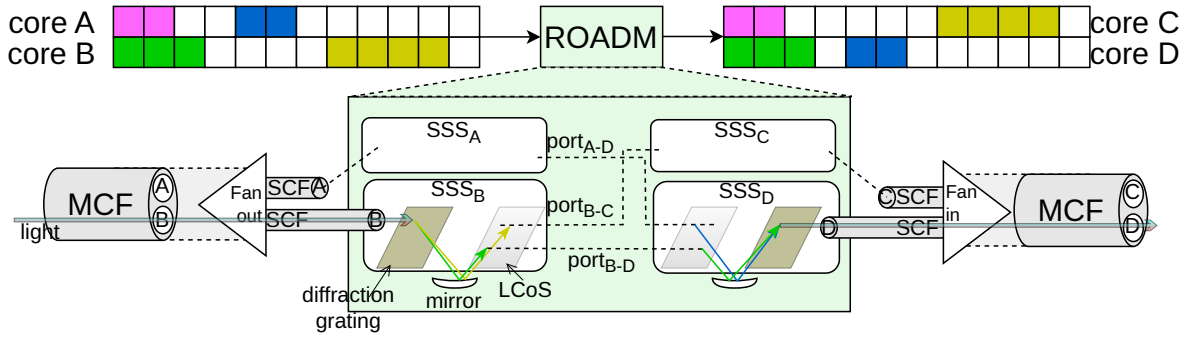

Figure (2.3) Detailed SSSs composing a ROADM.

millions of pixels on a *Liquid Crystal on Silicon* (LCoS) allow redirecting channels of varying widths to the selected SSS output port [38]. The LCoS presents no requirement for locking the spectrum to any predetermined channel. Afterward, the output port of an SSS connects to an input port of a different SSS according to the predefined connection setting. The procedure adheres to an inverse sequence in a given output SSS, aggregating all the circuits that need to switch to a specific core at its corresponding input SSS.

In summary, the core-constrained architecture is cost-effective and straightforward to implement and operate but lacks the flexibility of the spatial lane change architecture. Conversely, the SLC architecture is more expensive but provides enhanced flexibility and potentially better resource utilization in elastic optical networks. Choosing between these architectures depends on the specific requirements and budget constraints for network deployment.

2.2 Resource allocation problem

In many optical network architectures, the control plane or one of its components performs decisions regarding resource allocation. For example, in a *Generalized Multi-Protocol Label Switching* (GMPLS)-controlled optical network, the resource allocation mechanism is decoupled to a dedicated component with an open and well-defined interface and protocol called Path Computation Element (PCE) [39]. Fig. 2.4 presents the control plane and the data plane of a network.

The PCE is responsible for the path computation and resource selection. In the example, the GMPLS protocol disseminates information regarding the network state, both topology and resources. The Traffic Engineering Database (TED) stores the updated information, maintaining a global picture of current network topology and resource availability. The communication between PCE and GMPLS occurs with the help of Path Computation Service and Protocol (PCEP). The PCE can be centralized or distributed,

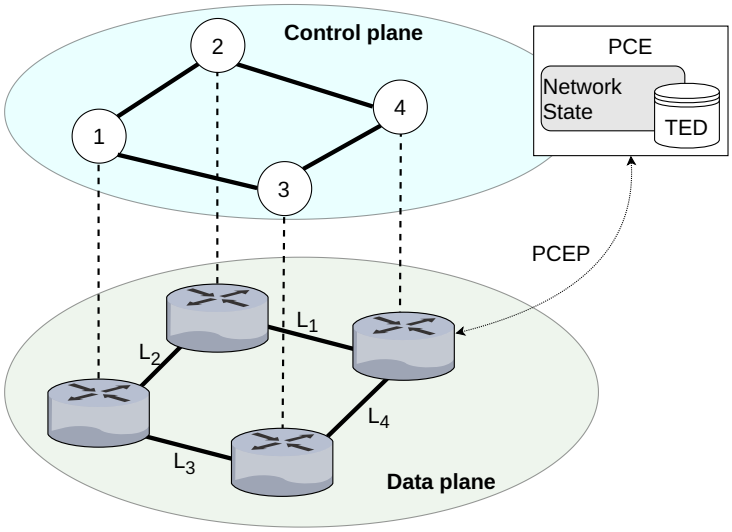

Figure (2.4) Path Computation Element (PCE) in control plane.

and in the last case, the resource allocation decision is a collaboration (with the PCEP protocol) between the multiple PCE instances.

The circuit establishment in optical networks requires resource allocation to enable data transmission. In a network with dynamic traffic, the request for new circuits arrives on different timestamps that are previously unknown. Whenever a new circuit request emerges, it brings information regarding its source and destination nodes $pair(s, d)$ and the minimal data rate required for transmission. On the other hand, in the static traffic scenario, the information about the circuits to create in the network is known in advance, and a traffic matrix with information on all the circuits is available as input. With this information, the resource allocation method should evaluate all the $pair(s, d)$ and define the best allocation setting.

For both traffic types, the resource allocation requires the fulfillment of a series of steps. The first step is selecting the appropriate route between $pair(s, d)$. The route is the fiber links and optical nodes that hold the circuit from its source until it reaches its destination. Some papers allocate the shortest path [40] or k-shortest paths [41] routes to efficiently accommodate the new circuit and save resources for future allocations.

After the route selection, the distance of the lightpath transmission becomes known. This information is important to solve the next step in the circuit establishment process: the choice of modulation level [42]. The optical signal can use different modulation levels by shaping characteristics of the lightwave, such as amplitude, phase, and polarity. The combination of different amplitude and phase levels applied to the optical signal enables the transmission of a higher bit amount per symbol when compared to the traditional model of one-bit per symbol *Binary Phase-Shift Keying* (BPSK).

The modulation level represents the density of the optical signal. Higher-level modulations allow the transmission of more bits per signal, while the lower-levels transmit fewer bits per signal. Thus, higher modulation levels require fewer spectral resources once they can transmit more data when compared to the lower-level signals. [42]. Fig. 2.5 presents characteristics for different modulation formats.

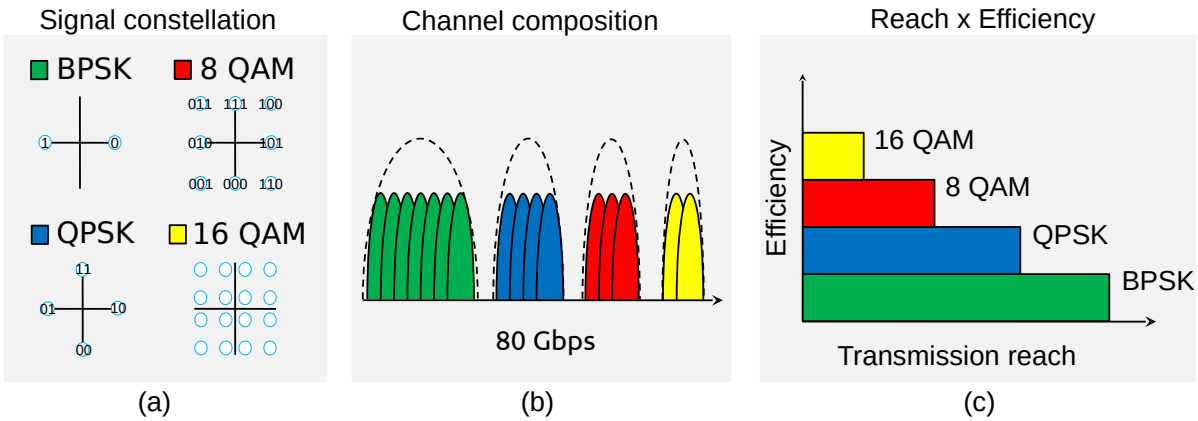

Figure (2.5) Application of different modulation formats.

The figure depicts the main differences regarding multiple modulation formats. As shown in Fig. 2.5 (a), the signal constellation corresponds to different variations on the lightwave characteristics such as amplitude and phase [43], and the number of bits transmitted by signal increases along with the number of possible combinations. We omit the bit combination in *16 Quadrature Amplitude Modulation* (16QAM) modulation for simplification. Fig. 2.5 (b) presents the slot efficiency for each modulation format to transmit the same data rate of 80 Gbps. While the 16QAM modulation requires only two frequency slots, the BPSK requires seven. However, the increased bit density makes the signal more fragile and susceptible to interference from the physical environment. In Fig. 2.5 (c), we show that the transmission reach is higher to simpler modulation formats, making them more robust to physical interference.

After defining the modulation level, measuring the frequency range required to transmit the demanded data rate is possible based on the capacity per slot provided by the chosen modulation. This information defines the channel spectral size that should be created for the new lightpath. In EON, the optical spectrum is systematized as a grid of 12.5 GHz, and these multiple frequency ranges are named slots. The slots are grouped to create a new channel to keep the new circuit. Thus, the next step of the circuit creation process is selecting the appropriate slot range.

Therefore, choosing the appropriate modulation level, route and slot range available to the circuit has become a problem frequently addressed in the EON literature, known as *Routing, Modulation Level and Spectrum Allocation* (RMLSA) [44].

The RMLSA problem can also be modeled to consider interferences of the physical environment in the signal propagation [45], [46]. In this context, the model is closer to reality because some constraints are added, such as the distance limitation for the modulation levels, the interference that occurs due to the fiber type used as propagation medium, and the interference between the circuits in the same fiber.

The use of MCFs enables the occurrence of SDM, which increases available spectral resources. Considering an EON with MCF, the RMLSA problem will present a new component characterized as *core selection*. Some papers refer to this new approach as RMSCA problem [16].

The MCF introduces a new dimension into the RMLSA problem since they have more than one core (usually 7), and each of these spatial dimensions has its own slot set, which can be allocated independently. Conceptually, each MCF operates as a pool of single-core fibers. The resource allocation solution must choose the most suitable core for new circuits. Fig. 2.6 presents a small network in which the RMSCA problem must be solved.

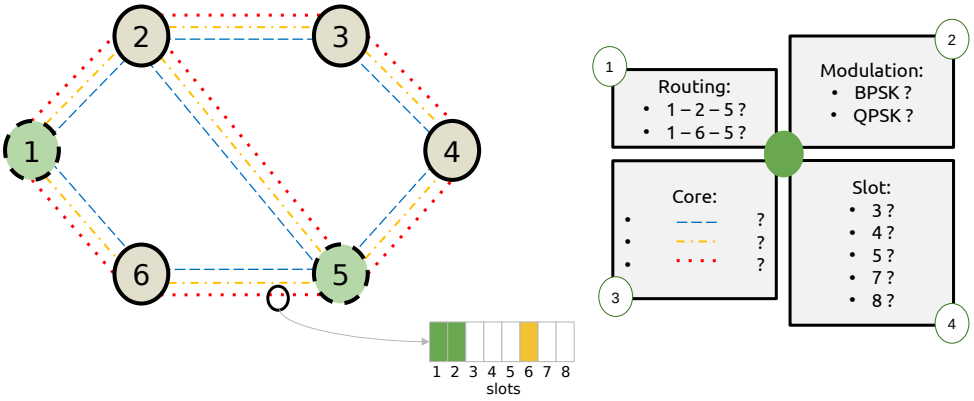

Figure (2.6) RMSCA problem to circuit between nodes 1 and 5.

Fig. 2.6 presents a network with 6 nodes and 7 bidirectional links. At a certain time, the control plane receives a circuit request of 20 Gbps between nodes 1 and 5. This request initiates the first step of the RMSCA problem: selecting the path. The node pair $1-5$ has two options for shortest paths based on the number of hops: $1-2-5$ and $1-6-5$. Once the routing problem is resolved, the total distance that the lightpath must travel becomes known. Based on this information, the modulation format used in the signal is selected. The modulation level is chosen based on the length of the route, as high-level modulations have a shorter reach due to the signal's fragility, which is affected by the transmission medium.

After selecting the modulation level, the control plane measures the number of slots required for the requested bandwidth. Considering the 20 Gbps in the example, the new circuit requires two slots if using the most robust modulation format in this scenario (BPSK) or a single slot for any more complex modulation format. The following steps are

the core selection (third step) and the slot allocation (fourth step). Since the decisions for core and slot range are highly dependent on each other, they are enclosed together. This phase must also consider the optical constraints outlined in the following section. Concluding the example, allocating a new circuit with one slot on the core represented by the red dashed line between nodes 6 and 5, without considering the guard band, can only occur on slots 3, 4, 5, 7, or 8. On the other hand, a circuit with two slots can only allocate slots 3, 4, or 7.

2.2.1 Optical constraints

Certain constraints regarding the optical transmission medium must be met to establish a new lightpath using EONs. These include spectral continuity, spectral contiguity, and core continuity. When allocating resources, it's essential to consider these constraints to ensure alignment with the optical equipment capability, reduce equipment deployment, minimize energy consumption, and optimize spectral occupation. Fig. 2.7 illustrates a scenario where the optical constraints compromise establishing a new circuit.

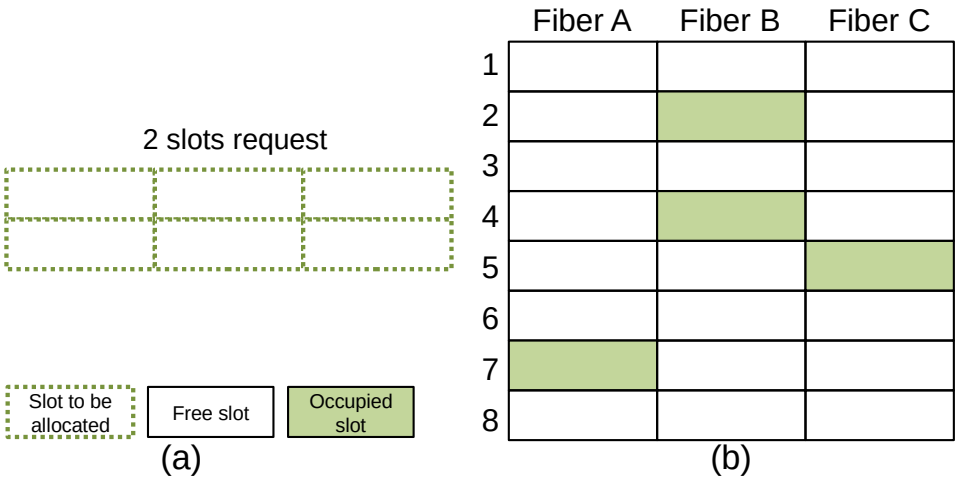

Figure (2.7) Continuity and contiguity restrictions block establishing a 2-slot circuit.

Fig. 2.7 illustrates the spectral state of fibers A, B, and C composing a route. The network must now allocate a two-slot request in the route A-B-C previously defined. Even though all the links have a low utilization (12.5%, 25%, and 12.5% respectively for links A, B, and C), the request is not allocable due to the optical constraints.

The spectral continuity constraint makes the permanence of the optical signal in the same slot range between source and destination nodes mandatory. Thus, the chosen slot set must be free in all links of the selected route. The SDM-EON scenario imports these same restrictions, which are relaxed now by the occurrence of the same slot frequency range in the multiple cores.

In the spectral contiguity constraint, the allocated slots must be adjacent in the spectrum. Therefore, a single transmitter is reserved for each circuit, and only one contiguous slot range is allocated.

Fig. 2.7 (a) presents a 2-slot circuit request, which must be served using the resources of Fig. 2.7 (b). The route was chosen in a previous stage, and the circuit must travel through the fibers A, B, and C. Considering the constraints, it is not possible to establish the circuit: there is no set of two adjacent free slots (contiguity constraint) maintaining the same index in all three links of the route (continuity constraint). The optical constraints stimulate the recurrence of scenarios such as Fig. 2.7, in which the control plane cannot allocate resources despite the high spectral availability on each link. Fragmentation is a common problem in spectral resource management, described in the following subsection.

A third optical constraint arises with the application of spatial division multiplexing. The application of core continuity constraint in spatially multiplexed fibers is a decisive point in the network design and the central matter of this thesis. When applying this constraint, the resource allocation module must always allocate the circuit in the same core along all the fibers composing its route. Network architectures with the core continuity constraint can use SSS with fewer ports, which reduces the general network cost.

When designing a network, the operators also have the chance to avoid the core continuity constraint by applying ROADMs with fully connected SSSs. This architecture corresponds to the full SLC and increases the flexibility of the resource allocator method when selecting the best core in every link of a route for new circuits. The full-SLC architecture relaxes the slot continuity constraint by providing the same slot index in the multiple cores of a given fiber. The slot continuity is still present, but with the full-SLC architecture, the resource allocator has more freedom to select the slot range for new circuits.

2.2.2 NP-Completeness analysis

This section discusses the complexity of the static RMSCA problem. The RMSCA problem contains the routing decision for all the node pairs with non-zero traffic demands, the modulation level, the core, and the slots allocation to satisfy the corresponding traffic demands. If the routing is already known or predetermined and only one modulation level is considered, the RMSCA problem is the static spectrum and core allocation (SSCA) problem. In the following, we show the NP-Completeness of the SSCA problem via its connection with the static spectrum allocation (SSA) problem in EONs. Therefore, the optimal RMSCA problem, which jointly optimizes the routing, modulation level, spectrum, and core allocation, is NP-hard.

SSA problem in the SLICE network

Define a network as $G(V, E, P)$, where V represents the set of nodes, E represents the set of directional fiber links between nodes in V, and P is the set of slots on each fiber, $|P| = \phi$.

Definition SSA problem - given a network $G(V, E, P)$, and a predefined set of spectrum paths request pair $SP = < p_r, t_r >$, where p_r is the path and t_r is the request size (in terms of the number of slots) of the r-th spectrum path, is it possible to establish each spectrum path in the set using consecutive slots, and satisfy the guardband constraint?

The SSA problem is proven to be NP-Complete in [47].

SSCA problem

Define a network as $G(V, E, C, P)$, where V represents the set of nodes, E represents the set of directional fiber links between nodes in V, C represents the set of cores in each fiber link, and P is the set of slots on each core, $|P| = \phi$.

Definition SSCA problem - given a network $G(V, E, C, P)$, and a predefined set of spectrum paths request pair $SP = < p_r, t_r >$, where p_r is the path and t_r is the request size (in terms of the number of slots) of the r-th spectrum path, is it possible to establish each spectrum path in the set using consecutive slots from a specific core, and satisfy the guardbands (GB) constraint?

Theorem 1: The SSCA problem is NP-Complete

In the following, we sketch the proof of Theorem 1. (i) $SSCA \in NP$. The certificate C is the spectrum allocation $< c_r, b_r, e_r >$ for each spectrum path p_r, where c_r is the chosen core, b_r, and e_r are the starting and ending slot index, respectively. The verifier: VF = "On input C":(1) Test whether each $< c_r, b_r, e_r >$ satisfies the traffic demand t_r and the index is no greater than ϕ. (2) For each spectrum path p_{r_1}, test whether it is separated by GB slots from any other p_{r_2} when they share a common core in a fiber link. (3) If both pass, accept; otherwise, reject. The verifier runs in time $O(|SP| + |SP|^2)$, which is polynomial in the size of the problem. (ii) The SSA problem is reducible to the SSCA problem. Given an SSA problem on the network $G(V, E, P)$; we can reduce it to an SSCA problem using the following construction. We construct the SSCA problem on a network $G(V, E, C, P)$ with $|C| = 1$. (iii) It is easy to see that the reduction is in the polynomial time of the problem size. (iv) The SSA problem has a solution if and only if the constructed SSCA problem has a solution.

Through the above reduction, we can see that the spectrum and core allocation problem alone is hard. The RMSCA problem is even more challenging since the routing and modulation level decisions must be jointly considered.

2.3 Fragmentation

Due to the mentioned optical constraints, small free spectrum portions spread out on the network interfere might the network operation since the resource allocator will block new circuits even if there are enough free slots. These available slots might be scattered across the optical spectrum due to the continuity and contiguity constraints (as in the example of Fig. 2.7), unable to be allocated. This problem permeates the EON literature and is defined as the *fragmentation problem* [48] [49]. High fragmentation increases the blocking of circuit requests, causing inefficient utilization of spectral resources [50].

The literature on EON includes manifold fragmentation metrics. It is, hence, hard to define a universal fragmentation metric without considering specific aspects of the system. This thesis considers multiple fragmentation metrics [51], [52] to highlight different features of the scenarios under evaluation. We consider the following variable list to define the different fragmentation equations.

- $e \in E$: Set of links in the topology.
- $c \in C_e$: Set of cores inside link e.
- s_{ec}^{max}: highest allocated slot index on core c of link e.
- $f \in F(e,c)$: set of free slot blocks f on core c inside link e.
- $F(r,c)$: set of free slot blocks on core c inside each link of lightpath r.
- $s \in S_{ec}$: set of slots s in core c inside link e.

The External Fragmentation (F_E) [52] is among the most simple fragmentation metrics, and its assessment provides an overview of the largest free slot segment in the spectrum. A slot segment corresponds to a set of contiguous slots with the same state (all free or all allocated). Equation 2.1 presents the external fragmentation.

$$F_E = 1 - \frac{max(F(e,c))}{\sum_{f \in F(e,c)} |f|}, \tag{2.1}$$

In Eq. 2.1, the function $max(F(e,c))$ retrieves the slot segment with the largest size in the set of segments inside core c. The size (amount of slots) of the largest segment f is then divided by the total amount of free slots inside core c.

The *Root Mean Square Factor* (RMSF) [51] accounts for the highest allocated slot index on each spatial channel and the number and size of free segments. The main factors intensifying the RMSF fragmentation are the increase of the last allocated slot index, the

number of free segments in each core (indicated by $|F(e,c)|$, and the size relation between small and large free segments. The RMSF is defined according to Equation 2.2:

$$F_e^{RMSF} = \frac{1}{|C_e|} \cdot \sum_{c \in C_e} \frac{s_{ec}^{max} \cdot |F(e,c)|}{\sqrt{\frac{\sum_{f \in F(e,c)} |f|^2}{|F(e,c)|}}}, \tag{2.2}$$

The Shannon Entropy [51] measures the spreadness of free slot segments in the spectrum of a link e. A large amount of small free slot segments intensify the entropy, and the presence of a few large segments reduces it. The value of $|f|$ indicates the size of the segment f. The slot index information does not play an important role in this metric. Equation 2.3 measures the spectral entropy:

$$F_e^{SE} = \frac{1}{|C_e|} \cdot \sum_{c \in C_e} \sum_{f \in F(e,c)} \frac{|f|}{|S_{ec}|} \cdot ln \frac{|S_{ec}|}{|f|}, \tag{2.3}$$

The *Root of Sum of Squares* (RSS) fragmentation [51] accounts mainly for the size of free slot segments, and it is measured by link e. Information about the number of channels or the allocated slot indexes does not interfere with the RSS fragmentation. Equation 2.4 measures the RSS fragmentation:

$$F_e^{RSS} = 1 - \frac{1}{|C_e|} \cdot \sum_{c \in C_e} \frac{\sqrt{\sum_{f \in F(e,c)} |f|^2}}{\sum_{f \in F(e,c)} |f|}, \tag{2.4}$$

The fragmentation metrics above are applied in some experiments in this thesis to provide more information about the performance evaluations. Another aspect revolving around multi-core fibers that plays an important role in the fragmentation levels is the crosstalk interference. The following section provides an overview of the influence of crosstalk.

2.4 Crosstalk impairment

The XT impairment is an important interference in MCF. To reduce its effects on multiple circuits, the resource allocation solution must observe the indexes of slots already allocated in the adjacent cores (or neighbors) on the core selection phase. The interference between cores should be considered in studies for closer proximity to real SDM-EON scenarios.

The XT is the main interference on MCF [35] and is classified as intra- or inter-core [53]. The intra-core XT occurs within a fiber core and is characterized mainly by the non-linear interferences (NLI) and the Amplified Spontaneous Emission (ASE) noise. We do not consider the intra-core XT in this thesis, and our focus is the inter-core XT. It occurs mainly at discrete points along the fiber called PMP, as illustrated in Fig. 2.8. The force of interaction between two cores occurs even with small perturbations in the fiber (radius of curvature $> 1m$) [11]. If this perturbation is larger than the nominal index mismatch between two neighboring cores, resonant coupling will occur. Fig. 2.8 shows an example of PMP occurrence in an MCF and (b) the power loss in several PMPs.

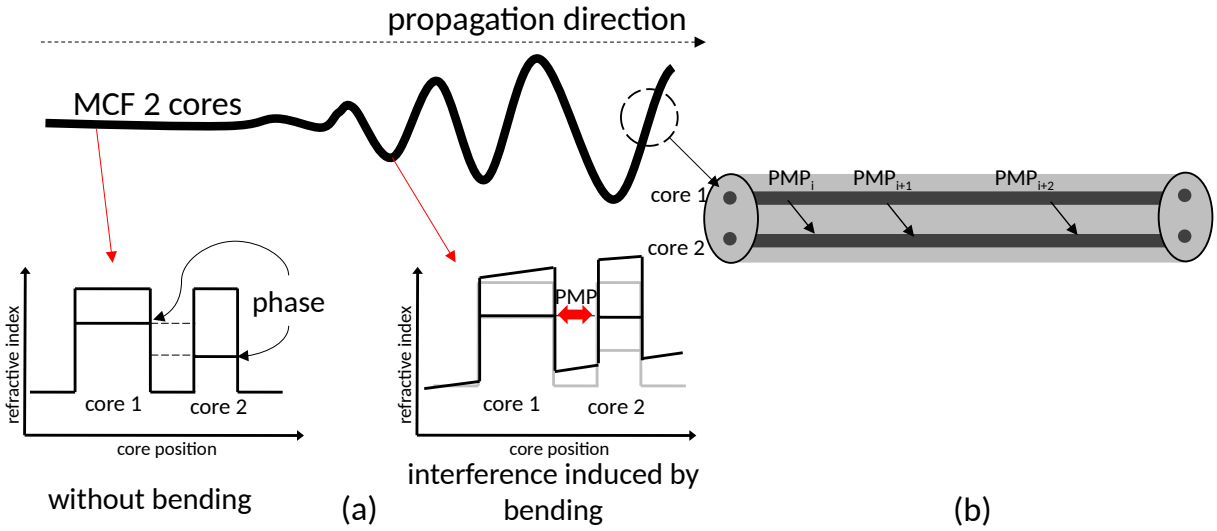

Figure (2.8) (a) Crosstalk occurrence in a Phase Matching Point PMP, adapted from [11] and (b) different PMPs along the fiber.

The crosstalk (after fiber propagation and installation) is a statistical value since the occurrence of XT in the PMPs is influenced by the phase-shift variations between the neighboring cores and because the phase displacement is easily varied by small changes in the conditions of the fiber, such as curvature and torsion [17].

Besides the number of cores, the core's arrangement and the fiber's physical properties have a strong impact on the XT between the cores. Fig. 2.9 shows the composition of a trench-assisted MCF model.

The use of trench-assisted MCF results in a reduction in the effects of XT. The power overlap of adjacent cores will be smaller because the trench (Fig. 2.9) reduces the power leakage for the cores. The crosstalk of a trench-assisted MCF is around 20 dB smaller than that found in a standard MCF [34]. The XT between neighboring cores has a strong dependence on the spacing between the cores (core pitch), and it can be reduced by increasing the space between cores or improving the confinement of each core like the

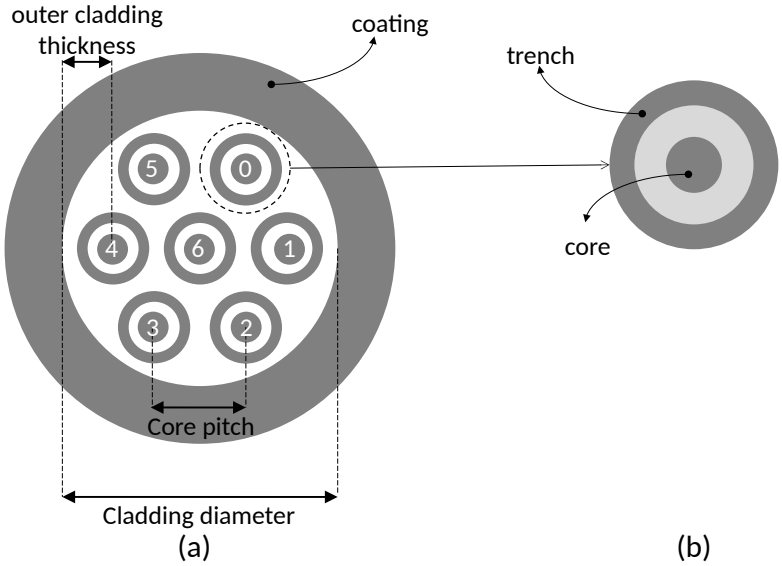

Figure (2.9) Layout of the elements of (a) a trench-assisted MCF and (b) of one core.

trench-assisted fibers [11]. The increase in core pitch causes a reduction in the number of cores since the diameter of the fiber should not increase proportionally.

The increase of outer cladding thickness was proposed [54] to avoid the increase of micro-bending loss in the outer MCF surface. However, fibers with a coating diameter larger than 200 μm are inappropriate because they are more susceptible to fractures. Thus, a thin outer cladding is favored to provide better core scattering, higher core density and to maintain the fiber mechanical flexibility [34].

Possible values for fiber parameters found in the literature are [17], [55], [33]: core pitch: 40.7 to 51 μm; cladding diameter: 144.6 to 188 μm; outer cladding thickness: 31.6 to 47.7 μm; coating diameter: 256 to 334 μm. The authors in [56] present a table with different parameter sets found in the literature and verify the impact of parameter variation on the network crosstalk calculation.

In Fig. 2.9 (a), a circuit allocated to core 0, slots 2, 3, and 4 would suffer XT interference if circuits are allocated in cores 1, 5, or 6, in slots 2, 3 and 4. The circuit signal becomes noise if its XT level exceeds the threshold allowed by the network. The crosstalk among cores is a physical impairment in SDM-EON networks that cannot be neglected. Thus, it is necessary to account for it in the network model. In section 3.2, we list the existing XT equations from the literature and select the most used for this thesis. We apply Equation 2.6 from [57] that measures XT values. Upon every circuit allocation request, the measured XT must be considered.

$$h = \frac{2k^2 r}{\beta w_{tr}}, \tag{2.5}$$

$$XT = \frac{n - n \cdot exp[-(n+1) \cdot 2hL]}{1 + n \cdot exp[-(n+1) \cdot 2hL]}. \tag{2.6}$$

In Eq. 2.5, h indicates the increment of XT per unit length, k is the fiber coupling coefficient, which is the percentage of power that leaks between cores. Variable r indicates the fiber bending radius, which is the radius of the mandrel in which the fiber is coiled [58], β is the propagation constant and describes the behavior of light as it travels through the cores, and w_{tr} is the distance between cores (core pitch), as defined in [59]. In Equation 2.6, n is the number of adjacent cores (neighboring cores), and L is the fiber length. Some papers propose a less complex way to calculate crosstalk by using lists to store information about the impact of crosstalk in slots, which reduces the number of XT verification [60]. Still, in these cases, the Eq. 2.6 is also used to measure crosstalk. Fig. 2.10 exemplifies the crosstalk occurrence in a 3-core fiber [61].

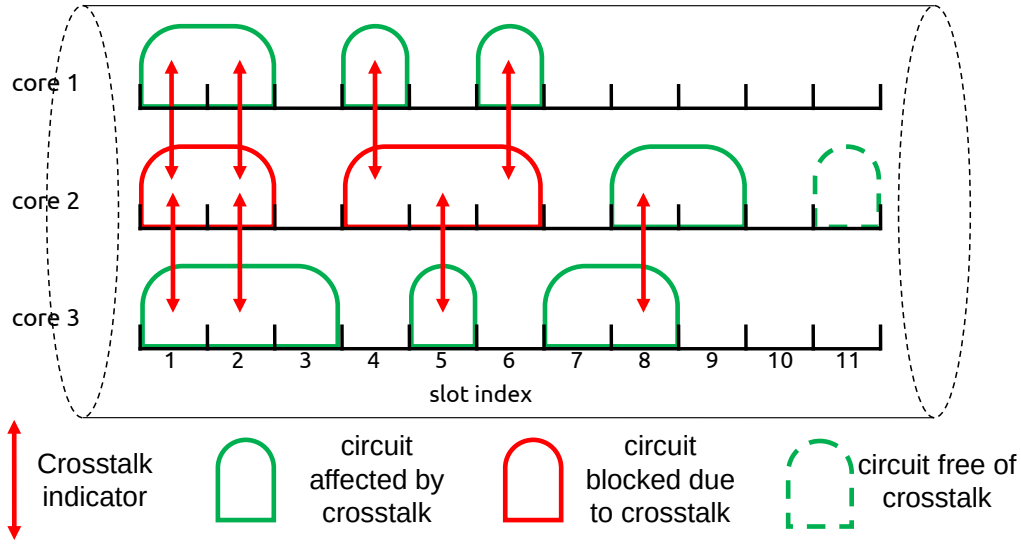

Figure (2.10) Crosstalk occurrence in 3-core fiber.

In Fig. 2.10, it is observed that core 2 suffers more intense crosstalk since two adjacent cores (1 and 3) present active circuits in the same range of slots, as the slots 1, 2, 4, 5, and 6. Therefore, the circuit allocation in MCF should verify the index of slots allocated in neighboring cores to avoid XT. This intensifies the spectral fragmentation because free slots cannot be allocated to reduce XT interference.

Crosstalk levels below -25 dB (threshold) are required to avoid significant penalties in transmission [5]. Circuits that reach a XT level below the threshold present problems in signal reading in the receiver. Therefore, circuit allocation should not occur in slots whose index is the same as occupied slots in neighboring cores to avoid interference. However,

this spectral allocation results in greater disorganization of circuits in the spectrum since it increases the spectral fragmentation.

In practical terms, if the XT level surpasses a certain threshold, it transforms the signal of a circuit into noise. Consequently, when allocating cores, it becomes imperative to consider the slot indexes already allocated in the adjacent cores, commonly referred to as neighbor cores. Crosstalk is a critical factor that must be meticulously factored into the allocation process, particularly in studies that aim to simulate real-world scenarios within the context of SDM-EON closely.

2.5 Network profile

In the scope of this thesis, we employ prevalent backbone topologies commonly referenced in optical networks literature: USA, PanEuro, and COST239. These topologies serve as proxies for real-world networks, mirroring continental scales with links spanning hundreds of kilometers. In all the experiments conducted here, we consider uniform traffic between all pairs of nodes. It means that node pairs have the same probability of becoming the $source - destination$ pair of a new circuit request. All scenarios experimented in this thesis are suitable targets for non-uniform traffic analysis.

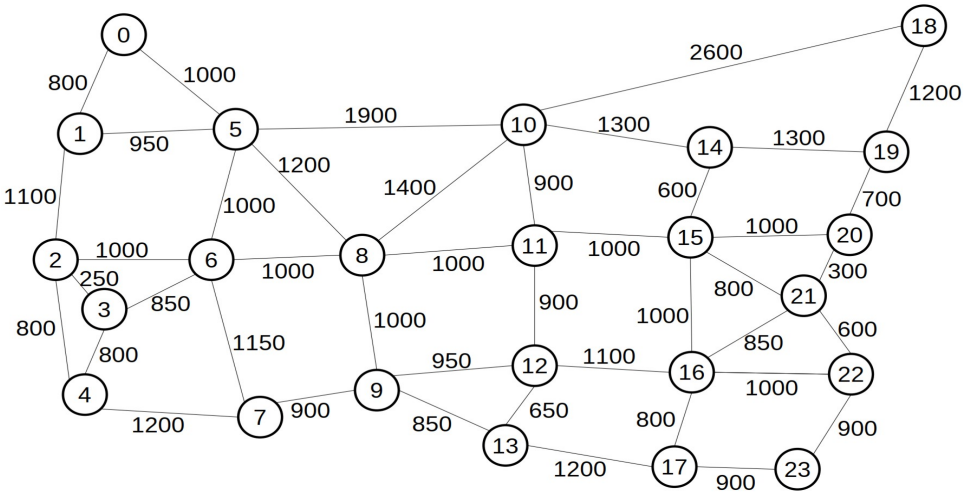

Figure (2.11) USA topology, with link distance in km.

The USA topology (Fig. 2.11) comprises 24 nodes interconnected by 86 links, encompassing the expanse of the United States territory. Conversely, the PanEuro topology (Fig. 2.12), reflective of European networks, features 28 nodes interconnected by 82 links. Similarly, the COST239 topology (Fig. 2.13), also spanning the European continent, comprises 11 nodes and 52 links.

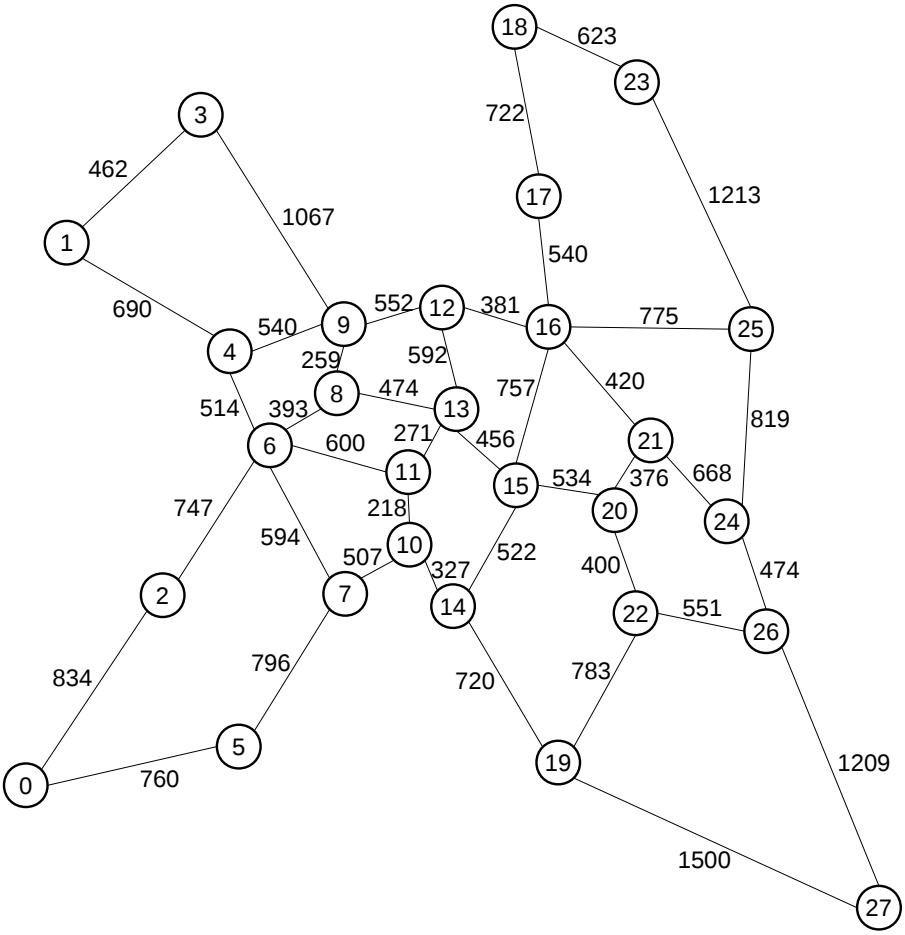

Figure (2.12) PanEuro topology, with link distance in km.

2.6 Concluding remarks

This chapter discusses the growing demand for bandwidth in transport networks due to the increasing volume of data transmitted, driven primarily by the rise of the Internet of Things (IoT) and mobile devices. In 10 years, the optical transport networks should provide 14 times higher capacity than the current scenario. Optical networks are highlighted as a prominent solution, utilizing light for data transmission to achieve high rates. The Elastic Optical Networks (EON) employ standardized frequency ranges (slots) for circuit allocation and reaches higher transmission capacity by grouping these slots, thereby enhancing network flexibility. In comparison to SCF, MCFs offer more cores, each with its own set of slots, allowing for improved data transmission efficiency. However, challenges such as signal crosstalk (XT) and its management are vital considerations in the deployment of MCFs, as high interference can lead to resource allocation difficulties.

Regarding the core switching capacity in a given network, two primary architectures are contrasted: the core-constrained architecture, which reduces costs by limiting switch-

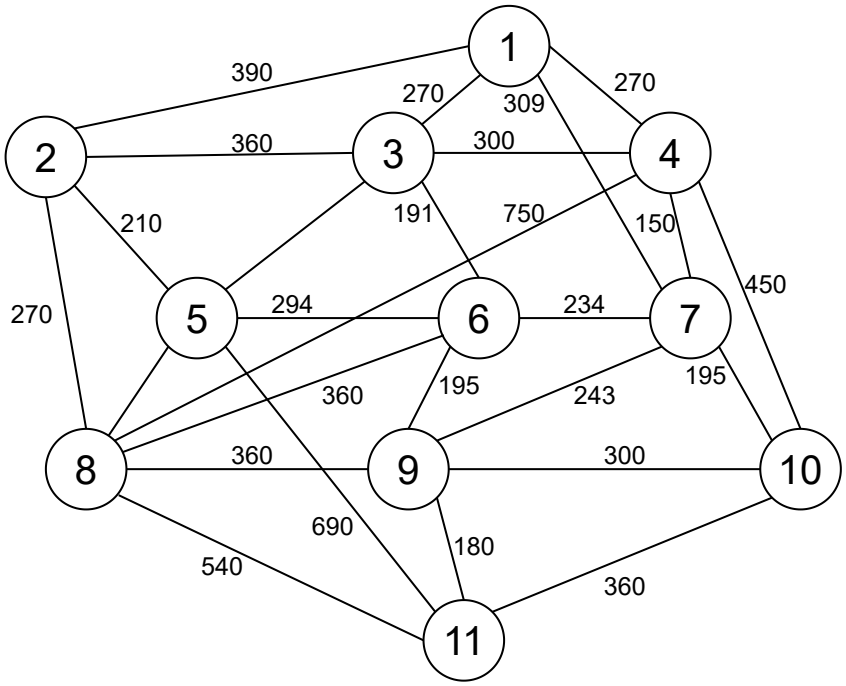

Figure (2.13) COST239 topology, with link distance in km.

ing options, and the SLC-enabled ROADM architecture, which offers greater flexibility at increased expenses. The crosstalk impairment is examined as a considerable factor impacting MCF performance, with methods for reducing its influence being crucial for the effective functioning of SDM-EONs. This comprehensive overview serves to underscore the complexities and technological advancements in optical networks while identifying challenges that arise in resource allocation and interference management in SDM-EON.

Chapter 3

State of the art

This chapter presents a survey on the literature around SDM-EON found in the main publication channels. In [5], the evolution of transmission capacity in optical fibers is shown. The authors state that the SDM concept is as old as the emergence of fiber-optical communication, but the current development of technologies that support the application of SDM has stimulated interest in the scientific community. In [28], a demonstration of the first EON with spectral-spatial division is presented, with an MCF of 7 cores. The authors construct a network of 4 nodes and 5 links (approximately 3 km each) and show the feasibility of adopting MCF in optical network scenarios. The authors also present results to show the occurrence of XT and other interferences from the physical environment. In [41], the performance of the different modulation levels is investigated in the SDM scenario. They also evaluate the performance of different switching models (independent switching, joint-switching, and fractional-joint switching) for MCF. In [62], an evaluation of different traffic aggregation policies is made in EON scenarios with SDM.

As shown, many papers in the literature highlight the feasibility and high performance on the application of MCF in EON. Surveys related to the SDM scenario found in the literature deal with equipment and technologies for using multi-core fibers [63], [31]. Authors in the survey [63] focus on spectrally and spatially flexible ROADM architectures, classifications, and their enabling technologies. Authors in survey [31] review research around SDM fibers, network components, and technologies (such as amplifiers, multiplexers, switches) and evaluate crosstalk interference in 7-core and 19-core fibers, considering different fiber lengths.

Especially the core allocation problem has recently attracted attention in the research community, with the novel constraint on resource allocation called *core continuity*. This constraint applies only to multi-core fibers. To this end, one line of work proposes to use the so-called SLC, e.g., [51], [64], which allows full switching between different cores along the lightpath route. Yet another line of works proposes to apply the core continuity

constraint, characterized by the continuation of the same core index in the entire route [65], [57]. Full switching has the advantage of flexibly switching along the route but requires prohibitively high capacity and equipment cost investments. Core-restricted switching, on the other hand, typically results in higher blocking.

3.1 RMSCA solutions

To reduce the fragmentation problem in fiber cores, some solutions proposed to the RMSCA problem create allocation priorities [66], [35]. Fig. 3.1 presents some allocation models with (a) priorities by slots index and (b) priorities per core.

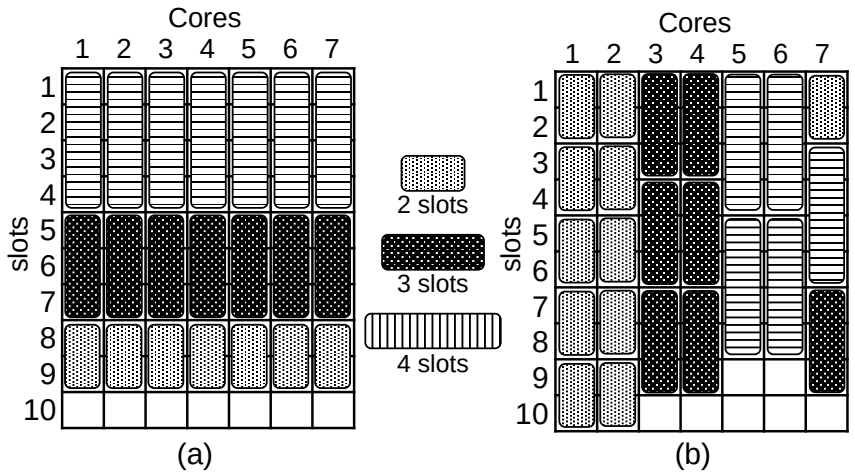

Figure (3.1) Circuits allocated and organized in (a) priority by slot index and (b) priority by core.

Fig. 3.1 (a) presents an example of allocations with prioritized areas delimited by a slot range [66]. In this case, slot sets in the spectrum are exclusive for allocating circuits with a specific number of slots. For example, in Fig. 3.1 (a), slots 1 to 4 are exclusive for 4-slot requests in all cores. Moreover, a slot range named *common area* is delimited, which should allocate circuits that cannot be allocated in its respective prioritized area due to resource unavailability or fragmentation. In the Fig. 3.1 (b), the circuits are allocated primarily in prioritized cores [35], [67]. For example, 4-slot requests are allocated primarily in cores 5 or 6. There is also a core used as *common area*.

Some authors evaluate the use of MCF on static traffic scenarios, in which the circuit requests have a source, destination, and bandwidth defined, and the traffic matrix is known. In [40], the crosstalk information is added as a constraint to the circuit establishment, and the algorithm *Shortest Path with Cumulative Spectrum Availability* (SPSA) is proposed for routing, core, and slot allocation. A 3-core MCF is considered in the evaluation. The authors observed that the effects of crosstalk are attenuated with the use

of fibers with higher slot availability. It reduces the interference between cores because the circuits can be scattered in the spectrum. In [16], an objective function is proposed to choose routes, slots, and cores. The preferred resources (route, slots, and core) meet the crosstalk threshold and maximize the objective function. The results show the performance of the proposed objective function, considering two different forms of modulation selection (*Modulation Format Fixed* (MFF) and *Modulation Format Switching* (MFS)).

The algorithm *Anycast Routing, Spectrum and Core Allocation with Shortest Path* (ARSCA-SP) is proposed in [68], and it allocates slots closest to the lowest index slot (*First Fit*) in all cores of the network links. An ILP strategy is used to make a performance comparison. In [69] is presented a crosstalk-aware RMSCA solution applied to scenarios with two request types: *advance reservation* (AR), which require reserved resources when they occur, and *immediate reservation* (IR), for which the resources are chosen at the moment it is generated, with no guaranty of availability. The proposal reduces both the maximum allocated slot index (F_{max}) and the Average Initial Delay Ratio (AID Ratio). The performance evaluation of AR and IR circuits is also made in [70], which uses a spectrum optimization scheme based on transfer learning to predict spectrum fragmentation and reduce blocking for incoming requests.

Some papers propose routing, modulation, core, and spectral range choice solutions in scenarios of SDM-EON with dynamic traffic. In [71], a Spectrum and Core Allocation (SCA) method is proposed for core and slot selection. The algorithm reserves cores for requests with a specified number of slots and uses priority levels for cores. A performance evaluation compares the proposal with the algorithms *First Fit* and *Random* in 7-core MCF. The proposal obtains a lower blocking ratio, smaller crosstalk average, and less fragmentation. A solution for core and slot allocation is proposed in [24]. The algorithm is compared with *First Fit* and *Random Fit* allocation algorithms in a 7-core fiber, and presents better performance. The proposal also has a smaller *crosstalk per slot*. The comparison with *First Fit* and *Random* algorithms is also done in [35], which proposes a method for core classification and prioritization, in which cores are exclusives to a given bandwidth request. The authors use 7, 12 and 19-core fibers, and check *crosstalk* through a crosstalk-by-slot (CpS) indicator, presented in Equation 3.1 and also used in other papers [24], [72]:

$$CpS = \frac{n_C}{n_T}, \tag{3.1}$$

In the equation, n_T represents the number of occupied slots in the link and n_C represents the number of occupied slots that are also occupied at the same index in adjacent

cores.

In [66], the *Intra-Area FF Assignment* algorithm is proposed for spectrum and core allocation. The algorithm creates "exclusive areas" in the optical spectrum for certain bandwidths and "common areas" for allocation if the exclusive areas are unavailable. The slot allocation inside the common area follows the policy *First Fit* to circuits with an even number of slots and *Last Fit* to circuits with an odd number of slots. The proposal is compared to *Random* and *First Fit*. The authors in [73] define the concept of *XT-prohibited slot*, free slots that can not be allocated since they allow the increase of crosstalk to the unwanted levels. In [74], the RMSCA algorithm RCSA-IC-SCM is proposed to reduce crosstalk. The results show that there is a reduction in the average crosstalk, but has a side effect in the increase of blockage due to increased spectral fragmentation.

The authors in [75] present a crosstalk-aware resource allocation. Also, they present an intra-node crosstalk modeling, which is a way to measure the occurrence of crosstalk within nodes, between fiber input and output ports, in the *Wavelength-Selective Switch* (WSS). The proposal is compared to the crosstalk-aware FF policy version. The authors in [67] show the service-classified routing, core, and spectrum assignment (SC-RCSA) algorithm, also crosstalk-aware, which allocates the spectral resources in dedicated cores. The algorithm is compared to the *First Fit* and *Random Fit* policies in crosstalk-aware and not-aware scenarios. The SC-RCSA proposal has a slightly higher blocking ratio than its competitors but has a lower average crosstalk and fragmentation rate than the other proposals evaluated.

In [76], the algorithm *Failure-Independent Path Protecting for Multi-Core network* (FIPPMC) is proposed for the survivability scenario in EON. The algorithm FIPPMC creates a list of "candidate paths", which corresponds to all possible combinations of route and spectrum available to the circuit. Each candidate path receives an evaluation value, which considers the occurrence of *crosstalk*. The candidate path chosen as the primary path is the one with the lowest evaluation value, and the path for dedicated protection is the one with the lowest evaluation value and links disjoint from the main path. In [77], the proposal of [76] is adapted to use shared routes for protection. The same authors, in [72], propose the algorithm *Minimum Interference and Failure-independent path protecting for MultiCore networks* (MIFMC), also for protection. In the proposed algorithm, the circuit is only established if there is an available disjoint route. If the disjoint route does not exist, another primary route is searched, and the disjoint routes are evaluated. This procedure is repeated until all possible primary routes are evaluated. The authors also propose RMSCA algorithm models to protection scenarios in [78] and [79].

The authors in [61] propose the algorithm *Crosstalk-aware provisioning strategy with dedicated path protection* (CaP) for primary and backup route selection. The algorithm

chooses two disjoint routes in the first available core and slots interval, which respect the crosstalk threshold. Authors in [80] propose an RCSA strategy to protect, named FIPP-p-cycles. The algorithm seeks a route for protection, disjoint from the primary route. The algorithm uses weights (W_i) to fetch available links and cores and look for a p-cycle to ensure protection. If no new p-cycle is found, the new circuit request is blocked.

Some papers take into account information about the network state during the operational phase, such as the spectral fragmentation. A spectral fragmentation analysis is done in [81]. The authors propose two fragmentation-aware algorithms for core and spectrum allocation: *First Fit Multidimensional Resource Compactness* (FF-MRC) and *Random Fit Multidimensional Resource Compactness* (RF-MRC). The authors compare the results with the implementation of *Dijkstra* for routing and *First Fit* for core and spectrum allocation. In [9] the same authors add *crosstalk* information to the core and spectrum allocation, and propose the *First Fit Crosstalk-Aware Spectrum Compactness* (FF-CASC) and *Random Fit Crosstalk-Aware Spectrum Compactness* (RF-CASC) algorithms. In [42] are created dedicated areas for the different request bandwidths. Besides, slot and core allocation are also fragmentation-aware. In [50], two fragmentation-aware RMSCA solutions are proposed. For the establishment of the circuit, the proposals use allocation with prioritized cores and take into account the level of spectrum fragmentation and the potential creation of bottleneck links.

A spectral defragmentation procedure can be used to overcome network fragmentation. The active circuits are reallocated to reduce the occurrence of small ranges of free slots and to enable the establishment of new circuits. Some papers [82] [83] discuss the push-pull mechanism for defragmentation, in which circuits are reallocated to different indexes and cores with no need for circuit shutdown. This is due to the circuit slide on empty slots. A defragmentation model is proposed in [84] and uses the SC (spectrum compactness) metric. The defragmentation will occur in cores with SC value under the threshold. Defragmentation is performed by reallocating the circuit in a different core (keeping the slot range) or in a different slot range (maintaining the same cores). Defragmentation solutions are also proposed in SDM-EON with time multiplexing [85].

In [86], a technique called *virtual concatenation* is proposed. This model allocates slots from the same circuit in different cores in a non-contiguous way, mitigating the fragmentation problem. This approach is less discussed in the literature since the equipment has not yet been developed to support this type of allocation.

To summarize the RMSCA proposals found in the literature, Tables 3.1, 3.2 and 3.3 are designed with important aspects of RMSCA proposals, clustered in tables for scenarios with static (Table 3.1) and dynamic traffic. The dynamic RMSCA algorithms are divided in two tables, which groups the XT-aware (Table 3.2) and XT-unaware (Table

3.3) algorithms. The designed tables use the following notation to describe the allocation models: RCSA to design routing, core, and spectrum allocation strategies; RSCMA to design routing, spectrum, core, and/or mode allocation strategies; RMSCA to design routing, modulation, core, and spectrum allocation strategies; and RSCTA to design routing, spectrum, core, and time allocation.

Table (3.1) Classification of static RMSCA proposals found on literature.

Reference	Core Continuity		XT-Aware	Protection	Contributions Highlights
	Yes	No			
A. Muhammad et al.[16]		√	√		Proposes strategies for the RMSCA problem that jointly optimizes the switching and spectrum resource efficiency.
G. Savva et al.[36]		√			Proposes XT-aware RCSA solutions to provide efficient resource utilization and minimize the number of connections that cannot be established due to low QoT.
L. Zhang et al.[68]	√				The first work that considers the anycast routing problem in SDM-EON with MCF. Proposes an RCSA algorithm to solve the problem.
A. Muhammad et al.[40]		√			Formulates the RCSA problem using integer linear programming. Proposes an algorithm and compares the performance with the ILP optimal solution
M. Yang et al.[87]		√	√		Formulates the RCSA problem using a node-arc-based ILP method and proposes an XT-aware-based heuristic algorithm.
S. Fujii et al.[71]	√				Proposes on-demand RCSA algorithm which constructs virtual grid for SDM-EON.
M. Yaghubi-Namaad et al.[88]	√				Formulates the RMSCA problem as an ILP path-based. Proposes a stepwise greedy algorithm and four different sorting policies to find near-optimal solution to RMSCA problem
E. Moghaddam et al.[69]		√	√		Models the RMSCA problem and XT in an SDM with Advance Reservation and Immediate Reservation traffic. The problem is formulated as a MILP and a heuristic is proposed to solve it.
F. Tang et al.[89]		√	√		Develops an ILP model to solve the RSCTA problem, with an auxiliary graph heuristic algorithm.

Table (3.2) Classification of dynamic XT-aware RMSCA proposals found on literature.

Reference	Core Continuity		Protection	Contributions Highlights
	Yes	No		
S. Fujii et al.[35]		√		Proposes RCSA algorithm which uses core prioritization policy to reduce crosstalk and core classification policy to reduce fragmentation.
Y. Tan et al.[61]		√	√	Investigates dedicated path protection considering XT in SDM-EON. Proposes an XT-aware RCSA provisioning strategy with dedicated path protection.
K. Hashino et al.[73]		√		Proposes an XT-aware RCSA with the concept of "crosstalk prohibited frequency slot" to suppress the crosstalk.
R. Zhu et al.[9]		√		Models the RCSA problem and uses the CASC metric to measure spectrum status. Proposes two XT-aware RMSCA algorithms combined with the CASC metric.
Y. Zhao et al.[86]		√		Proposes an XT-aware cross-core virtual concatenation (CCVC) RMSCA to solve the fragmentation in SDM-EON.
Q. Yao et al.[90]	√			Proposes a crosstalk estimation model with machine learning in Few-mode MCF. Also proposes an XT-aware RSCMA algorithm to resource allocation (core, mode, and spectrum).
Q. Zhu et al.[67]		√		Proposes a service-classified RCSA to improve spectral efficiency in SDM-EON.
K. Hashino et al.[60]		√		Proposes a strict and less computationally RCSA with xt-prohibited slots, to reduce the processing complexity and avoids the XT influence.
K. Walkowiak et al.[91]		√		Proposes an RCSA algorithm based on worst-case crosstalk estimation. The lightpath should attend the XT threshold in a translucent SDM-EON with distance adaptative transmission and signal regeneration.
M. Klinkowski et al.[65]	√			Proposes two XT-aware RSCMA algorithm that consider the worst-case XT and the precise-case XT.
K. Kubota et al.[75]		√		Proposes an RCSA with prohibited frequency slots and node interaction cost to suppress crosstalk at fiber and nodes in SDM-EON.
Y. Lei et al.[74]		√		Proposes a RCSA which evaluates the inter-core crosstlak spectrum crosstalk measurement (IC-SCM) in SDM-EONs.

Both tables present the main characteristics of the RMSCA proposals found in the EON-SDM literature. There is a higher utilization of dynamic traffic scenarios (Tables 3.2 and 3.3), corresponding to 73.08% of the evaluated papers. Dynamic traffic scenarios

Table (3.3) Classification of dynamic XT-unaware RMSCA proposals found on literature.

Reference	Core Continuity		Protection	Contributions Highlights
	Yes	No		
H. Tode et al.[66]		√		Introduces MCF or MMF and proposes a RSCMA which exploits prioritized area concept, and is XT-aware depending if the MCF or MMF supports XT.
H. M. Oliveira et al.[77]		√	√	Proposes an RCSA algorithm to dynamically generate primary and backup paths using a shared backup scheme.
H. M. Oliveira et al.[72]		√	√	Proposes an RCSA algorithm to provide failure-independent path protecting p-cycle with minimum interference.
R. Zhu et al.[81]		√		Designs a metric named "multi-dimensional resource compactness and proposes two RCSA algorithms based on it, with first-fit and random-fit allocation policies.
S. Sugihara et al.[42]		√		Proposes an RMSCA algorithm with prioritized areas to reduce fragmentation and controls the service level of Advance Reservation and Immediate Reservation requests.
H. M. Oliveira et al.[76]		√	√	Introduces an algorithm based on p-cycle to provide failure-independent path protection in elastic optical networks.
K. Walkowiak et al.[23]		√		Proposes an RCSA algorithm for lightpath provisioning in translucent SDM-EON, with signal back-to-back regeneration and modulation conversion.
H. M. Oliveira et al.[92]		√	√	Investigates the problem of dynamic protection against two simultaneous failures in SDM-EON. Proposes a path-protection sharing spectrum and stradding p-cycle FIPP algorithm.
H. M. Oliveira et al.[93]		√	√	Proposes an RMSCA algorithm to generate primary and backup paths using a shared backup scheme in SDM-EON.
S. Fujii et al.[94]		√		Proposes an energy-efficient network system with architecture on demand satisfies (AoD) nodes. Also, proposes an on-demand RCSA algorithm that satisfies the restricted spectrum arrangement required by the AoD nodes.
S. Iyer[80]		√		Proposes an RCSA algorithm for provisioning spatial super channels, which ensures the spectral requirements and reduce of transceivers utilization.
H. M. Oliveira et al.[95]		√	√	Proposes an RMSCA algorithm for path protection to provide failure-independent path protecting p-cycle.
S. Iyer et al.[96]		√	√	Designs a independent-failure p-cycle RCSA, which provides disjoint protection to primary routes.
S. Trindade et al.[50]		√		Proposes two RMSCA proactive algorithms to avoid spectral fragmentation. The algorithms consider the spectral fragmentation state and potential bottleneck formation.
Q. Yao et al.[70]		√		Proposes an RCSA strategy based on transfer learning in SDM-EON, considering a scenario with Advance Reservation and Immediate Reservation.
H. Oliveira et al.[79]		√	√	Proposes an RCSA algorithm that employs minimum interference routing, FIPP p-cycle, traffic grooming, and spectrum overlap to increase spectral efficiency in protected SDM-EON.
H. Oliveira et al.[78]	√		√	Proposes an RCSA protection algorithm using hybrid routing and FIPP p-cycle. The algorithm prioritizes the use of single path routing and multipath if no single path is available.
P. Lechowicz et al. [51]	√	√		Evaluates several fragmentation metrics in SDM-EON. Proposes a fragmentation-aware RCSA algorithm that uses information about fragmentation metrics.

are more similar to real scenarios, in which information about future circuit requests, such as duration, required bandwidth, and source and destination nodes are unknown. In addition, most of the papers do not consider the core continuity constraint (84.46%). If the core continuity is considered, a circuit must use the same core for all the links in its route. Therefore, removing the core continuity constraint implies the relaxation of the slot continuity constraint once it is possible to maintain the same allocated slot range through the whole route and switch between cores in different links. Authors in [51] perform comparisons around scenarios with and without core continuity.

The XT-aware RMSCA proposals are also evaluated. These algorithms use information about crosstalk measurement to choose the best spectral resources for new circuit requests. Around 30.77% of RMSCA proposals are XT-aware. Lastly, 26.92% of the RMSCA proposals found are adapted to protection scenarios.

3.2 Measuring crosstalk

Two groups can be created to classify the SDM-EON papers in literature based on the number of neighbors accounted for the XT measurement. The first group uses a fixed value as the number of neighbors, which is $n = 3$ to peripheral cores and $n = 6$ to central core [16], in scenarios with 7-core fibers. Some papers classify it as a worst-case crosstalk estimation [91]. The second group uses a dynamic number of neighbors and counts only those with active circuits in the same slot index of the evaluated circuit [66]. This case is defined as a precise XT estimation [65]. Fig. 2.10 can be cited as an example, in which the circuit allocated in slots 8 and 9 of core 2 has $n = 1$ because it has one active neighbor (slots 7 and 8 in core 3).

Besides the problem of using static or dynamic n values, we also highlight another concern around the crosstalk effect. In some papers, when establishing a new circuit, the crosstalk validation is also performed on active circuits of neighboring cores [9]. This recurrent evaluation must occur in scenarios with dynamic traffic, in which the number of active circuits in the neighboring cores varies. Scenarios with a static XT evaluation already use the maximum neighbor capacity (3 to peripheral cores and 6 to the central core) and do not require reassessment. Table 3.4 presents the classification of papers related to SDM-EON literature considering the crosstalk calculation.

According to Table 3.4, most papers consider scenarios with *static n* or *without crosstalk*. Using scenarios without crosstalk is most appropriate for cases where the applied MCF is a bundle of SCF, and crosstalk has no impact between cores [41]. Nevertheless, the crosstalk verification is recommended in multi-core fiber scenarios since it is the most significant interference [9]. Using the highest possible value as a static number of neighbors (3 for peripheral cores and 6 for the central core) simplifies the crosstalk evaluation since there is no need to reassess the number of neighbors on new circuit establishments.

Some papers consider a *dynamic number of neighbors*, in which crosstalk occurs only in slots with active neighboring cores on the same slot index. These papers can be divided into two groups: one with crosstalk reassessment of previously established circuits (when their n values are changed), and the other group without this reassessment. We emphasize that the use of *dynamic n* implies a slightly complex evaluation since the crosstalk of many circuits will be calculated multiple times.

It is also possible to consider other physical layer interferences besides XT. In [102], the authors call *3D* the EON that use the three domains: temporal, spectral and spatial. The authors propose two physical impairment-aware algorithms (*Fragmentation-Aware Routing, Spectrum, Spatial Mode and Modulation Format Assignment* (FA-RSSMA) and *Fragmentation-Aware Routing, Spectrum, Spatial Mode and Modulation Format Assign-*

Table (3.4) Classification of crosstalk on evaluated papers.

Static N	Dynamic N without Neighbors XT	Dynamic N with Neighbors XT	Without XT	Without Classification
Yuanlong Tan et al. [61]	K. Hashino et al. [73]	R. Zhu et al. [9]	Richardson et al. [5]	H Tode et al. [66]
Y. Zhao and J. Zhang [86]		H. Tode et al. [66]	H. M. Oliveira et al. [77]	K. Takenaga et al. [34]
A. Muhammad et al. [16]		G. Savva et al. [36]	H. M. Oliveira et al. [72]	K. Imamura et al. [97]
L. Zhang et al. [68]		K. Hashino et al. [60]	R. Zhu et al. [81]	K. Imamura et al. [98]
A. Muhammad et al. [40]		M. KlinKowski et al. [65]	S. Sugihara et al. [42]	Y. Cao et al. [99]
M. Yang et al. [87]		F. Tang et al [89]	H. M. Oliveira et al. [76]	J. Zhu et al. [100]
D. Kumar et al. [101]			P. Khodashenas et al. [41]	K. Walkowiak et al. [23]
Y. Zhao et al. [84]			R. Proietti et al. [102]	M. Cantono et al. [103]
H. M. Oliveira et al. [92]			Rui Tian et al. [62]	S. Trindade et al. [50]
Y. Zhao et al. [104]			S. Fujii et al. [71]	K. Kubota et al. [75]
T. Hayashi et al. [17]			H. M. Oliveira et al. [93]	
S. Fujii et al. [35]			D. M. Marom et al. [63]	
Q. Yao et al. [90]			S. Fujii et al [94]	
K. Takenaga et al. [105]			Iyer S. [80]	
T. Hayashi et al. [106]			M. Yaghubi et al. [88]	
G. M. Saridis et al. [31]			H. M. Oliveira et al. [95]	
K. Takenaga et al. [107]			S. Iyer et al. [96]	
M. Klinkowski et al. [108]			Q. Yao et al. [70]	
Q. Zhu et al. [67]			H. Oliveira et al. [79]	
K. Walkowiak et al. [91]			P. Lechowicz et al. [51]	
H. Oliveira et al. [78]				
E. Moghaddam et al. [69]				
Y. Lei et al. [74]				

ment with Congestion Avoidance (FA-RSSMA-CA)), and evaluate performance compared to SP-FF (*Shortest Path* and *First Fit*). The *Quality of Transmission* (QoT) of the signal is also considered.

3.3 Technologies and equipment for core switching

Equipment that allows the circuit switching between different cores along the route enables the SLC [109] and brings significant innovation to the SDM-EON scenario. The use of MCFs, and consequently the expansion of the link transmission capacity, coupled with the greater flexibility of switch between cores, leads to a relaxation of the RMSCA problem constraints. However, a few papers in the literature attempt to propose a system model adapted to the scenario of SDM-EON. A more in-depth analysis is presented in [5], [63], [109]. Fig. 3.2 presents a node model with support for SDM fibers.

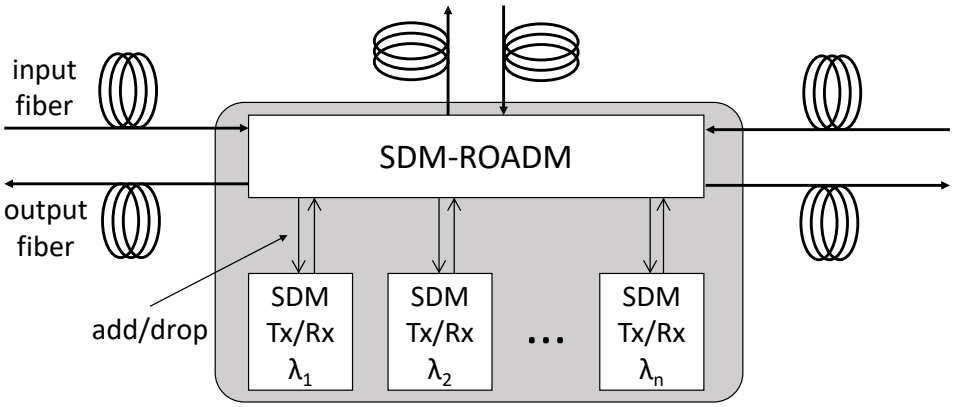

Figure (3.2) Potential architecture of a SDM node, adapted from [5].

Current optical networks have flexibility due to ROADM, which allows the establishment of independent lightpaths within an optical fiber, as well as making it possible to switch them when necessary. It is considered that future SDM-EON will enable this same flexibility. The Fig. 3.2 presents a ROADM adapted to SDM scenario (SDM-ROADM), which performs the circuit switching between fiber cores, besides the add/drop function to transmitters and receivers (Tx and Rx, respectively) [5]. More detailed information around components, equipment cost, power consumption, and transceiver models can be found in [109].

During its propagation, a circuit in an SDM-EON crosses at least two nodes (source and destination). On each node beside the source, the MCF with c cores goes through an SDM demux, which splits the cores into c SCFs to enable switching or circuit drop. In the case of circuit switching, the SCF is conducted to an SDM mux, which couples c input SCF into a single MCF with c cores. The source node performs the same coupling

operation when adding a circuit for transmission. Some equipment can be adapted as SDM mux/demux, such as *photonic-lantern multiplexer* (PLM) [12], which compresses c low capillary SCF to a MCF with c cores [12]. Fig. 3.3 illustrates a PLM.

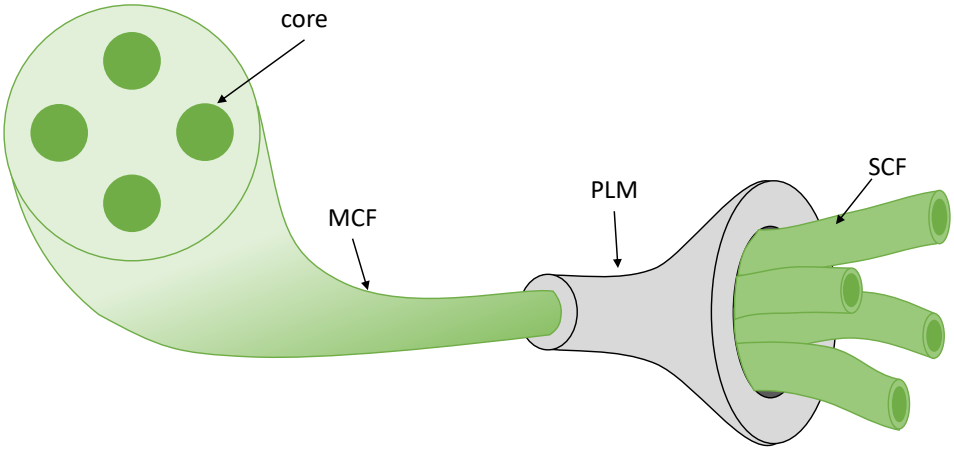

Figure (3.3) Photonic-lantern multiplexer [12].

Based on the observation of papers related to SDM-EON equipment proposals, it is concluded that there is no precise definition of the architecture to be adopted. There are also no detailed studies of financial or energy cost for the proposed architectures, which opens up research opportunities on the topic. Thus, the definition of switching architecture plays an important role in network design, in which the proper switching architecture is chosen according to the services the network provides.

The SDM-EON literature relies on different degrees of flexibility to provide alternative architectures of core switching. When referring to transponder architecture, the most common approach for architecture definition [13], [110], [111], [109] discusses the role of three types of super-channels for data transmission is flexible SDM optical networks: spectral super-channel (*Spec SpCh*), spatial super-channel (*Spa SpCh*), and spectral-spatial super-channel (*Spa & Spec SpCh*).

The *Spec SpCh* [109] is the most common approach for EON, in which several continuous slots compose a channel to serve a single connection with high bandwidth requirements. The high efficiency comes with the flexibility of the channel capacity. The *Spec SpCh* only considers the spectral domain and the resource allocator evaluates each core in an MCF as an independent parallel fiber.

The *Spa SpCh* [109] method extends the *Spec SpCh* to the spatial domain, and the super channel composition encompasses the same frequency range in all the spatial dimensions of an MCF. This approach has two downsides: i) the channels in each core would require a guard band, increasing the amount of wasted spectral resources if compared to the *Spec SpCh*; ii) this approach is not suitable for fibers with possible XT interference.

The *Spa & Spec SpCh* [109] is a hybrid of the previous two approaches. This type of super-channel is a combination of multiple *Spec SpCh* in the same spectral ranges over different spatial dimensions. The allocation flexibility covers both the spectral and the spatial dimensions, in which c x s *SpCh* indicates the number of spatial (cores c) and spectral (amount of slots s) dimensions. Fig. 3.4 illustrates the three scenarios with the different types of super-channels.

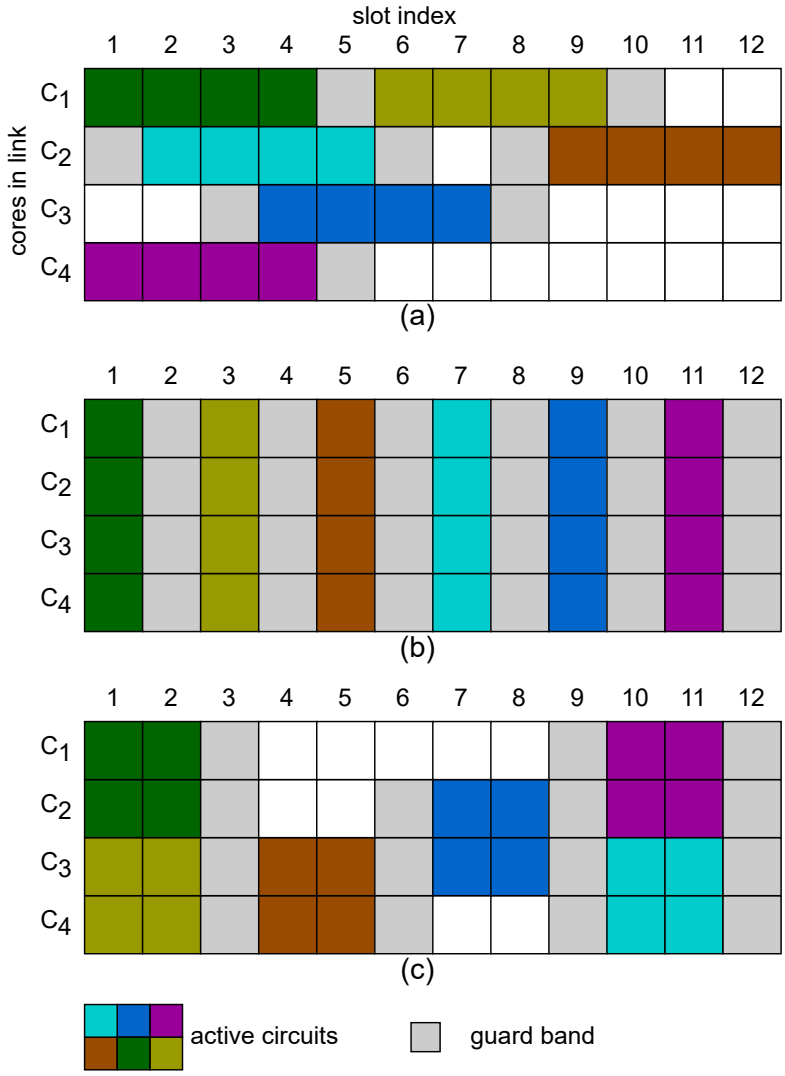

Figure (3.4) Super-channels types in SDM-EON: a) *Spec SpCh*, b) *Spa SpCh*, c) *Spa & Spec SpCh*.

In Fig. 3.4 a), the circuits only occupy the spectral dimension, and each channel allocates in a single spatial dimension. Fig. 3.4 b) presents Spa SpChs, and each circuit allocates a single slot across all the available cores. Finally, Fig. 3.4 c) depicts the hybrid architecture with Spa & Spec SpCh, in which channels with dimension $cxs = 2x2$ occupy the spectrum across multiple slots and cores. A guard band of 1 slot isolates the circuits and reduces interference in all scenarios.

In the whole scope of this thesis, we only consider the creation of Spec SpCh, mainly because of the crosstalk effect. Including the application of other types of super-channels requires more complex fibers in the network composition, such as uncoupled and trench-assisted MCF [112]. The next chapter presents a proposed solution for resource allocation in core-constrained SDM-EON architectures with use of dedicated cores.

3.4 SDM-EON in a nutshell

The use of multi-core fibers guarantees higher resource availability because each core of MCF is equivalent to a single-core fiber of the standard EON. Regarding the papers found in the literature of SDM-EON, Fig. 3.5 presents a characterization of them.

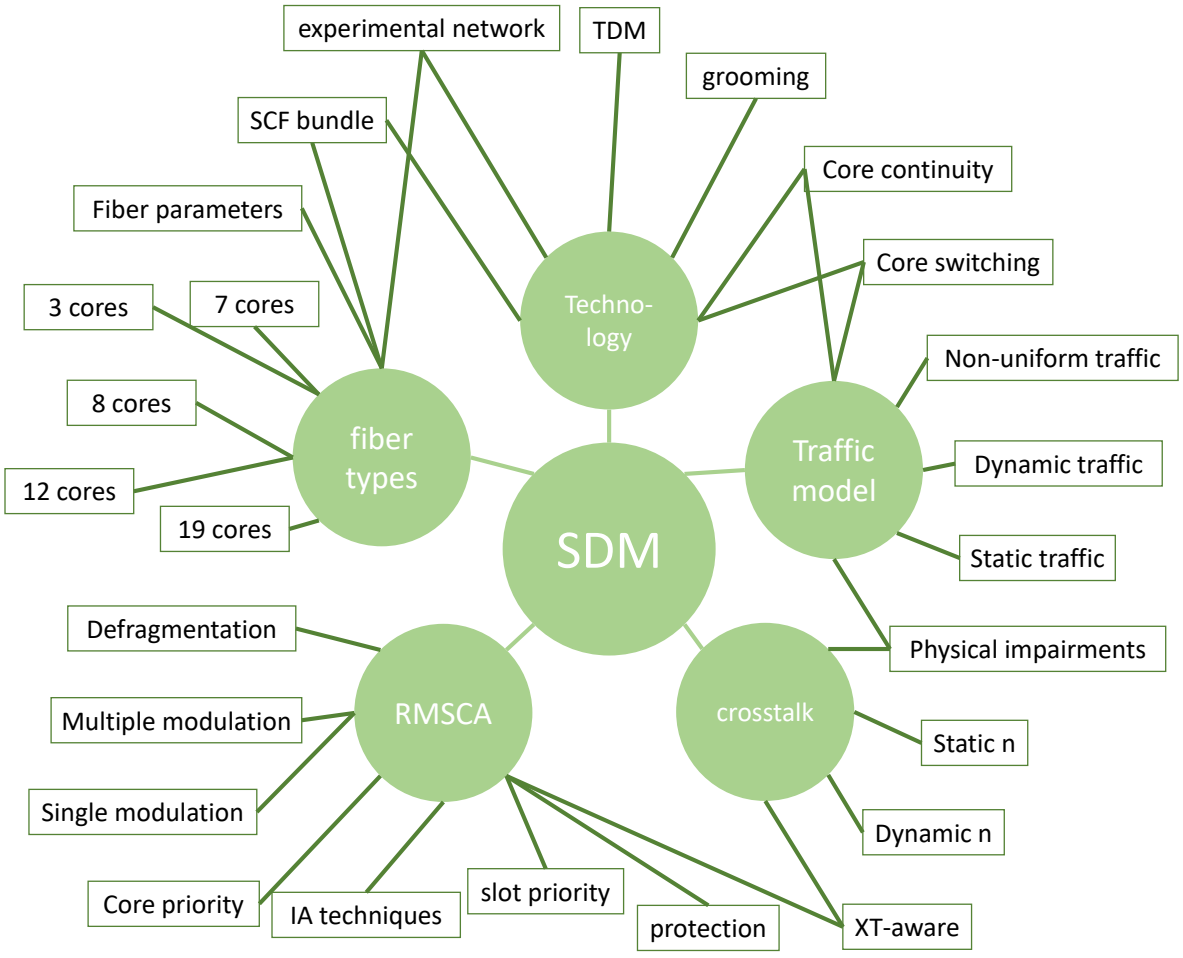

Figure (3.5) SDM related papers classification.

There are a variety of traffic scenarios, equipment, fiber types and RMSCA solutions. Table 3.5 presents the distribution of some references according to the characteristics presented in Fig. 3.5.

This literature collection leads to the conclusion that most of the papers use dynamic traffic configuration. Besides, there are several spectrum and core allocation solution proposals. However, the solutions are compared to classic algorithms, which are not crosstalk-aware. There are no comparisons between the new proposals. Furthermore, the *crosstalk* is a significant problem in the SDM-EON scenario because employing information of the physical layer approximates the model performance to real scenarios of data transmission. Few papers consider survivability (8 papers) and traffic grooming (3 papers).

Table (3.5) SDM related papers classification.

Type (Fig. 3.5)	**References**
TDM	[102] [89]
grooming	[62] [113] [79]
core continuity	[90] [114] [65] [78] [51]
core switching	[9] [77] [41] [72] [86] [63] [104] [88] [89] [51] [23] [67] [96] [50] [60] [70] [91] [79] [75] [69] [74]
non-uniform traffic	[99] [62] [91]
dynamic traffic	[9] [81] [62] [73] [42] [72] [61] [77] [104] [84] [95] [113] [80] [35] [67] [96] [50] [60] [56] [70] [91] [65] [79] [75] [74] [51]
static traffic	[40] [68] [100] [87] [88] [115] [36] [108] [69] [89]
physical impairments	[36]
static n	[9] [16] [61] [86] [101] [87] [92] [104] [84] [113] [35] [90] [31] [106] [56] [91] [65] [69] [74]
dynamic n	[73] [65] [89]
xt-aware	[16] [73] [86] [61] [100] [87] [104] [99] [84] [89] [36] [67] [60] [56] [91] [65] [75] [69] [74]
protection	[61] [77] [92] [93] [95] [113] [79] [78]
slot priority	[66]
ia techniques	[90] [70]
core priority	[71] [67] [50] [69]
single modulation	[62] [68] [86] [92] [104] [99] [84] [90] [70] [79] [78] [75]
multiple modulation	[114] [16] [116] [66] [71] [42] [41] [94] [93] [88] [23] [95] [80] [35] [115] [88] [36] [56] [50] [108] [91] [65] [69] [89] [51]
defragmentation	[85] [83] [84] [82]
19 cores	[116] [73] [104] [98] [35] [88] [31] [36] [89]
12 cores	[116] [101] [100] [104] [35] [88] [65] [51]
8 cores	[42]
7 cores	[9] [114] [16] [116] [81] [28] [66] [62] [71] [73] [72] [86] [61] [34] [77] [55] [100] [94] [87] [92] [104] [93] [97] [84] [113] [35] [90] [88] [31] [89] [106] [107] [67] [96] [50] [60] [56] [70] [91] [65] [79] [75] [69] [74]
3 cores	[40] [100] [87] [96] [65] [69]
fiber parameters	[9] [40] [16] [33] [5] [86] [34] [55] [101] [87] [92] [97] [85] [89] [11] [17] [98] [59] [90] [31] [106] [107] [67] [56] [65] [69] [74]
SCF bundle	[117] [115]
experimental network	[28]

In SDM-EON literature, some scenarios are predominant, such as dynamic configuration for request generation, 7-core fibers, consideration of *crosstalk*, and consideration of multiple modulation format in the signal allocation. There are also many improvement opportunities, such as the comparison between already proposed slot and core allocation techniques, the application of other physical layer effects besides *crosstalk*, and the proposition of impairment-aware allocation algorithms.

3.5 Concluding remarks

In conclusion, the current literature on SDM-EONs highlights several key areas of focus and reveals both advancements and gaps in research. Predominantly, studies have centered on dynamic traffic configurations, the utilization of 7-core fibers, and the incorporation of crosstalk effects in resource allocation. Dynamic traffic scenarios are crucial as they simulate real-world conditions, enhancing the accuracy of network performance evaluations. The focus on 7-core fibers strikes a balance between complexity and capacity, providing a manageable framework for investigating core-switching mechanisms. Additionally, crosstalk consideration is critical for realistic modeling of multi-core fiber networks, where interference between cores can significantly impact performance. The integration of multiple modulation formats further illustrates the ongoing efforts to optimize network capacity and efficiency. Despite these advancements, there is a notable gap in the comparative analysis of different slot and core allocation techniques.

There is a need for more detailed comparisons between existing slot and core allocation methods to identify the most effective strategies. The application of additional physical layer effects beyond crosstalk, such as fiber nonlinearity and signal degradation, could provide a more comprehensive understanding of network impairments. Additionally, the development of impairment-aware allocation algorithms could significantly enhance network performance by accounting for various physical constraints. While some studies have addressed survivability and traffic grooming, these areas remain underexplored, presenting avenues for future research. Addressing these gaps will not only improve the current models but also drive innovation in SDM-EON technology, leading to more efficient and resilient optical networks.

Chapter 4

Crosstalk assessment

XT evaluation is critical in SDM-EONs due to its impact on network performance. The XT affects each modulation format differently since each modulation can tolerate different levels of XT intensity according to its XT threshold. The values for XT thresholds define the acceptable interference levels for the various modulation formats.

This chapter evaluates the equivalent crosstalk thresholds corresponding to the distance thresholds for various modulation formats. The XT measurement for different distance thresholds associated with each modulation helps to define a more precise crosstalk threshold. The study aims to illustrate the significant impact of crosstalk on network performance and the necessity for tailored crosstalk thresholds based on traffic profiles and network configurations.

Following the threshold evaluation, we identify in the literature of MCF two primary methodologies for XT evaluation, which we classify as static and dynamic assessments. The evaluations differ in complexity and accuracy. Static XT evaluation employs a fixed number of interfering neighboring cores, simplifying the modeling process. For instance, in a 7-core fiber, the peripheral cores are assumed to have three neighbors, while the central core has six. This worst-case approach ensures that a network can handle the maximum possible interference, providing a conservative estimate of network performance. However, it may lead to an overestimation of XT in scenarios where not all neighboring cores are actively transmitting, potentially resulting in underutilized network resources and increased circuit blocking. On the other hand, dynamic XT evaluation considers the actual state of the network, accounting for the active neighboring cores that share the same slot index. This method provides a more precise estimation of XT, adapting to the current traffic conditions and active connections.

Dynamic XT evaluation can be further classified into scenarios with or without reassessment of XT on neighboring active circuits. When including reassessment, the XT impact on established circuits is recalculated whenever new connections arrive in the

network, ensuring accurate interference levels. This approach is more accurate but increases computational complexity. Without reassessment, dynamic evaluation simplifies the process but may underestimate XT in highly dynamic networks.

4.1 Calculating crosstalk thresholds

The paper presented in [16] defines different XT thresholds for each modulation level, calculated with an empirical model proposed in [118]. However, it is noted that the distance thresholds found in the literature [44] for modulation levels are overestimated when compared to the crosstalk threshold. In other words, the crosstalk thresholds [16] would cause lower blocking when compared to the scenario in which only the distance threshold [44] is considered equivalent to the physical impairment.

Experiments are used here to estimate the equivalent crosstalk threshold for the distance thresholds of each modulation format in the literature. The goal is to measure the resulting crosstalk for the different distances corresponding to the modulation thresholds. The EON papers found in the literature consider different reach for different modulation levels. For example, the BPSK modulation (with low spectral efficiency) has an optical threshold of 8000 km, while the 64QAM modulation (high efficiency) has a threshold of only 250 km. In this experiment, Eq. 2.6 measures the crosstalk value for each modulation distance threshold, resulting in a more precise crosstalk threshold.

The *Optical Networks Simulator* (ONS) [119] is the tool used to run all the simulations in this thesis. In all scenarios, the independent replication method was employed to generate confidence intervals with 95% confidence level and 10 replications. Connection requests follow a Poisson process with a mean holding time of 600 seconds, according to a negative exponential distribution and uniformly distributed among all node pairs.

The simulations for this current scenario consider 100.000 requests with the following connection request rates: 10, 20, 40, 80, 160 e 200 Gbps, all with the same arrival probability. To do the crosstalk evaluation, the following values are used in Equation 2.6: $k = 4 * 10^{-4}$, $r = 50mm$, $\beta = 4 * 10^6$ e $w_{tr} = 40\mu m$ as defined in [16].

A pair of nodes is considered, with one bidirectional link. We run a sequence of 12 simulation scenarios in which the link length varies from 1,000 to 10,000 km in a step of 1,000 km. Moreover, we add the evaluation of links with 250 km and 500 km since they represent the reach of 64QAM and 32QAM modulations, respectively. The granularity of frequency slots is 12.5 GHz. The fiber is a 7-MCF (Fig. 1.1(a)), with 320 slots in each core. The guard band between two adjacent lightpaths is one slot. The load for all the simulations is 1000 Erlangs because it generates a high blocking rate in this scenario. The purpose of high link congestion is to generate a scenario with intense crosstalk impact. Fig.

4.1 depicts the average crosstalk for the simulations compared to the crosstalk threshold found in the literature.

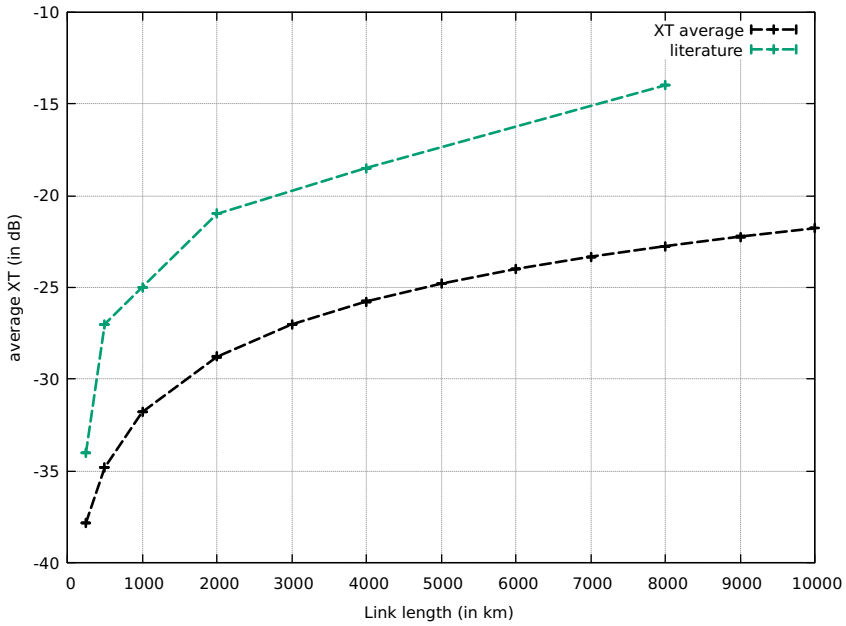

Figure (4.1) Crosstalk variation with increasing of distance.

The evaluation shows that the crosstalk average for each distance threshold is more strict than the XT threshold established in the literature for all the modulation formats. This simple experiment evidences two possible directions: i) the XT threshold must be redesigned for each specific scenario since it has a high dependence on the traffic profile and the network setup and load; ii) The distance threshold associated with the modulation formats requires redimensioning in spatial-multiplexed networks when the XT interferes in the circuit allocation.

Considering the evaluation made in the scenario of Fig. 4.1, XT thresholds were defined for the modulation levels according to their respective distance threshold. Table 4.1 synthesizes the crosstalk thresholds equivalent to the reach of the modulation levels.

Table (4.1) Definition of modulation threshold for the respective distance reach.

Modulation	**Transmission Capacity**	**Distance Reach (km)**	**Crosstalk Threshold**	**Threshold in literature [16]**
BPSK	12.5 Gbps	8000	-22.75	-14.0
QPSK	25 Gbps	4000	-25.76	-18.5
8QAM	37.5 Gbps	2000	-28.77	-21.0
16QAM	50 Gbps	1000	-31.79	-25.0
32QAM	62.5 Gbps	500	-34.80	-27.0
64QAM	75 Gbps	250	-37.81	-34.0

4.2 Defining interference among neighbors

Besides the constants from the physical characteristics of the MCF (such as bending radius and core pitch), two variables must be considered for crosstalk calculation. The distance L, which is obtained by the chosen route length, and the number of neighbors n of the core chosen for allocation.

Another feature contributing to the increase in complexity is the crosstalk evaluation when the number of active neighbors n is zero. In this case, there should be other ways to consider interferences, or there will be no impairments in the established circuit, and any modulation level will be allowed, even those with low reach and high efficiency. To avoid this scenario, we consider the modulation distance threshold to represent other physical layer impairments besides crosstalk.

Experiments were made to evaluate the performance of choosing a static or dynamic number of neighbors. The modulation thresholds presented in Table 4.1 are used. Cases with and without reassessing crosstalk in the active circuits are considered in the dynamic number of neighbors scenario. The simulation scenarios have the same parameters as the evaluation performed in Fig. 4.1. The USA topology (24 nodes and 43 3 links, detailed in Fig. 2.11) is used. The allocation of resources is made by *FirstFit* policy for the choice of core and the choice of slots.

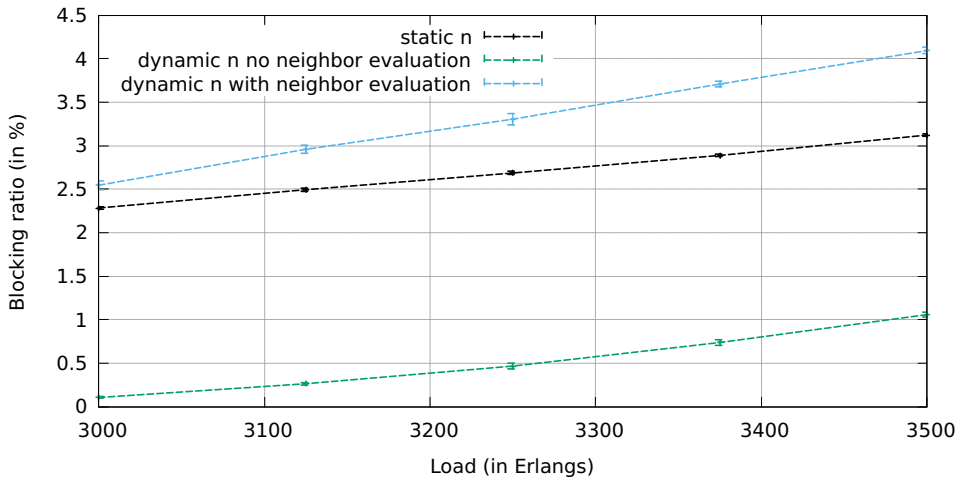

Figure (4.2) Blocking variation with static and dynamic values of n.

For the performance evaluation shown in Fig. 4.2, it is noticed a lower blocking ratio for the scenario with a dynamic number of neighbors without the crosstalk assessment for neighbors. In this scenario, there is a high occurrence of $n = 0$, which results in remarkably low crosstalk and favors the adoption of higher-level modulations for the majority of circuits.

The worst performance occurs for the scenario with a dynamic number of neighbors and crosstalk reassessment for neighbors. As in the previous scenario, the dynamic number of neighbors allows the occurrence of cases where $n = 0$. When the circuits with $n = 0$ are established, higher-level modulations are applied because, at this moment, there is no crosstalk impact. Then, when occurs resource allocation in their neighboring cores, circuits previously established prevent the establishment of new circuits. It occurs because the previously established circuits use higher-level modulation, which has lower crosstalk threshold, and the modification of n (from 0 to 1, for example), would change their crosstalk value to values higher than the threshold allowed by the modulation level.

The choice of the crosstalk model plays an important role in the modeling of the SDM-EON scenario since it causes a variation in the blocking rate results. In the scenario with the dynamic number of neighbors and no crosstalk assessment for neighbors, there is a blocking reduction of 66.09% when compared to the static number of neighbors evaluation and 74.13% when compared to the dynamic number of neighbors evaluation with crosstalk reassessment for active circuits. It is important to emphasize that the evaluation performed here can present different behavior, depending on the scenario settings: generated bandwidth, topology structure, traffic profile, and others.

An evaluation of the crosstalk model is also made in [65], in which the authors define variations of the crosstalk calculation model, defining the worst case (static number of neighbors) and the precise calculation case (dynamic number of neighbors), evaluated in fibers of 3, 7 and 12 cores. The authors propose and compare solutions to the resource allocation problem, based on variations of the First Fit policy (which may be per core or slot index), and compare different models of calculating crosstalk (worst case or precise calculation). The results indicate that 12-core fiber is less likely to block circuits using the crosstalk precise calculation model. Overall, the choice between static and dynamic XT evaluation significantly influences network design and performance, with dynamic evaluation offering the potential for higher efficiency and lower blocking rates at the cost of increased complexity.

4.3 Concluding remarks

In summary, this chapter underscores the role of XT evaluation in the performance of SDM-EONs. By analyzing the crosstalk thresholds corresponding to various modulation formats and their distance thresholds, we highlight the significant impact of crosstalk on network efficiency and the necessity for tailored XT thresholds. The comparison between static and dynamic XT evaluation methods reveals a trade-off between complexity and accuracy. Static XT evaluation simplifies modeling by assuming a fixed number of

neighboring cores, thus ensuring a conservative estimate of network performance but potentially leading to underutilization of resources. In contrast, dynamic XT evaluation, which accounts for the active state of neighboring cores, provides a more accurate estimation of crosstalk but introduces increased computational complexity. This precision can be further enhanced by including or excluding reassessment of XT on active circuits, each affecting the blocking rate and overall performance.

Our experiments, conducted with a variety of modulation formats and distance thresholds, reveal that the crosstalk thresholds established in the literature may not always align with empirical data. The results indicate that the XT thresholds should be recalibrated for specific scenarios to accurately reflect the impact of crosstalk in spatially multiplexed networks. Additionally, our evaluation of static versus dynamic crosstalk models demonstrates that dynamic evaluation, particularly without reassessing crosstalk for neighbors, can significantly reduce blocking rates compared to static methods. However, this approach may lead to complications when neighboring cores become active, affecting previously established circuits. The choice of crosstalk model and evaluation method profoundly influences network design and performance, suggesting that an approach tailored to the specific network setup and traffic profile is essential for optimizing SDM-EON efficiency.

Chapter 5

Core-constrained SDM-EON

As demonstrated in the previous chapters, there are multiple architectures for implementing SDM technologies. The key components to determine which technology suits best are the traffic profile and the equipment/budget availability. This decision strongly impacts the flexibility of resource allocation and utilization.

A reduced switching capacity results in lower routing flexibility but reduces the equipment cost and the power consumption [26]. The core-constrained architectures are more suitable for scenarios with a limited budget or high concern regarding environmental footprint. This architecture requires the least number of ports on the SSS equipment inside the ROADMs, which reduces complexity and power consumption. Considering the high sustainability foreseen for future network generations, the core-constrained solutions are relevant as resource-saving solutions.

5.1 Allocation with Strengthened Medium Core

This chapter presents the *Allocation with Strengthened Medium Core* (ASMC) algorithm as a solution to the RMSCA problem in a core-constrained architecture. The ASMC allocates robust circuits in the central core subject to greater impact of crosstalk. In addition, the other circuits are allocated in the peripheral cores according to parity (odd or even), resulting in a greater spectral organization. The ASMC is compared with other RMSCA solutions found in the literature and shows a reduction in blockage of at least 43.64%.

The central idea of the algorithm is to allocate circuits with less spectral efficiency (defined by the more resistant modulation level) in the central core. These types of circuits use more robust modulations and have higher XT thresholds, which makes them more tolerant to XT interferences [16]. The other types of circuits are allocated in the peripheral cores and separated in odd and even according to the respective amount of

slots in an attempt to reduce fragmentation. Fig. 5.1 shows the ASMC flowchart. The information

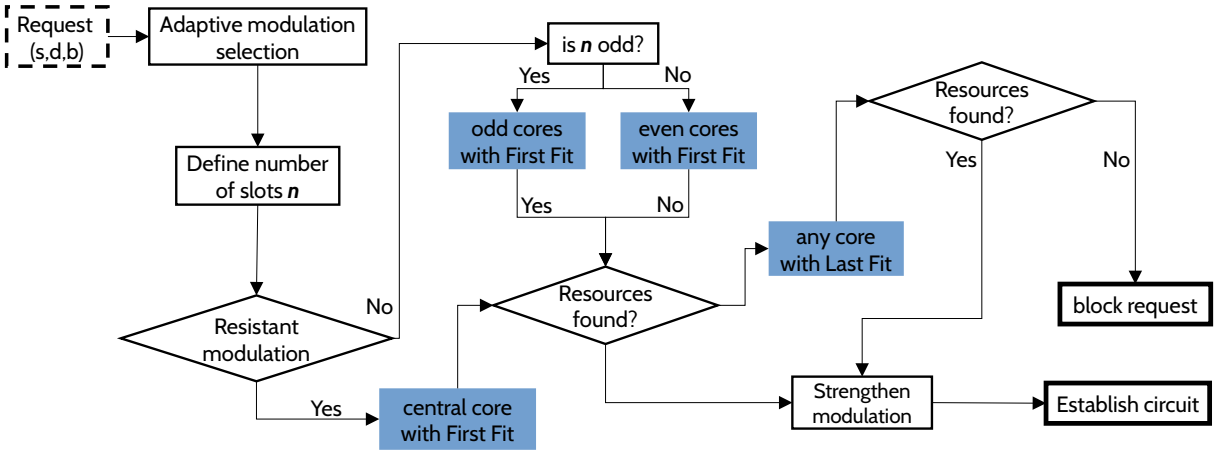

Figure (5.1) Flowchat of ASMC algorithm.

In the routing phase, ASMC uses the Dijkstra algorithm. The most spectral-efficient modulation that respects the crosstalk threshold is chosen by finding the shortest route. The threshold is calculated according to the Equation 2.6.

For core selection, the adopted modulation level is the first point to consider. The ASMC presents dedicated cores, which are exclusive for allocating specific circuit types. Thus, lower-level modulations, which have lower XT_{TH} (BPSK and QPSK, in this scenario), are allocated in the central core. This aims to maintain the circuits with higher resilience to the crosstalk effects in the central core.

If the circuit modulation is more complex than the BPSK and QPSK, the core is chosen based on the number of slots in the circuit. Circuits with an even number of slots are allocated in even index cores, and those with odd numbers of slots are allocated in odd index cores. Considering the selection of odd and even cores, the core and slot allocation is done by *First Fit* (FF) policy. Finally, if a circuit can not be allocated on the medium core or one of the priority cores, the last allocation attempt is made with the *Last Fit* (LF) policy in the highest available slot index considering all fiber cores. If none of the above requirements is met, the circuit is blocked.

Through the flowchart, the following allocation sequence can be observed: central core with FF (BPSK or QPSK modulation circuits only), peripheral cores through FF, in which odd and even circuits are separated, and finally LF allocation in the slot with highest index among all cores.

If the algorithm finds adequate spectral resources, there is still a final step: the attempt to strengthen the chosen modulation [120]. At the beginning of the circuit establishment process, the chosen modulation is as efficient as possible for the route length. However, in some cases, applying different modulation levels implies the same amount of slots for a

given bandwidth. As an example, 50 Gbps bandwidth circuits require two slots for QPSK (around 25 Gbps per slot) or 8QAM (around 35.7 Gbps per slot) modulation levels, and 10 Gbps bandwidth circuits use only one slot, considering any of the available modulations. With this feature, ASMC attempts to change the modulation previously selected to the most robust format possible without changing the number of slots. That is, the chosen modulation will be the most robust, using the same number of slots of the most efficient and viable modulation for the bandwidth and route considered. Fig. 5.2 illustrates the operation of the ASMC solution.

Fig. 5.2 illustrates how ASMC works in three distinct cases: (a) the allocation of a robust circuit (QPSK) in the central core, (b) the circuit allocation in peripheral cores, and (c) robust circuit allocation (BPSK) in the peripheral core. According to the ASMC operation, more robust circuits (with BPSK or QPSK modulations) should be allocated in the central core using the FF policy for both core and slot definition. In Fig. 5.2 (a), the 3-slot circuit with QPSK modulation should be allocated in core 1 (central core), if it has available slots. In this case, the allocation is feasible and occurs in slot indexes 3 to 5. In Fig. 5.2 (b), an 8QAM modulated circuit with an even number of slots (4 slots) is allocated. For the allocation of this circuit, a viable core must first be selected for allocation through the FF policy, considering only even index cores (cores 2, 4, and 6). Looking at the arrangement of the slots, it is concluded that core four will be selected. Slots must also be chosen according to the FF policy, and slots 5, 6, 7, and 8 will be selected. Next, an 8QAM modulated 3-slot circuit is allocated. Considering that only the odd index cores will be evaluated (cores 3, 5, and 7, except central core 1), the 3-slot circuit will be allocated to core 3 in slots 4, 5, and 6. In Fig. 5.2 (c), a new robust 4-slot circuit (BPSK modulation) will be allocated. Looking at the spectrum, it is noted that there are no slots available for allocation in the central core. Then, according to the ASMC algorithm, circuits that cannot be allocated in their priority area should be allocated according to LF policy at the highest slot index among all cores. The last fit slot indices for cores 1, 2, 3, 4, 5, 6, and 7 are 8, 8, 8, 2, 8, 6, and 8 respectively. The feasible allocation occurs at core five because it has enough free slots.

The ASMC algorithm will be executed $|R|$ times, where $|R|$ represents the number of circuit requests generated on the network. The route search does not present complexity during the operational phase of the network since each pair of nodes $pair(s, d)$ has a fixed route, defined by the Dijkstra algorithm [121] before the operational phase. The algorithm then goes through the $|M|$ modulation list, searching for the appropriate and most efficient modulation for the B bandwidth considering the already defined route. Then, the list of cores (odd or even) C is traversed, and the FF policy is used to search the interval of slots to allocate in slot set S of the chosen core. In the worst case, this

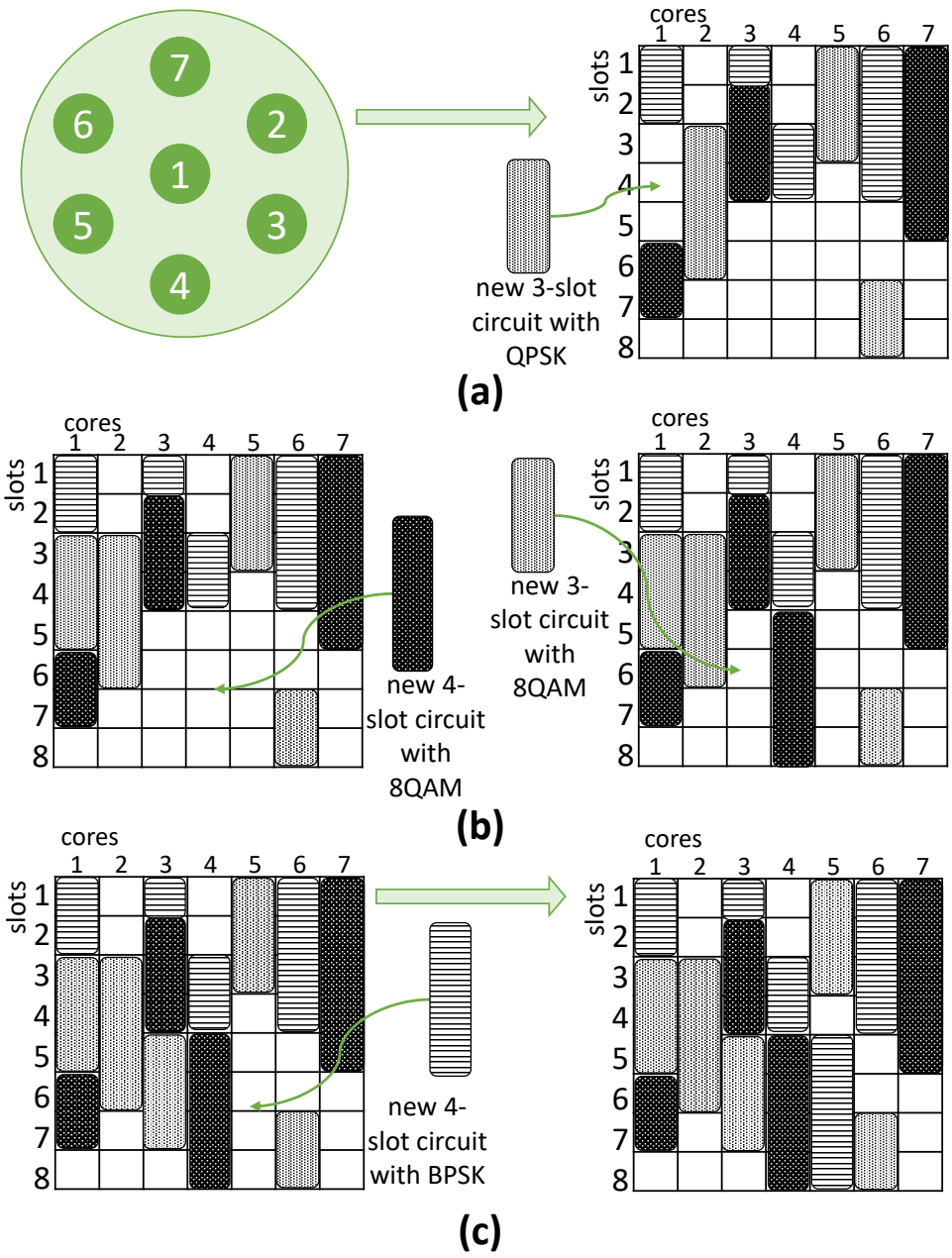

Figure (5.2) Example of ASMC algorithm in three scenarios: (a) allocation of a robust circuit in central core, (b) circuit allocation in peripheral core and (c) robust circuit allocation in peripheral core.

step takes time $O((|C|/2) \cdot |S|)$, where $|C|$ represents the number of fiber cores and $|S|$ represents the number of slots in each core. Suppose the algorithm does not find available resources. In that case, the C core list is traversed again, and the S slot set for each core is traversed through policy LF to find any available interval of slots with the highest index. In the worst case, this step takes time $O(|C| \cdot |S|)$. If resources are found, there is still the attempt of circuit strengthening, which can be executed up to $|M|$ times. The final complexity of the algorithm is given by $O(|M| + (|C|/2 \cdot |S|) + (|C| \cdot |S|) + |M|)$,

Table (5.1) Modulation formats with the respective transmission rate per slot and crosstalk threshold.

Modulation	**Transmission capacity**	**XT Threshold**
BPSK	12.5 Gbps	-22.75 dB
QPSK	25 Gbps	-25.76 dB
8QAM	37.5 Gbps	-28.77 dB
16QAM	50 Gbps	-31.79 dB
32QAM	62.5 Gbps	-34.8 dB
64QAM	75 Gbps	-37.81 dB

which can be represented by $O(|M| + (|C| \cdot |S|))$.

5.2 Performance evaluation

In this evaluation, five replications were used at each loading point. Each replication involved 10^5 requests, all with the same arrival rate. The topology considered in the simulations is the USA with 24 nodes and 43 bidirectional links. Fig. 2.11 shows link distances in kilometers. The granularity of the frequency slot is 12.5 GHz. Each fiber is a 7-MCF, with 320 slots in each core. The guard band between two adjacent lightpaths is assumed to be one slot.

The metrics evaluated are circuit block rate and bandwidth blocking rate. The circuit blocking rate is the relation between the number of blocked circuits and the total number of generated circuits. The bandwidth blocking rate considers the bandwidth information of all circuits. It represents the relation between the sum of bandwidth for the blocked circuits and the sum of bandwidths in all circuits generated.

The simulations are performed in a crosstalk-aware scenario, in which the blocking may occur due to high crosstalk levels for the selected modulations, and different modulation formats are used. The number of active neighboring cores n is dynamic in Equation 2.6, and when a new circuit is about to be established, the crosstalk of already established circuits is checked. The available modulation formats used are presented in Table 5.1 with the respective transmission rate and XT threshold XT_{TH}. The XT evaluation in Equation 2.6 considers the following parameters: $k = 3.16 * 10^{-5}$, $r = 55mm$, $\beta = 4 * 10^6$ and $w_{tr} = 45\mu m$, as defined in [16]. The following connection request rates are 10, 100, and 400 Gbps, all with the same arrival probability.

All compared algorithms use Dijkstra as the routing algorithm [121]. We picked three algorithms for comparison in an attempt to demonstrate the performance of different forms of resource allocation (shown in Fig. 3.1). The first one, called *FF-CASC*, is an adaptation of the FF algorithm. It uses FF allocation policy for slot and core selection.

When it is unfeasible to allocate the FF slot due to interferences, the FF-CASC uses the CASC metric to search for another slot to increase the spectrum compactness. The second algorithm is RF-CASC [9], which consists of the random selection of spectral resources (cores and slots), always respecting spectral continuity and contiguity constraints. The RF-CASC also uses the CASC metric if no slot is allocable in the random selection phase. The third algorithm is the Intra Area [10], which allocates resources according to priority areas of slots. The main idea of this assessment is to show the comparison between algorithms that cause more spectral fragmentation (RF-CASC) with an algorithm that prioritizes the organization of the allocated resources (Intra Area), besides showing the performance of the two techniques compared with a classic algorithm of the literature (FirstFit, used in FF-CASC) that maintains a certain level of organization of resources. The load range is defined to display the blocking variation from 0 to 1% for ASMC. Fig. 5.3 shows the circuit block probability result in USA topology.

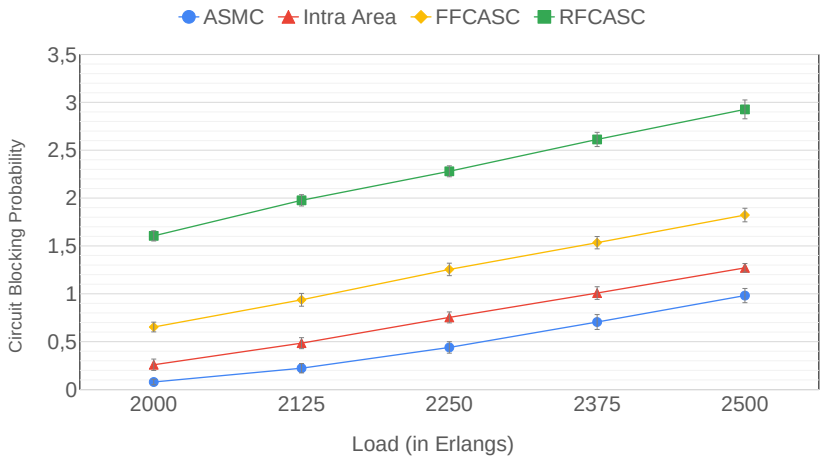

Figure (5.3) Circuit blocking probability on USA topology.

The circuit blocking probability measures the number of circuits blocked in the network concerning the total generated circuits. The spectral organization provided by the ASMC algorithm allows a larger number of circuits to be accommodated in the spectrum, resulting in a lower blocking rate. The Intra Area algorithm performs closer to ASMC because it maintains a particular spectral organization by allocating slots in exclusive ranges. However, Intra Area makes no differentiation for allocating high modulation levels, with high XT_{TH}. The FFCASC, in turn, forces the allocation of all circuits in the first cores without differentiation as to the modulation adopted or the number of slots of the circuits. Thus, when allocating the central core, the new circuit suffers great crosstalk interference since all peripheral cores will already be allocated. Thus, in scenarios with crosstalk interference, the central core has low spectral use in FFCASC, and it causes a

great impact on the blocking rate. Finally, the RFCASC algorithm causes the spreading of the circuits in the spectrum, generating large fragmentation and a high circuit blocking rate. Fig. 5.4 shows the results of bandwidth blocking probability.

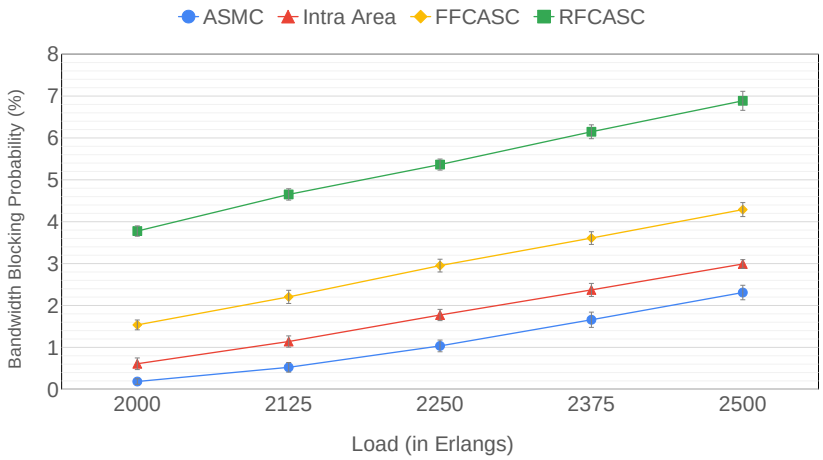

Figure (5.4) Bandwidth blocking probability on USA topology.

The bandwidth blocking probability measures the total bandwidth blocked on the network. When looking at the Fig. 5.3 and 5.4 results, there is a small variation in the behavior of the graph. The ASMC algorithm presents an average reduction of 43.64% in the bandwidth blocking probability compared to the Intra Area, 65.88% compared to FF-CASC, and 80.81% compared to RF-CASC. Therefore, it is observed that the ASMC algorithm can be applied to solve the RMSCA problem, obtaining a good performance in scenarios with crosstalk evaluation.

The studies around SDM-EON have grown in the literature since MCF appear as promising proposals to support the growing data traffic in EON. Using multi-core fibers ensures greater availability of resources as each core is compared to a single-core fiber of the traditional EON. However, the physical proximity of the cores in the fiber causes *crosstalk* more accentuated in the SDM-EON scenarios.

5.3 Concluding remarks

In summary, ASMC algorithm represents a significant advancement in solving the RMSCA problem within core-constrained architectures. By strategically allocating circuits based on modulation robustness and core location, ASMC achieves a notable reduction in both circuit and bandwidth blocking rates. The results from the simulations underscore its efficacy, with ASMC demonstrating up to 80.81% improvement in bandwidth blocking

rate over other algorithms like FF-CASC and RF-CASC, and close performance to the Intra Area algorithm.

This performance improvement is crucial given the increasing complexity of optical networks and the demand for efficient spectrum utilization. ASMC is an approach that not only optimizes resource allocation but also considers the physical constraints and interferences inherent in multi-core fibers, paving the way for more resilient and efficient network designs. Future research could explore further enhancements in RMSCA strategies and their integration into SDM networks, as well as the application of ASMC to larger and more diverse network topologies to fully validate its scalability and robustness.

Chapter 6

SLC-enabled SDM-EON

The ability of core switching (SLC-enabled scenarios) increases the number of solutions for the resource allocation problem and improves its efficiency. SLC-enabled SDM-EON architectures are prone to support more parallel circuits due to their higher spectral organization.

The SLC causes a relaxation of the slot continuity constraint, increasing flexibility (and thus complexity) for resource allocation. However, with connections established and disconnected at high incidence, spectral resources tend to be highly fragmented due to multiple reduced gaps of free slots scattered in the spectrum. The spectral fragmentation problem [122] corresponds to the dispersal of free resources across the spectrum, but in a way that turns its allocation unfeasible for most requests, degrading network performance.

SLC-enabled architectures contribute to reducing spectral fragmentation, yet they cannot eliminate it if there are connection requests of two or more slots. To further mitigate network fragmentation, it is essential to reorganize the allocated circuits when fragmentation levels become sufficiently high to disrupt circuit allocation.

In the scope of the fragmentation problem, spectral defragmentation techniques come into play [49] [123], rearranging existing optical circuits to prevent a new connection from being blocked [124]. Many defragmentation solutions found in the SDM-EON scenario propose circuit interruption in the defragmentation process, which can lead to poor quality of service for traffic requests.

This chapter proposes the application of *push-pull* and *fast-switching* defragmentation techniques, which do not interrupt the active circuits in the network. The techniques are applied in an RMSCA algorithm that executes a spectrum defragmentation mechanism.

We elaborate a defragmentation mechanism that does not interrupt the active circuits through push-pull technique. This defragmentation mechanism is applied to an RMSCA algorithm found in the SDM-EON literature, and the performance is compared to other SDM-EON defragmentation proposals found in the literature. The simulation results show

that the proposed algorithm allows the defragmentation of the spectrum without interrupting the circuits, maintaining a blocking rate similar to defragmentation mechanisms that cause network interruption.

6.1 Fragmentation in SDM-EON

The principal cause of fragmentation in optical networks is the impact of optical constraints, since in a scenario without them, the resource allocation might fill any gap of free slots. The process of establishing and finishing connections, along with optical constraints from the propagation medium, inevitably creates small non-contiguous spectrum fragments, which cannot be allocated and lead to the problem of spectral fragmentation [122]. With the introduction of spatial dimension, the issue of spectrum fragmentation becomes more complex in SDM-EONs, as the crosstalk effect causes intensified spectrum fragmentation in cores.

The resource allocation solution must observe the slot continuity and contiguity constraints mentioned in previous chapters, plus the core continuity if the network scenario uses the core-constrained switching paradigm. As a consequence of these restrictions, the presence of small free slot intervals interferes with the network operation, and it becomes impossible to establish some circuits even if the fiber has enough free slots. This is because these slots will be scattered in the optical spectrum (as in the example of Fig. 2.7), unable to be allocated due to the continuity and contiguity constraints. The fragmentation is an important problem in the optical networks literature [48] [49].

Some defragmentation techniques are proposed by the literature in both SDM-EON and EON scenarios [49] [123]. Many defragmentation solutions found in the SDM-EON scenario propose circuit interruption in the defragmentation process, which can lead to poor quality of service for traffic requests. Thus, the fragmentation problem also becomes an important subject of study in the SDM-EON scenario. Defragmentation techniques can be classified mainly into action time, routing, and traffic interruption [49, 124]:

Action time: The techniques can be classified as reactive or proactive. Reactive mechanisms are invoked when a new request cannot be fulfilled, whereas, in proactive mechanisms, spectrum allocation takes into account a slot arrangement to leave a reserve for future allocations, performing defragmentation periodically or when a certain fragmentation threshold is reached.

Routing: Rerouting approaches reallocate existing optical circuits to the same or different slots by changing their routes to avoid the effects of fragmentation. Non-

rerouting techniques, however, do not allow existing circuits to change their routes, only relocating slots.

Traffic interruption: The techniques can be classified as hitless and non-hitless. Approaches with impact are those that, while maximizing the size of contiguous blocks of unallocated frequency resources, cause traffic disruption and are unsuitable for EONs. Hitless techniques defragment without causing service disruption, or at least minimizing the traffic disruption.

The four main defragmentation techniques are (i) *re-optimization*, (ii) *make-before-break*, (iii) *push-pull* and (iv) *hop-tuning*. The first was proposed in [125], and the idea is applied firstly to *Flexible Wavelength-Division Multiplexing* (FWDM) networks. *The re-optimization* consists of the active circuit shutdown with the subsequent creation of a new circuit for traffic reestablishment. This causes a delay in data transmission, which may impair the *Quality of Service* (QoS). It is classified as proactive, rerouting, and non-hitless. The other three techniques are classified as hitless, and the first of these, known as *make-before-break*, was proposed in [126]. An additional circuit between the same source-destination pair is established while the original circuit is still active. The routes of these two circuits must have disjoint links, and resources are allocated in advance so the traffic can switch between them. After the transmission starts using the new circuit, the previously allocated resources are released.

The last two techniques are the *push-pull* [127] and *hop-tuning* [128]. Both consist of shifting the spectrum of conflicting connections without changing the route. In *push-pull* technique, initially, the number of slots allocated to the circuit is increased while its central frequency slides in the spectrum to a new position. When it reaches the destination, the number of slots decreases to its original size. There is no rerouting, is hitless and proactive. In *hop-tuning* technique, the circuits are suspended and reallocated in available spectrum slots without trying to slide the circuit, as done by *push-pull*. When switching the center frequency of the circuit, the reset time causes the transmission interruption. The interrupt time depends on the transponder tuning speed, which can be less than $400ns$, as shown in [129]. Thus, the *hop-tuning* is non-hitless, proactive, and non-rerouting.

The disadvantage of non-hitless defragmentation techniques is that they cause circuit interruption, which might add undesired latency in data transmission. Thus, for this work, we chose to use a hitless approach. Among the hitless approaches, the hop-tuning technique provides the best performance in terms of spectrum defragmentation efficiency. However, in addition to the high costs of its equipment, there is no technology to perform hop-tuning in networks with fine granularity as the 12.5 GHz, equivalent to an SDM-EON slot [49]. As for the make-before-break technique, its main drawbacks are: (i) sacrificing additional resources and transmitters to be able to perform defragmentation, and (ii)

requires additional optic layer operations to avoid interference on other active circuits. Thus, the push-pull technique is discussed below.

Push-pull and Fast-switching

The push-pull technique enables defragmentation without allocating additional resources and without the need for traffic interruption [127]. Due to these advantages, we evaluate the push-pull technique in an EON-SDM scenario, where defragmentation does not disrupt network activity. Along with the push-pull, the fast-switching [123] technique was also applied to perform high-speed switching and fast reconfiguration without disruption between cores for defragmentation purposes. Fig. 6.1 presents the process of relocating a circuit using both push-pull and fast-switching techniques.

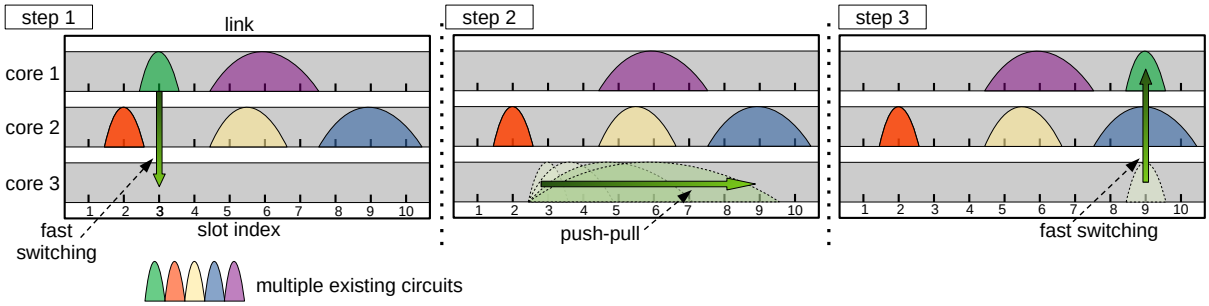

Figure (6.1) Fast switching and push-pull techniques.

The relocation made in Fig. 6.1 is intended to change the slot index of the allocated circuit from slot 3 to slot 9. In *step 1*, it is not possible to perform circuit shifting by push-pull only, as there is an active circuit that prevents the reservation of existing slots between the 3 and 9 indexes in the chosen core. To make the shift possible, fast-switching is done to switch the circuit to a core that contains all free slots between source and destination indexes (from 3 to 9). In *step 2*, push-pull is performed from slot 3 to slot 9. To operate push-pull, the entire interval of slots between the source and destination indexes is allocated. Then, the center frequency of the circuit slides in the spectrum by means of laser frequency tuning, until it reaches the spectral position indicated by the new allocated slot. Finally, slots that are not occupied by the circuit are released after changing the center frequency. In *step 3*, a new core switch is made with *fast-switching*, and at this point, the circuit returns to the source core.

The fragmentation problem and defragmentation techniques have already been discussed and evaluated in EON topologies [49]. However, few studies consider spatial multiplexed EON scenarios. In [83], a defragmentation procedure that enables fast circuit switching and displacement without interruption is proposed and implemented. The au-

thors highlight the type of equipment (integrated dual output intensity modulator (Photline MX-DOIM)) used for switching on multi-core fibers, which can be applied even to high transmission capacity links. The same equipment is also cited in [123].

In [84] is proposed the *Crosstalk-Aware Spectrum Defragmentation* (CASD) algorithm, which is based on *Spectrum Compactness* (SC) metric, used to measure the degree of organization of allocated slots and calculated for each core in the network. This chapter evaluates the application of push-pull and fast-switching defragmentation techniques, which do not interrupt the active circuits in the network, in an RMSCA algorithm that proposes a spectrum defragmentation mechanism. The Equation 6.1 present the SC metric [84]:

$$SC^{c,l} = \frac{s_{max_{e,c}} - s_{min_{e,c}} + 1}{\sum_{i=1}^{P} B_i^{c,e}} \cdot \frac{\sum_{j=1}^{G^{c,e}} g_j^{c,e}}{G^{c,e}} \tag{6.1}$$

In equation 6.1, $s_{max_{e,c}}$ and $s_{min_{e,c}}$ represent the maximum and minimum occupied slot in the core c of link e, respectively, $B_i^{c,e}$ represent the *ith* connection in the core c of link e, $G^{c,e}$ is the number of available spectrum segments in the core c of link e, and $g_j^{c,e}$ denotes the spectrum resources of the *jth* available spectrum segment in the core c of link e. The following section presents the operation of the CASD algorithm, with the adaptation proposed in this paper for the reallocation of circuits without interruptions in the network.

6.2 Push-Pull CASD

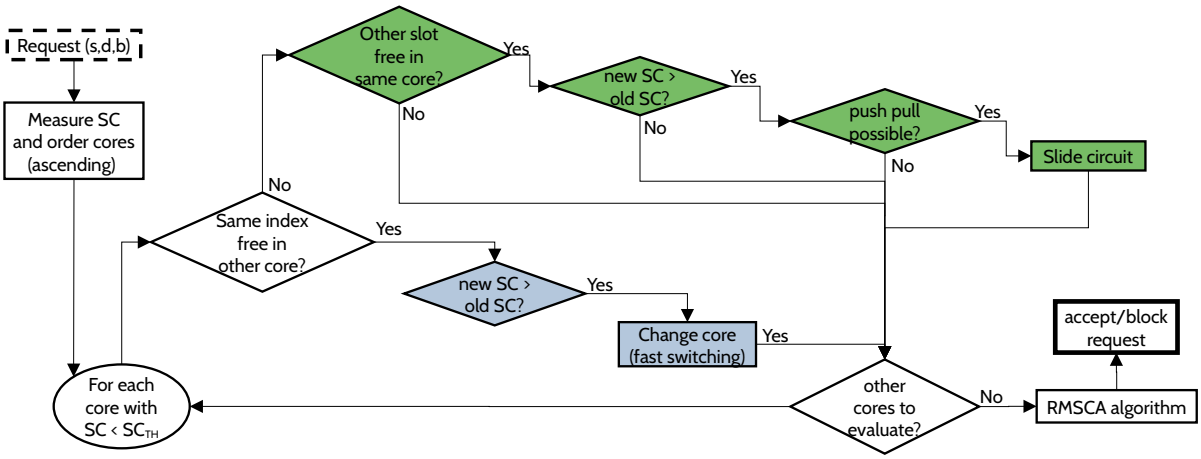

Figure (6.2) CASD algorithm

Fig. 6.2 shows the flowchart of the CASD algorithm. In a dynamic traffic scenario, connection requests arrive one by one, stay for a certain period on the network, and then

depart. Each connection request is represented by $R = \{sr, d, B\}$, where sr is the source node, d is the destination node, and B is the requested bandwidth. The evaluation of the network fragmentation state is always made with the arrival of a new connection request. At this point, the SC of all cores in all links on the network is calculated. All cores in the network are sorted by their SC value, increasingly, and those with SC below a predefined SC threshold (SC_{TH}) will undergo a defragmentation attempt.

The cores that will be defragmented undergo a resource availability assessment. At this time, an attempt is made to relocate all circuits allocated to the core in question. First, whether the circuit established in the core to be defragmented can obtain a higher SC value if relocated to another core of the same fiber at the same slot index is checked. If possible, the circuit reallocation is made and the algorithm goes to evaluate the next circuit. This step is called the *same spectrum different core* (SS-DC), highlighted in Fig. 6.2.

If the other cores in the link cannot support the circuit, the algorithm attempts to relocate the circuit to the same core at a different slot index. This step is called *different spectrum same core* (DS-SC) and is only performed if the slot index was chosen as the target results in SC greater than SC before relocation. The attempt to relocate circuits by SS-DC or DS-SC is performed for all circuits on all cores with SC below SC_{TH}. After the defragmentation phase, the RSA algorithm chosen for the scenario is applied.

In this evaluation, modifications were made to reallocate the CASD solution. In the proposal found in the literature, there is interruption of network operation whenever it is necessary to perform a defragmentation. The adaptation made in this document, called *push-pull CASD*, the reallocation is done through fast-switching and push-pull techniques, only when possible. In this case, network operations are not interrupted, and the defragmentation process becomes less costly.

Throughout the CASD step, the CASD push-pull algorithm operates in the same way as the flowchart presented in 6.2. The difference occurs in the process of reallocating the circuit. To perform the $SS-DC$ step, push-pull CASD looks for free slots with the same indexes of the circuit to be relocated on other cores, just like CASD, but does the core change by fast-switching. At this point, there is no increase in complexity compared to CASD, but there is a change in the way of allocating the circuit, which becomes hitless in push-pull CASD. To perform the $DS - SC$ step, CASD deactivates the circuit at the slot indexes before relocation and turns it on at the slots chosen for reallocation. Push-pull CASD, on the other hand, needs to verify that all slots are free between the slot indexes before relocation and the slot indexes after relocation to be able to push-pull between indexes. If there are occupied slots preventing movement, push-pull CASD checks if the same movement range is free in the other cores of the same fiber for all links

in the allocated circuit route. If the CASD push-pull encounters at least one core with free movement range (which can occur on different cores for each link in the route), it uses the core in question to perform the push-pull. It is important to highlight that the change of cores in the link is made by fast-switching and does not insert interruptions in the network. The core is used only for the push-pull, and then the circuit returns to its source core by fast switching. If at least one allocated circuit link does not have cores with this free slot range for the move, the $DS - SC$ step is not performed for the core in question.

The following section presents the comparison between the CASD proposal found in the literature and the adaptation *push-pull CASD*.

6.3 Performance evaluation

Simulations evaluate the performance of the proposal *Push-Pull CASD* in comparison with the *CASD* and the base algorithm (*Baseline*). All algorithms have the classic allocation scheme based on the shortest path routing, with the First Fit (FF) core and spectrum allocation policy. To provide an upper bound, the *Baseline* algorithm does not perform defragmentation. The *CASD* and *Push-Pull CASD* algorithms attempt to defragment each new demand based on the SC_{TH} values of 1000 and 5000, the best values found in a previous threshold test. The lower the threshold, the fewer defragmentation attempts the algorithm will propose.

Five replications were performed for each loading point. Each replication involved 100.000 requests with ten evenly distributed granularity levels, ranging from 12.5 Gbps to 125 Gbps with steps of 12.5 Gbps. The topologies considered in the simulations were the USA (Fig. 2.11) and the PanEuro topology (Fig. 2.12. The granularity of the frequency slot is 12.5 GHz. Each fiber is a 7-MCF, with 320 slots in each core. The guard band between two adjacent lightpaths is assumed to be two slots. Each node in the topology is equipped with sufficient transmitters and receivers, each capable of transmitting up to 10 slots. We use the threshold of modulation reach and crosstalk as defined in the literature, shown in Table 4.1.

Bandwidth blocking rate

The *Bandwidth Blocking Rate* (BBR) (Figs. 6.3 and 6.4) shows the bandwidth blocking rate on the network. The higher the BBR, the larger the bandwidth blocked on the network and the worse the algorithm performs. The CASD and Push-Pull CASD algorithms show equivalent BBR results at their respective SC thresholds, a variation of less than 1% within the confidence interval for both topologies. It is important to note that both

algorithms work the same way, with the difference that CASD uses the re-optimization technique for defragmentation. The results demonstrate that while the push-pull technique adds a new constraint to the defragmentation problem, as presented previously, the blocking rate shows results similar to re-optimization, which interrupts the network flow.

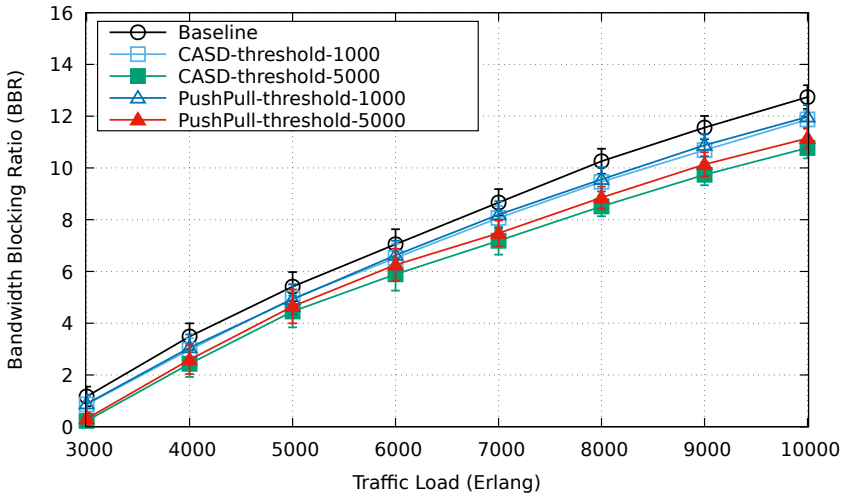

Figure (6.3) Bandwidth Blocking Ratio (BBR) for USANet topology.

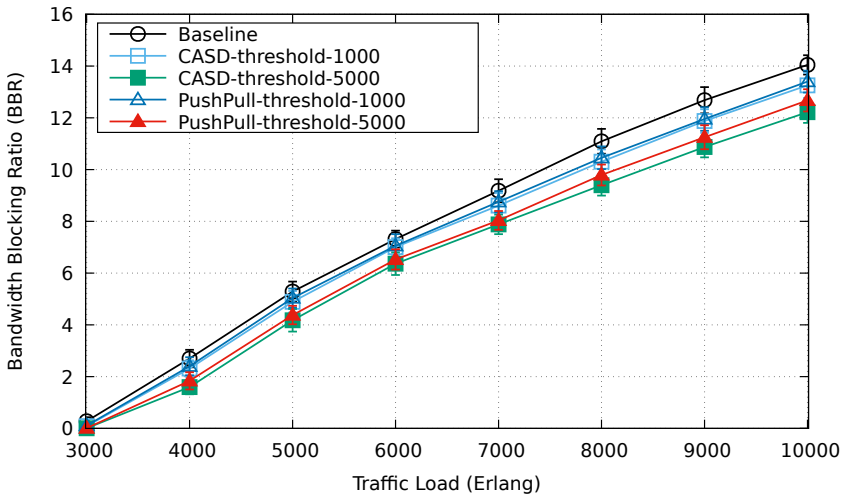

Figure (6.4) Bandwidth Blocking Ratio (BBR) for PanEuro topology.

Spectrum moving times

The metric *spectrum moving times* (SMT) (Figs. 6.5 and 6.6) shows the ratio of the total number of attempts of spectrum reallocation to the total number of successes in the reallocation. This metric is completely related to the SC threshold, so the higher the threshold, the more often the CASD will try to reallocate (defragment) the spectrum. The Baseline algorithm does not perform defragmentation, so it will not appear in the graphics. It can be observed that algorithms with $SC_{TH} = 1000$ have values of 4 orders

of magnitude higher than algorithms with $SC_{TH} = 5000$. This means that algorithms with low SC_{TH} will only propose defragmentation when the spectral fragmentation is high. Therefore, their chance of defragmentation success is much lower, which causes high values in SMT.

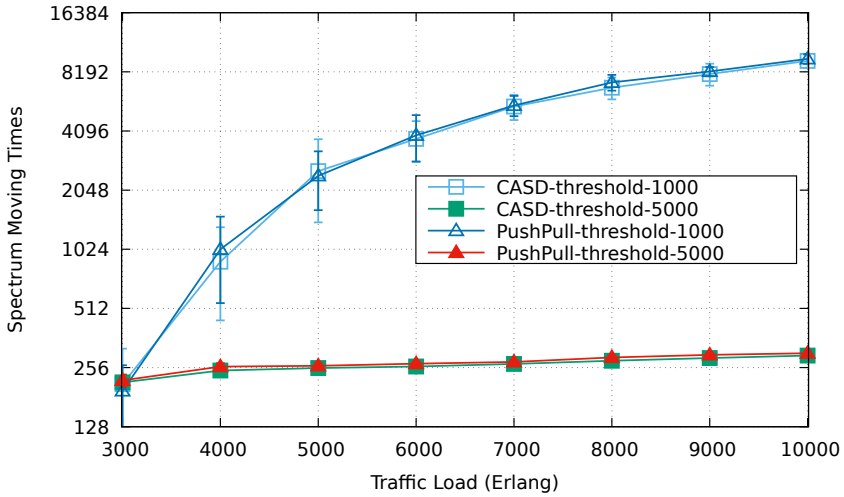

Figure (6.5) Spectrum Moving Times for USANet topology.

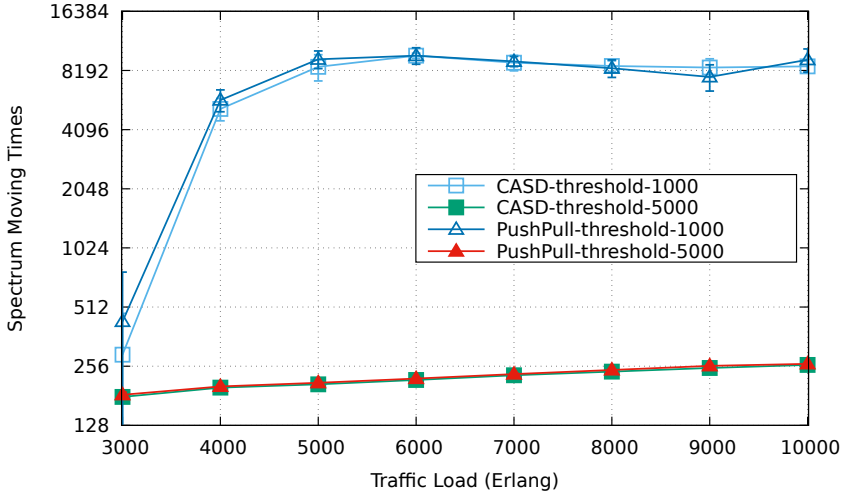

Figure (6.6) Spectrum Moving Times for PanEuro topology.

Spectrum defragmentation latency

The spectrum defragmentation latency (Figs. 6.7 and 6.8) denotes the cost of defragmentation and refers to the average time taken for defragmentation of the spectrum, measured in seconds (s). Spectrum defragmentation latency measurement refers to the circuit deconfiguration time plus its configuration time in another part of the spectrum. The configuration and deconfiguration time (ST) is calculated as the sum of the processing, configuration, and propagation times according to the following Equation [130]:

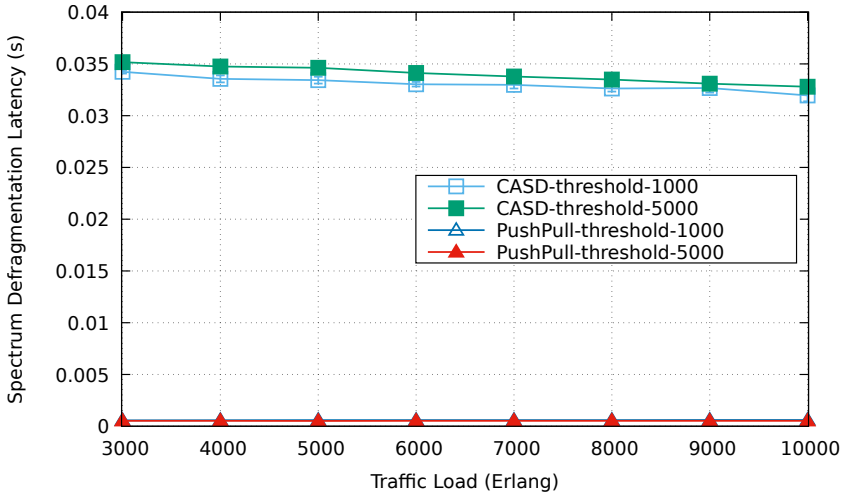

Figure (6.7) Spectrum Defragmentation Latency (s) for USANet topology.

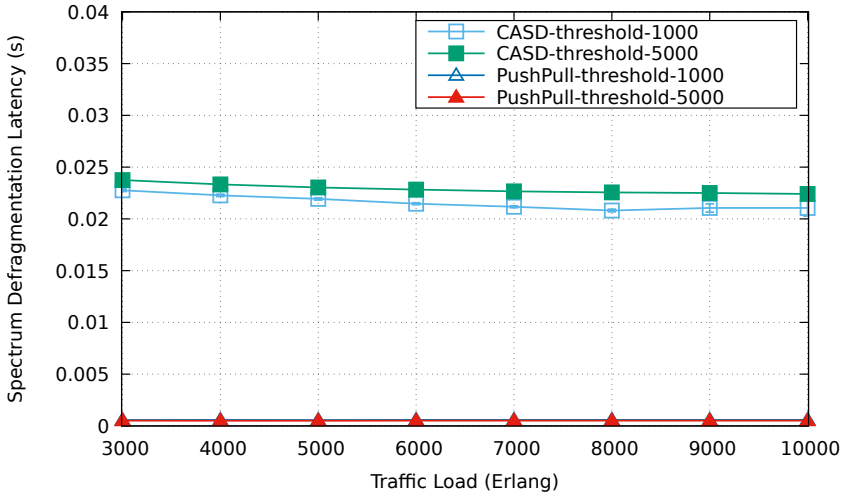

Figure (6.8) Spectrum Defragmentation Latency (s) for PanEuro topology.

$$ST = \underbrace{(hp+1)*D}_{\text{processing delay}} + \underbrace{(hp+1)*O}_{\text{configuration delay}} + \underbrace{\sum_{i \in E} P_i}_{\text{propagation delay}} \tag{6.2}$$

where hp is the number of hops on the route, D is the message processing time, O the *Optical Cross Connect* (OXC) configuration time, and P_i the propagation delay on the i link. For the CASD Push-Pull algorithms, we only calculate the time spent in *fast switching* to be equal to $10\mu s$ [123], since the push-pull operation does not interrupt network traffic. The Baseline algorithm does not perform defragmentation, so it will not appear in the graphics.

Algorithms that implement Push-Pull CASD have a spectrum defragmentation latency of up to 99% lower than CASD algorithms. This is because CASD uses the re-optimization technique for the defragmentation process, while the Push-Pull CASD defragmentation process interrupts the traffic only on *fast switching*. Thus, as presented in [83], the traffic

interruption time is so low that it is considered negligible and easily recovered by *Foward Error Correction* (FEC).

In addition, it is observed that the latency caused by defragmentation to lower SC_{TH} is slightly lower due to the number of possibilities available when the mechanism is activated. For higher thresholds (as $SC_{TH} = 5,000$), spectrum movement possibilities are greater, allowing the defragmentation algorithm to perform more complex movements which cost more time. When the SC_{TH} is lower (as $SC_{TH} = 1,000$), the state of the network is so critical that it allows for small spectrum movements that are faster in turn. The same goes for load growth, where the higher the load, the more difficult the spectrum movement, and therefore, the latency is lower for higher loads.

6.4 Concluding remarks

In this chapter, we examined the issue of spectral fragmentation in SDM-EONs and introduced an innovative approach to spectrum defragmentation. We focused on the application of hitless defragmentation techniques, specifically the push-pull and fast-switching methods, to manage spectral fragmentation without disrupting active network operations. Traditional defragmentation techniques, such as re-optimization, inherently involve interruptions that can degrade network performance and quality of service. Our proposed approach integrates these advanced techniques into a reconfiguration algorithm that aims to minimize or eliminate traffic disruption. Through extensive simulations, we demonstrated that the proposed algorithm achieves performance levels comparable to conventional methods, and offers a robust solution to the fragmentation problem by effectively balancing defragmentation efficiency with operational stability. This balance is crucial for maintaining high-quality service in dynamic network environments where minimizing service disruption is of paramount importance. Overall, the proposed method provides a significant advancement in spectral defragmentation, showcasing that it is possible to address fragmentation challenges in SDM-EONs without sacrificing network performance or service quality. The small differences in blocking rates between the proposed and traditional methods underline the effectiveness of the non-intrusive defragmentation approach. This contribution is particularly valuable for evolving optical networks that demand high levels of flexibility and reliability. The next chapter will explore the sparse core switching paradigm, which promises additional cost savings and performance improvements. By leveraging the insights gained from this study, future research and implementations can focus on optimizing network architectures further, paving the way for more efficient and resilient optical networks.

Chapter 7

Sparse core switching

This chapter proposes a new heuristic approach to core switching, referred to as *sparse core switching* (SCS), to balance the capacity and equipment cost of SSS through the proper distribution of the available equipment budget. With sparse core switching, SSSs only connect ports between specific core pairs. Depending on the number and distribution of these ports, the blocking performance should improve concerning restricted switching. We postulate, however, that a naive sparse-switching solution could lead to a significant deterioration of network performance if we do not consider the inter-dependence between XT and the related aspects of spectrum fragmentation when allocating resources.

The core switching occurs inside the ROADM, which interconnects the different fiber cores and add/drop modules [131]. ROADMs are composed of SSSs, which are connected to the fiber cores and present input/output ports for switching to/from the respective core. The SSS component switches any frequency slot on its input port to any output port and is the most expensive element in the ROADM composition [131], [37]. Changing the number of SSS in a ROADM and the degree of connectivity between different SSS on the same node makes it possible to create different switching architectures in a network.

We propose an initial evaluation to reckon the impact of using high switching capacity nodes in the network. In the following simulations, the goal is to show the impact provided by the crescent utilization of nodes with full-SLC capacity. The simulations are performed initially in a core-constrained scenario (no-SLC). Then, in each following point, the number of full-SLC nodes is increased by 1. The definition of the nodes with full-SLC follows a sequential selection, and new full-switching nodes are added gradually to the set of nodes used in the previous scenario. The evaluation is performed on the USA topology (Fig. 2.11). The following chart presents the BBR, which reflects the amount of bandwidth not allocated in the network. The BBR is the ratio of the total blocked bandwidth to the total generated bandwidth. The x-axis defines the number of employed full-SLC nodes, with a maximum of 24 to USA topology. Fig. 7.1 shows the BBR result.

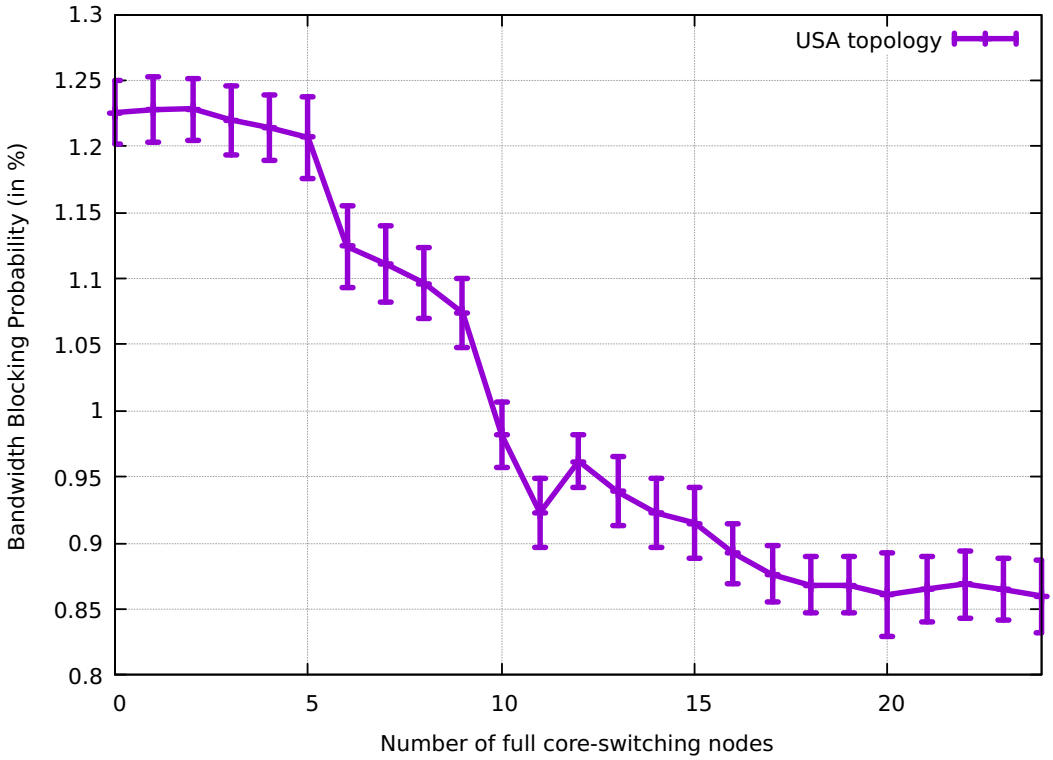

Figure (7.1) BBR by increasing full-core switching nodes.

A general decreasing blocking behavior in Fig. 7.1 confirms that the application of SLC-enabled nodes can improve the network performance. In some points, the blocking reduction is more intense, which shows that the increased SLC capacity may provide more benefits with a specific number of SLC nodes. It is also verified that after node 15, the blocking value starts to stagnate (note the confidence intervals), which indicates that it is unnecessary to enable SLC in all nodes to obtain the best performance.

We emphasize that the sequence of node selection may cause a cascade effect in blocking reduction. The node groups with the highest blocking reduction might not have the same impact without the assignment of previous nodes with full-SLC capacity. It is also noted that adding full-SLC capability to some nodes might cause a small increase in the BBR. Therefore, the relevance of exploring the sparse-SLC allocation problem is clear. Moreover, it is also important to analyze the cost-benefit of using partial-SLC at different nodes.

Enabling the core switching feature is a crucial decision in SDM-EON design. It highly impacts the process of circuit establishment in terms of bandwidth blocking and the RMSCA solution. The non-linear blocking decrease presented in Fig. 7.1 shows that some nodes are key candidates for improving the network performance with minimum effort.

The goal of this chapter is to analyze this effect precisely. To this end, we analyze the

performance of sparse, full, and networks without SLC with crosstalk awareness, given the availability of switching port resources (budget) to perform the sparse distribution. We numerically show that efficient sparse core switching can improve the network performance and even exceed the performance of full core switching with just a fraction of additional ports compared to restricted switching. To the best of our knowledge, this is the first time this approach is used to address the performance of sparse core switching.

The ROADMs are today essential building blocks in elastic optical networks [31], [15]. The idea behind core-switching architectures implemented in ROADMs is to balance the trade-off between ROADM cost, power consumption, and routing flexibility [29]. In any SDM-EON architecture, ROADM is characterized by its SLC capabilities and the number of SSS ports. The latter plays an essential role in the overall cost and complexity of the equipment. Fig. 7.2 illustrates a network scenario with three ROADMs (A, B and C) in a space division multiplexed network interconnected by two MCF a and b. In every ROADM, the input MCF passes through a splitter (fan-out), on which each core becomes a separated SCF. The SCF goes through an ROADM internally, with one SSS piece of equipment dedicated to each core. The SSS has output ports connected to the SSSs on the destination core or to the add/drop module in the node. When crossing an SSS, a circuit is directed to the proper output, as predefined by the resource allocation method implemented in the control plane.

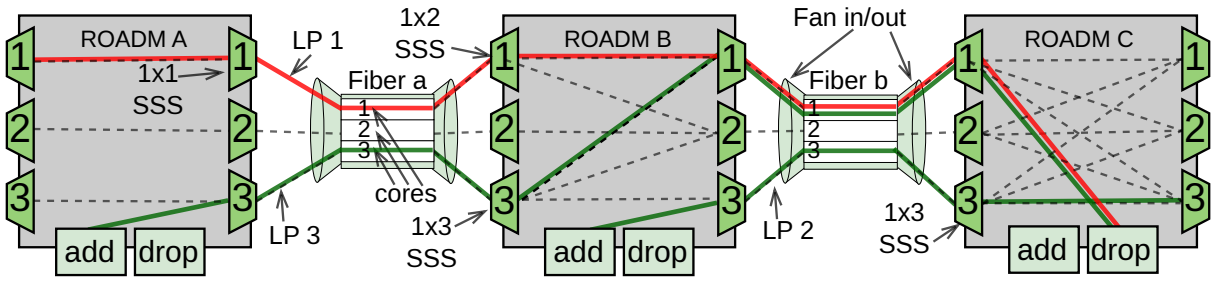

Figure (7.2) Spatial lane change in an SDM network with Spectrum Selective Switches (SSS).

The main difference between ROADMs with and without SLC is in the configuration of ports and the connection between SSS ports. In Fig. 7.2 node A exemplifies a switching architecture *no-SLC*. In such ROADMs, SSSs have port connections only between cores with the same index in addition to an extra port to the add/drop module (not illustrated in Fig. 7.2 for simplicity). Such architecture imposes the core continuity constraint and has a comparably lower implementation cost. ROADM B and C, on the other hand, have an SLC architecture with different degrees of flexibility. ROADM C represents an architecture with *full-SLC*, in which any input core can switch to any output core. However, this configuration requires a high implementation cost.

In Fig. 7.2, there are three established lightpaths: $LP1$ passes through nodes A and B and terminates in node C. $LP2$ initiates in node B and passes through node C. Neither $LP1$ nor $LP2$ perform SLC, and both maintain the respective core index along the path. On the other hand, $LP3$ initiates in node A and core 3, switches to core 1 in node B (thus performing SLC), and terminates in node C. We illustrate the SSS port connection on ROADM B with dashed lines, whereby input core 2 has no SLC capabilities, while cores 1 can change lane to core 2, and core 3 can switch to any output SSS. Thus, ROADM B illustrates what we refer to as *sparse-SLC* allocation. Such ROADM architecture can be applied in variable SSS port setups for network nodes.

According to [131], selective switches are the most expensive elements in the ROADM design. Paper [13] provides an equation to measure the normalized cost for the different architectures according to the number of cores, the node degree, and the switching granularity. For instance, the architectures with the core continuity (referred to here as *no-SLC*) require comparably lower-cost infrastructure, also resulting in less implementation complexity [29].

Besides core continuity constraint (when applicable), when allocating resources over the control plane, we need to consider RMSCA. As a result, two other main optical network constraints are critical to solving the RMSCA problem. The first one is the slot contiguity constraint, meaning that the slots for the same circuit should be adjacent in the spectrum. The second constraint is slot continuity, which requires the maintenance of the selected slot range in all links of the selected route.

When allocating frequency slots (resources) with consideration of the previously described constraints (slot contiguity, slot continuity and core continuity), XT is one of the basic and most critical physical layer impairments to consider in MCF scenarios [57]. The receiver at the destination node cannot receive data from the affected lightpath if the crosstalk power reaches a threshold (also a factor of the modulation format applied).

It should be noted that despite the popularity of the SLC architectures, no solutions so far considered the impact of XT, which is a critical physical effect to multi-core fibers. When core switching is enabled, the control plane can choose algorithms to allocate small free-spectrum fragments on the cores, avoiding fragmentation. In the case of core continuity, however, the fragmentation problem in MCF networks is inevitable. By not considering the impact of XT, spectrum fragmentation can significantly worsen, further increasing the number of unused spectrum blocks. An over-optimization of XT leads to the degradation of the other, as shown in [57].

7.1 Model and algorithms

This section presents a novel algorithmic solution for the sparse core-switching planning problem. Fig. 7.3 illustrates the overall analysis approach and the performance measures used. The overall process consists of test and evaluation phases. In the test phase, upon every circuit request, we apply the cross-talk model to the network resource allocation problem before allocating the circuit. We evaluate the best distribution of SSS ports in the network and rank the order of the cores to place them. This ranking is then used as the basis for performance measurements. In the evaluation phase, we measure blocking and network fragmentation. In both phases, we consider crosstalk.

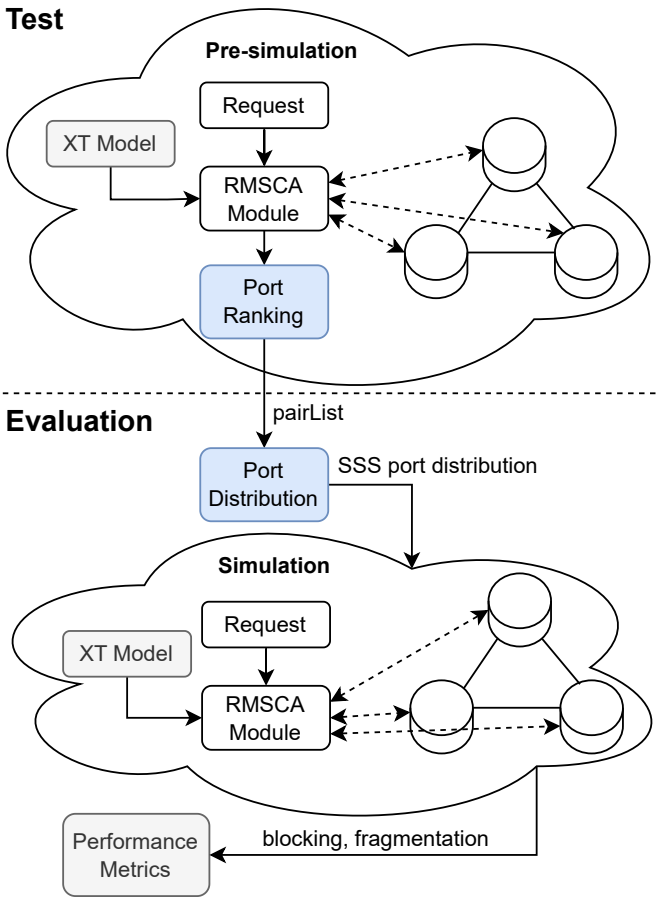

Figure (7.3) Heuristics application on test and evaluation phases.

The crosstalk is measured (based on Eq. 2.6 and Fig. 7.3) whenever a request for a new circuit arrives and based on the RMSCA resource allocation algorithm used. When the selected core and slot allocation exceed the crosstalk value defined, the RMSCA algorithm seeks to find another available slot where crosstalk is within permissible values. Such a process results in spectrum fragmentation, and the fragmentation metrics are obtained

during the evaluation phase (Fig. 7.3) to help analyze the performance of various switching architectures.

Port ranking and distribution algorithms

We now present the algorithms for port ranking and distribution. The SSS port distribution defines a maximum value α to limit the core-switching capacity in a node. α represents the top percentage of core-switching that a given node can have, in relation to the same node with full switching capacity. According to an available budget, the algorithm distributes switching ports between the SSSs. In the distribution, it prioritizes nodes with more simultaneously active circuits. That is why the test phase is necessary to reach the steady state *a priori*.

Algorithm 1 describes the port ranking algorithm executed in the test phase. It is called whenever the control plane enables a new *circuit* in the network through resource allocation algorithms. A loop is used between lines 1 and 7 to traverse nodes on the route of the new circuit. On line 2 is checked whether the current node is the source or destination of the path. As this algorithm aims to evaluate the nodes where there is switching, source and destination nodes are neglected. Lines 3 and 4 retrieve information about the cores allocated by the circuit in incoming and outgoing fiber on *node*. Function *count_active_circuits*() on line 5 checks how many active lightpaths are switching in the same core pair c_s and c_d. The algorithm stores a *node.counter* to keep track of the peak amount of active circuits during the simulation for each pair c_s, c_d in a node. In lines 6 and 7, *node.counter* updates when a new peak is found.

Algorithm 1 *Port_ranking*(*circuit*)

```
1: for node ∈ get_route(circuit) do
2:     if node! = source(circuit) & node! = destin(circuit) then
3:         c_s ← get_input_core(circuit, node)
4:         c_d ← get_output_core(circuit, node)
5:         counter = count_active_circuits(c_s, c_d)
6:         if counter > node.counter(c_s, c_d) then
7:             node.counter(c_s, c_d) ← counter
```

As shown in Fig. 7.3, when the test ends, a list *pairList* is built with all pairs of input and output cores in decreasing order. This list is the input to the second algorithm that distributes port distribution in the evaluation phase. Algorithm 2 presents the SSS port distribution.

The loop in lines 1 to 6 in the pseudo-code 2 iterates over all sorted pairs from *pairList*. In line 3, the function *cost_port_insertion* measures the cost of port insertion to the current *pair*, which includes the expense of output and input ports in the source and

Algorithm 2 *Port_distribution*($pairList, budget, \alpha$)

```
1: for pair ∈ pairList do
2:     node ← get_node(pair)
3:     cost ← cost_port_insertion(pair)
4:     if budget ≥ cost & relative_port_count(node) < α then
5:         connect_ports(pair)
6:         budget ← budget − cost
```

destination core, respectively. In line 4, the following conditions are verified before adding the ports in the SSSs: (i) if the cost of the new ports is lower than the remaining budget and (ii) if the number of ports in the node is lower than the maximum α threshold. If both conditions are verified, on line 5, the new ports are added to the network, and the remaining budget is updated. This process repeats until the *pairList* is empty.

The goal of adopting the α threshold is to avoid the algorithms creating the same architecture as if it were a full-switching one. Thus, no more ports are deployed in a node that reaches the α value, even if a budget is available. This approach saves resources for *pair* with less circuit utilization (lower value of *counter* in Algorithm 2). It also prevents the investment of all the budget in a small fraction of nodes. The proposed heuristic is not proven to be the optimal solution. The Algorithm 1 has complexity $O(C^2)$ and Algorithm 2 has complexity $O(|C| \cdot |L|)^2$, where $|C|$ is the number of cores and $|L|$ is the number of links. Both heuristics are useful in the network planning phase for adding SCS capabilities.

7.2 Performance evaluation

This thesis highlights the economic gain of performing sparse core switching by saving the number of equipment (ports). Two crucial observations are essential in performance evaluation. First, by comparing the sparse core distribution to full-switching, we aim to show the performance gain due to the impact of SCS on both fragmentation and crosstalk. Second, the results will show the harmful effects of a "naive" SCS distribution that can worsen the network performance as compared to the standard (*no-SLC*) scenario.

Based on Fig. 7.3, we run event-driven simulations in the test phase to check and rank order those core ports that are simultaneously used under the tested (hypothetical) network traffic. Considering a *full-SLC* architecture with crosstalk constraints, this is done. The subsequent evaluation considers this port ranking precisely (*pairList*). Moreover, several simulations were carried out to fine-tune the value for α to be used as the capacity limit for port distribution. Fig. 7.4 presents the impact according to variations on α, from 0.1 to 0.9 in a step of 0.2. Other α values were tested, but removed from the Fig. 7.4 to improve visualization. It is important to mention that this evaluation is sensitive

to traffic profile variation and needs a reassessment whenever it changes. This solution also has low tolerance against failures or other events that might change the topology arrangement. These events also require a revaluation of the port distribution.

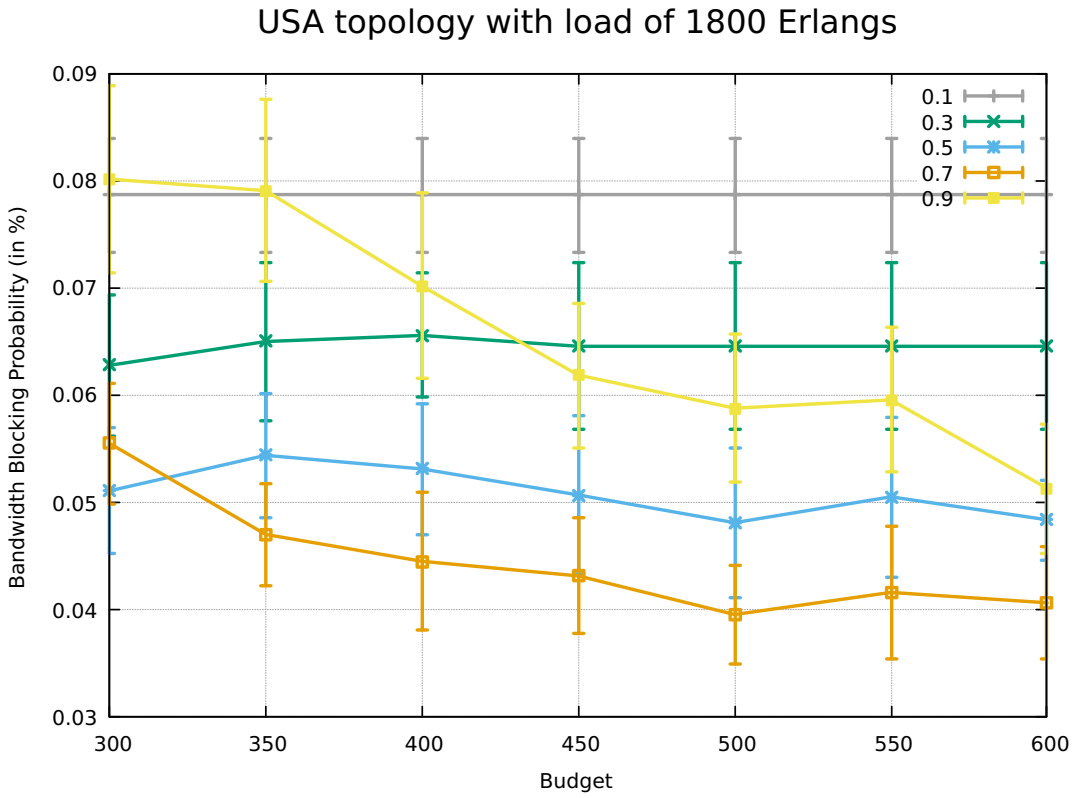

Figure (7.4) Impact of α variation in USA topology.

The results in Fig. 7.4 show that the α value causes a big variation in the network performance. A small α reduces the flexibility and has an impact similar to the no-SLC scenario. On the other hand, a high value of α (e.g. 0.9) brings the behavior close to the full-SLC scenario, which also hurts the network in terms of blocking rate. Finally, the best performance in this scenario was the one with $\alpha = 0.7$, which reaches the lowest blocking rate for higher budget availability. It is possible to perform this evaluation according to any new scenario to find the most suitable α value. Besides that, a more fine-tuning evaluation might find more precise values for α.

Finally, the available budget is evaluated increasingly from \$300 to \$700, with a step of \$50. We emphasize that in this document, the budget accounts only for the expenses beyond the cost of a no-SLC architecture. Furthermore, the SSS unitary cost is proportional to the cost of $1x9$ port SSS, and the \$ sign merely represents a monetary value not associated with real values. Thus, the no-SLC corresponds to the scenario with a

budget equal to 0. The cost is measured exclusively through port availability on the SSSs equipment [13], as described in Table 7.1.

Table (7.1) Relative cost of SSSs with different port counts [13].

Port count	1x5	1x9	1x20	1x40	1x80	1x160	1x320
Cost	\$0.63	\$1	\$1.58	\$2.5	\$3.95	\$6.25	\$9.87

All links in the following simulations are 7-MCF with 320 slots inside each core, on USA topology (2.11) and COST239 (Fig. 2.13)). Each chart point is the average of 10 replications created with the independent replication method, with a confidence level of 95%. Each replication consists of the generation of 10^6 circuit requests. The circuit requests follow a Poisson process with a mean holding time of 600 seconds, according to a negative exponential distribution and uniformly distributed among all node pairs. The generated circuit bandwidth requests vary from 1 to 32 slots (depending on the number of Gb/s requested, distance, and modulation applied) and are uniformly distributed. The guard band between adjacent circuits is one slot. A set of fragmentation metrics is also computed for all the simulation runs.

To solve the RMSCA problem, the K-shortest path algorithm is used for route selection ($K = 4$), and the first-fit policy is applied for both core and slot selection. The definition of modulation format follows adaptive modulation, and the available modulation formats are BPSK, QPSK, 8QAM, 16QAM, 32QAM, and 64QAM, with distances threshold as defined in Table 3.4. The following fiber parameters k, r, β and w_{tr} values applied for crosstalk evaluation are (Eq. 2.6) 4×10^{-4}, $50mm$, 4×10^{-6} and $45\mu m$, respectively. We emphasize that the resource allocation solutions are aware of XT, and all avoid allocation in slots with XT impact beyond the threshold.

Bandwidth blocking probability

To obtain blocking results closer to 1%, the network load was set to 1800 and 8700 Erlangs for the USA and COST239 topologies, respectively. It is essential to notice that the same simulation parameters and RMSCA module must be used for both the test and evaluation phases (Fig. 7.3). While the choice of RMSCA method without a doubt impacts the outcome of the port distribution algorithm, the fact that we use the same one both in the testing and evaluation phases allows us to achieve valid and comparative numerical values for all studied scenarios, including *full-SLC*, *no-SLC*, and *Random* distribution algorithm.

Fig. 7.5 shows BBR for each architecture under an increasing budget scenario. The USA topology with *no-SLC* needs \$1739.08 units of extra budget to become a *full-SLC* network. However, our heuristic reaches the performance of *full-SLC* architecture with significantly less budget, around \$350. Thus, it uses only 20.12% of the budget required

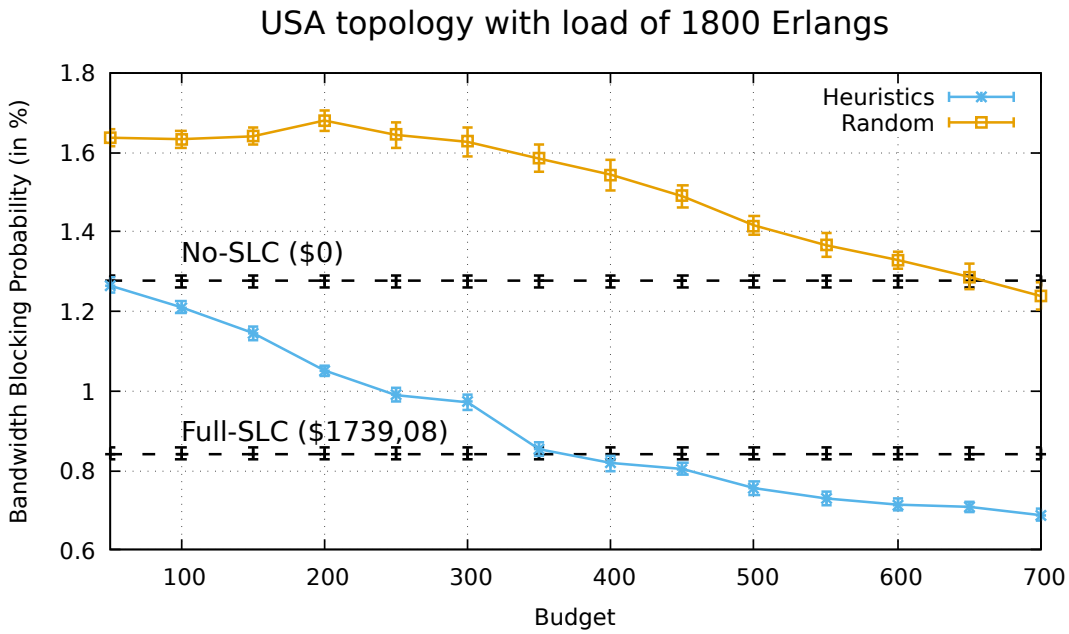

Figure (7.5) Bandwidth Blocking Rate in USA topology.

by *full-SLC* distribution to achieve the same blocking performance. In addition, with a budget above $350, it achieves an even lower BBR compared to all the other scenarios. This performance overlap is due to the high impact of crosstalk, which is more pronounced in *full-SLC*. From these results, it can be seen that a random distribution has a significant impact on BBR. *Random* is inferior to *no-SLC* network for a budget lower than $650. At the same time, the heuristic performs better than *full-SLC*. Thus, the insertion of core-switching ports requires efficient node selection and distribution strategies. By doing so without performing any evaluation (random), the network performance deteriorates by increasing the degree of resource fragmentation.

Fig. 7.6 presents the same analysis for COST239 topology, with budget $1388.59 used to upgrade from *no-SLC* to *full-SLC*. Fig. 7.6 shows that our heuristic performs comparably concerning *full-SLC* with only 14.4% of its budget requirements ($200). In addition, its performance exceeds *full-SLC*, and with an investment of only $400, 28.8% of the *full-SLC* budget, when it reaches a reduction of 31.34% in BBR. The chart also shows the best performance for the heuristic with a budget of $400. After that point, using more budget results in an increased BBR. This behavior is maintained as the investment grows and the SCS architecture approaches *full-SLC*. This result illustrates that adding a higher budget does not necessarily improve network performance. Fig. 7.6 illustrates an inflection in the blocking rate line after $400 budget point. A more flexible core-switching generates a more compact spectral allocation, which escalates the crosstalk impact. We can also observe here that a naive distribution can have adverse effects, see *Random*. In

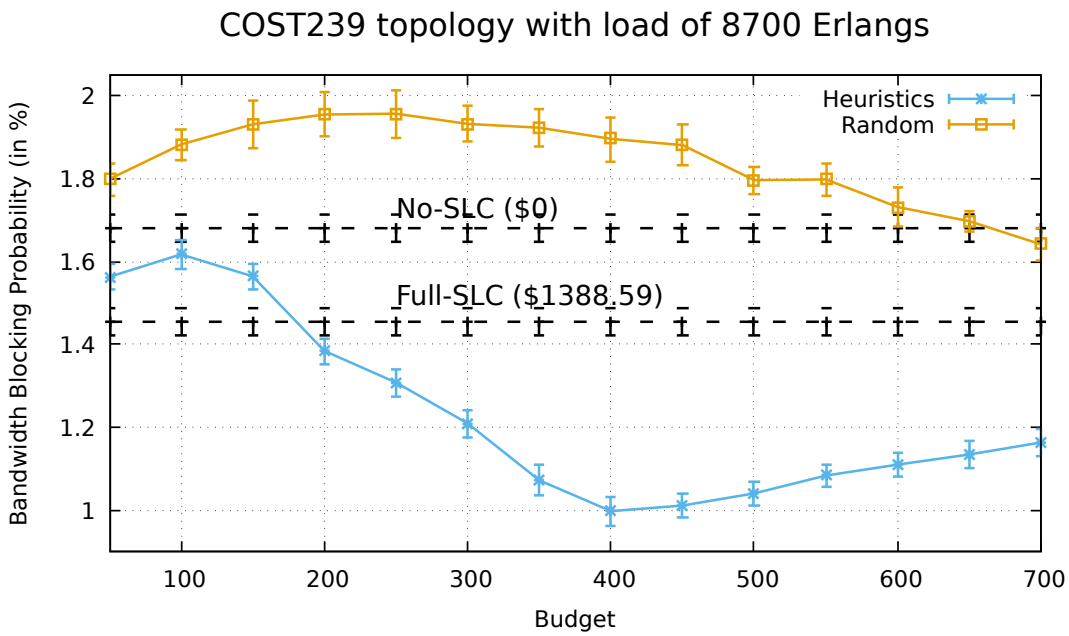

Figure (7.6) Bandwidth blocking probability in the COST239 topology.

Fig. 7.6, for the same investment of $400, *Random* distribution leads to 89.77% in BBR increase as compared to our heuristic.

Fig. 7.7 shows the values of RMSF fragmentation in COST239 topology. It should be noted that in all scenarios evaluated, since the blocking values are higher than zero (Fig. 7.6), the resources are considered busy in the optical spectrum; for $BBR > 0$, at least one circuit is blocked because no free spectrum can be found for it. Therefore, the information regarding the highest allocated slot index does not play a fundamental role in RMSF. In Fig. 7.7, RMSF primarily reflects the number of segments and the occurrence of smaller-sized free slot blocks. *full-SLC* architecture presents higher RMSF fragmentation, with the trend to generating more fragments of smaller granularity. The maximum flexibility of *full-SLC* allows free slot blocks to be allocated until they are reduced to smaller free segments; however, these slots are harder to allocate due to crosstalk. Fig 7.7 shows *No-SLC* architecture with less fragmentation for RMSF. It reflects the presence of larger segments than smaller ones. This is due to the rigid switching capacity, which makes slot allocation more difficult. Our heuristic has a slightly reduced fragmentation than *Random* since it employs core switching ports between cores with more utilization.

Fig. 7.8 shows the entropy fragmentation (measured by Eq. 2.3. The higher entropy shows that *no-SLC* architecture has a more spread spectrum due to the lowest flexibility. On the other hand, *full-SLC* architecture has maximum flexibility, which results in a more compact spectrum. The heuristic and *Random* have increasing flexibility along the x-axis. Since it contributes more to highly utilized nodes, our heuristic generates lower

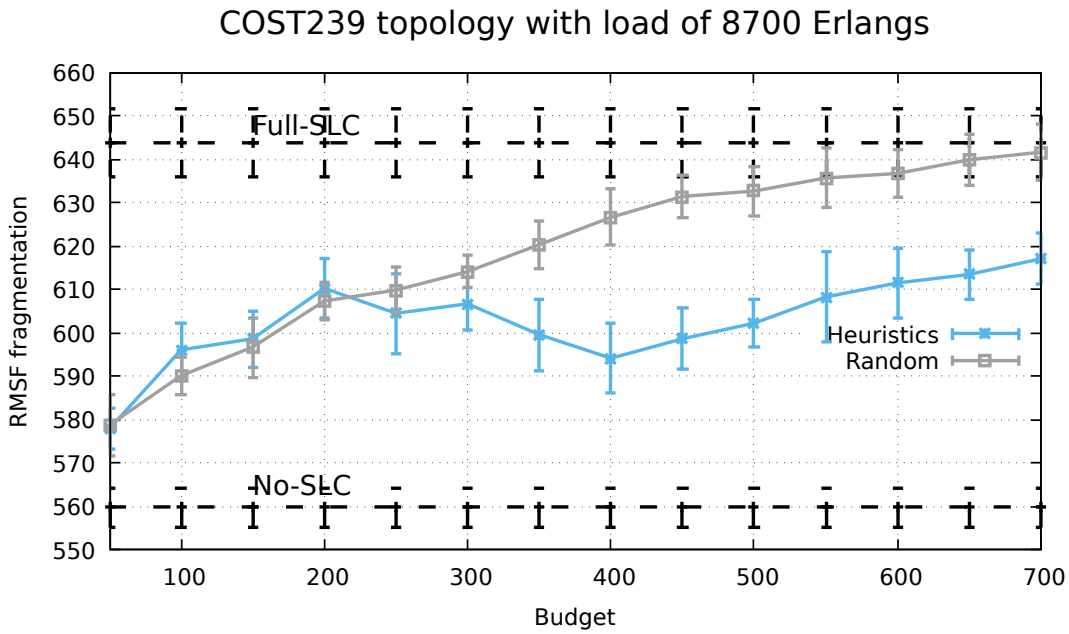

Figure (7.7) RMSF fragmentation in COST239 topology.

spectral fragmentation than *Random*.

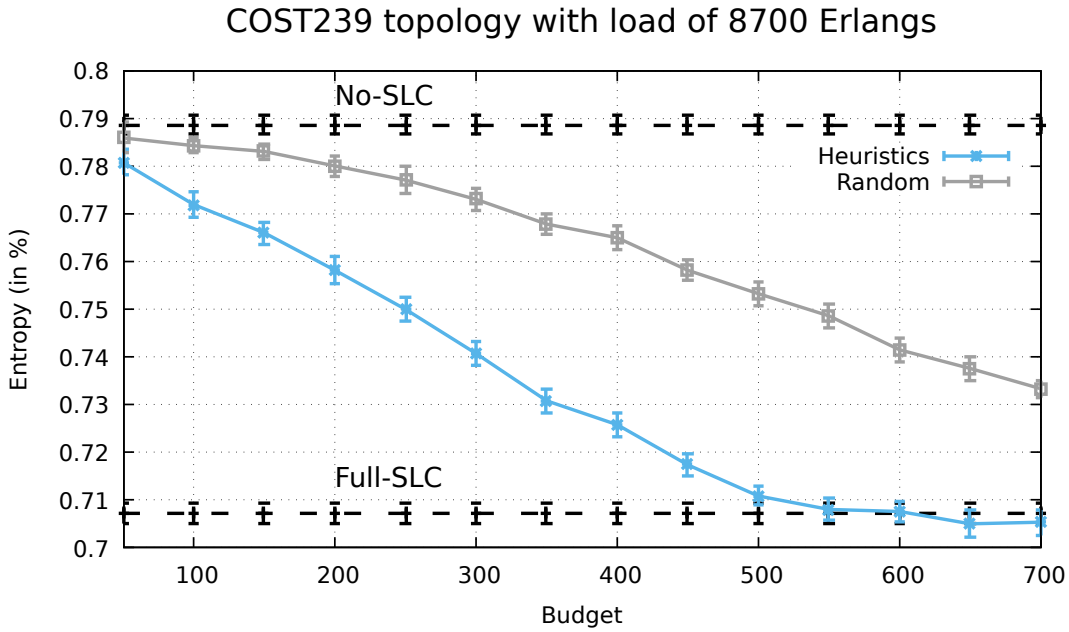

Figure (7.8) Spectral entropy in COST239 topology.

Fig. 7.9 presents the percentage of accepted circuits of a range of bandwidth requests. Since requests with closer bandwidth values can be served with the same number of slots, the performance line has a stepped appearance. In Fig. 7.9, our heuristics accepts more

circuits than others, which increases with an increased bandwidth request. This behavior reflects the ability of our heuristics to hold larger blocks with free slots, which *full-SLC* architecture does not do due to its higher spectrum compression due to switching flexibility and ability to fill smaller spectrum gaps.

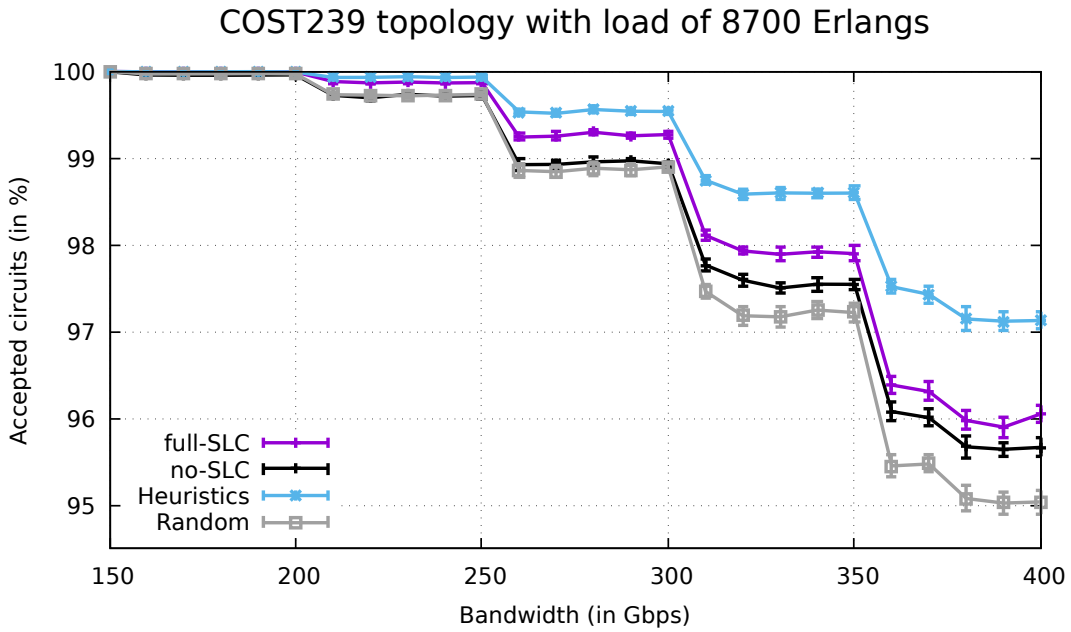

Figure (7.9) Percentage of established circuits per each generated bandwidth.

Fig. 7.10 presents the RSS fragmentation evaluation (according to Eq. 2.4. This fragmentation is affected mainly by the size of all free segments. Information about the number of segments and the highest allocated index does not affect this metric. This fragmentation grows with the presence of large segments over the tiny ones. Due to its reduced flexibility, the no-SLC solution has large segments of free slots, reaching a higher fragmentation than the full-SLC. The heuristic solution has large segments of free slots with less budget (up to 200). After this point, the value of this metric decays to a level lower than the full-SLC (after 350 of budget). At this point, the heuristic solution allocates more circuits, and fewer empty slots are scattered as small segments in the spectrum.

Cost-benefit evaluation

We also perform a cost-benefit evaluation to relate the applied budget and resulting blocking rate and identify the budget point at which the monetary application brings benefits. The methodology is similar to the model applied in [132] and [133]. Eq. 7.1 represents the bandwidth blocking probability gain.

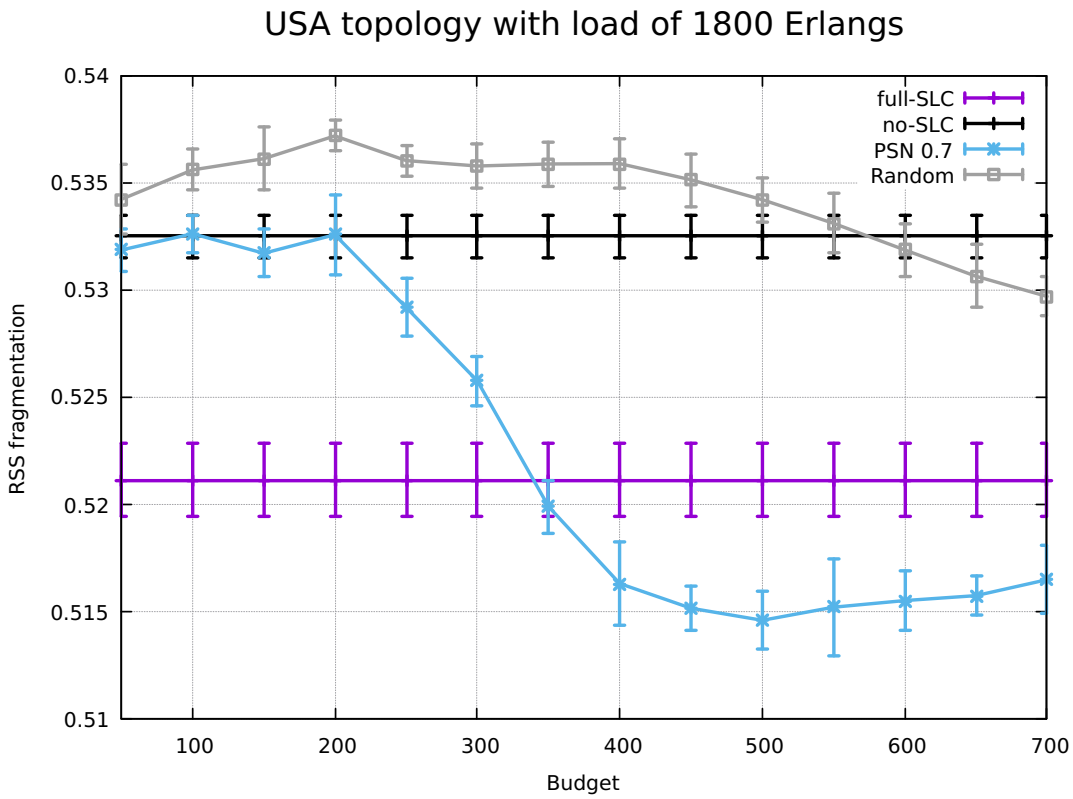

Figure (7.10) RSS fragmentation.

$$G_{BBR} = \frac{BBR_{noSLC} - BBR_b}{BBR_{noSLC} - BBRfullSLC}, \tag{7.1}$$

Equation 7.1 represents the performance gain for the evaluated budget values. The BBR_{noSLC} and $BBR_{fullSLC}$ values indicate the static bandwidth blocking rate for no-SLC and full-SLC scenarios, respectively. BBR_b represents the bandwidth blocking rate for the budget point under evaluation. The G_{BBR} is the first component of the cost-benefit evaluation. Eq. 7.2 presents the gain in equipment cost.

$$G_{cost} = \frac{C_b}{C_{noSLC}}, \tag{7.2}$$

The G_{cost} relates the cost increase between the scenario without core switching and the different budget points. C_b represents the cost of the budget point under evaluation, and C_{noSLC} represents the cost of the no-SLC architecture. To perform this measurement, we added the values 758.52 and 492.31 to all the budget points in topologies USA and COST239, respectively. The values also are added to the no-SLC and full-SLC costs. This

value corresponds to the actual cost of the no-SLC architectures, considering the number of SSS ports applied to maintain exclusively the core continuity constraint. This addition avoids a zero division in the G_{cost} evaluation. Finally, Eq. 7.3 describes the cost-benefit measurement.

$$G = \frac{G^b_{BBR}}{G^b_{cost}}, \tag{7.3}$$

In Eq. 7.3, the G^b_{BBR} indicates the bandwidth blocking gain, according to Eq. 7.1 for the budget point under evaluation, and the variable G^b_{cost} indicates the cost gain for the same budget point (based on Eq. 7.2). The cost-benefit result is the relation of the two previously mentioned variables and reflects the impact of budget distribution directly on the bandwidth blocking rate. Figs. 7.11 and 7.12 illustrate the G_{BBR} for the heuristic solution in USA and COST239 topologies, respectively.

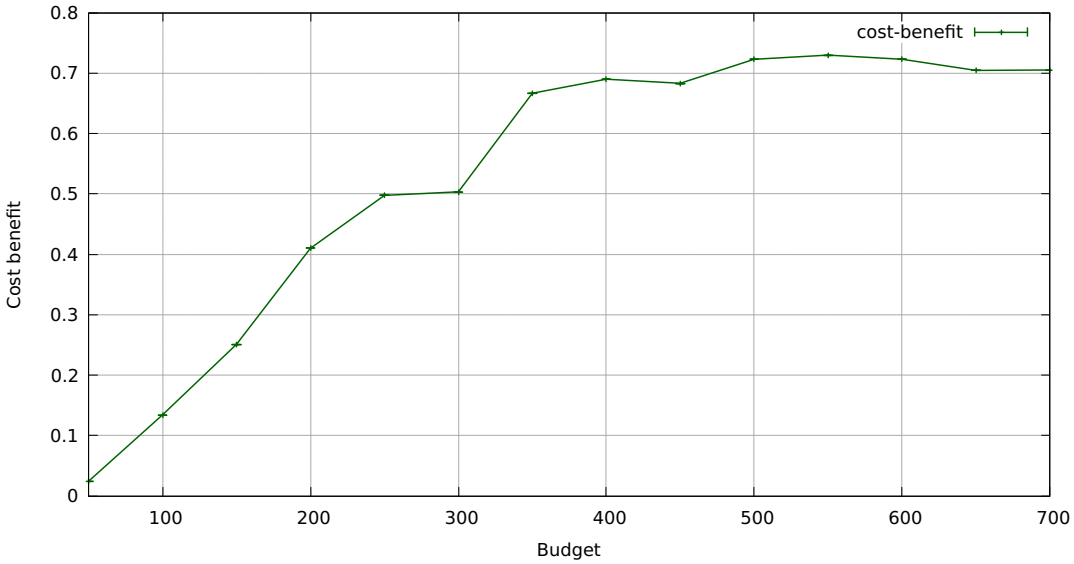

Figure (7.11) Cost-benefit evaluation for USA topology.

The cost-benefit evaluation for the USA topology (Fig. 7.11) presents an increasing behavior and stabilizes with an investment of around 350. After this point, the financial investment brings low to no benefits to the network in the evaluated scenario. For the COST239 topology evaluation (Fig. 7.12), there is a peak cost-benefit gain at the point of 400 budget. This turning point indicates the budget investment that gets more compensated when looking into the impact on the bandwidth blocking rate. The lower cost-benefit points before and after the 400 point represent reduced performance in terms of blocking rate and/or a very high investment that does not pay back in terms of performance.

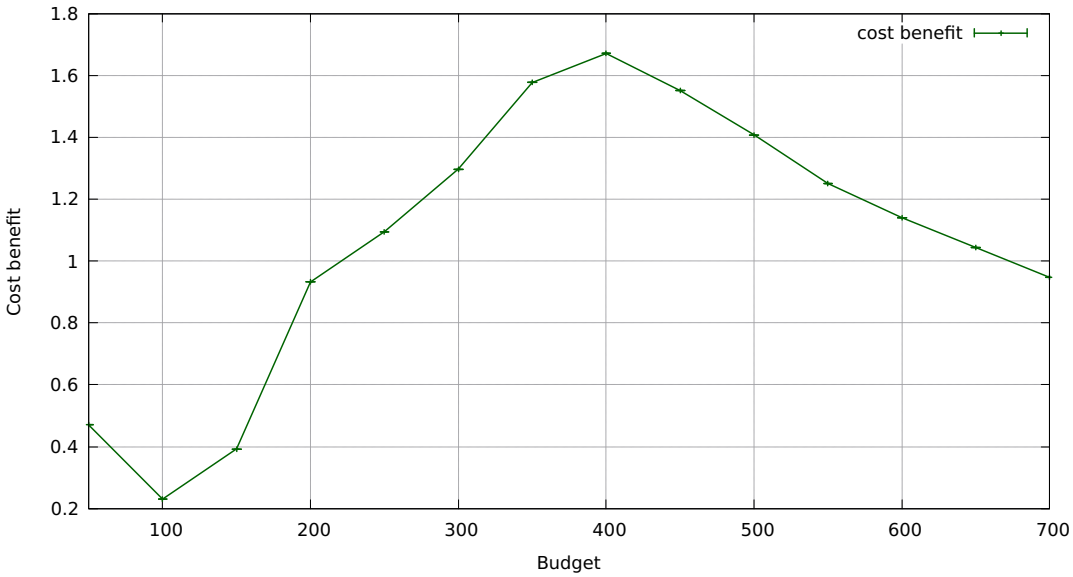

Figure (7.12) Cost-benefit evaluation for COST239 topology.

With this evaluation, we can conclude that the best budget investment in a sparse core switching architecture for the USA and COS239 topologies is 350 and 400 of budget, additionally to the no-SLC cost. We emphasize that this evaluation, as the sparse core switching heuristic, is highly dependent on the scenario parameters and should be reassessed if any scenario information changes, like the topology composition, fiber types, generated bandwidth, etc.

7.3 Concluding remarks

In this thesis, we have extensively evaluated the concept of sparse core switching within SDM-EONs, revealing its significant economic and performance benefits. Our research demonstrated that a well-optimized sparse core-switching distribution can effectively balance the trade-offs between crosstalk and fragmentation, offering performance comparable to full-core switching scenarios but at a substantially reduced cost. By systematically analyzing the impact of varying the parameter α and evaluating different budget scenarios, we identified an optimal budget investment of approximately \$350 for the USA topology and \$400 for the COST239 topology. These findings highlight the potential of sparse core switching to provide a cost-effective alternative to full-core switching, reducing the required budget by over 80% while still achieving high network performance and low bandwidth blocking rates. The evaluation also underscores the importance of strategic port distribution and careful consideration of traffic profiles to maximize the benefits of sparse core switching.

Furthermore, the comparison between heuristic and random distributions illuminated the detrimental effects of unplanned sparse core switching on network performance. Our heuristic approach consistently outperformed random distributions, illustrating the need for deliberate and informed core-switching port allocation strategies. The cost-benefit analysis further reinforces the advantages of the proposed sparse core-switching framework, demonstrating that, with appropriate budget allocation, the sparse core-switching architecture provides substantial performance gains without incurring excessive costs. This research not only advances the understanding of core-switching in optical networks but also sets the stage for future work in optimizing network deployment and addressing other physical impairments beyond XT. The proposed framework, while effective, also presents opportunities for further refinement and broader application, particularly in analyzing node costs and energy consumption, which could further enhance its practical utility in real-world scenarios.

Chapter 8

Conclusions and research challenges

The ever-increasing bandwidth requirements for data transmission demand an infrastructure capable of supporting high data rates with low latency, and the employment of SDM-EON ensures augmented resource availability. The flexibility of EON, combined with the high resource availability of SDM, increases the search space for resource allocation and spectrum handling.

The XT effect constitutes a significant interference factor for SDM-EON. Resource allocation strategies must be aware of XT, especially in scenarios characterized by high XT occurrence. This thesis undertakes a comparative analysis of XT thresholds associated with various modulation formats as proposed in the literature, against XT measurements corresponding to different modulations based on their respective distance reach. Furthermore, the thesis identifies multiple methodologies for crosstalk measurement, exposing their distinct impacts regarding the blocking rate. Our findings reveal significant disparities in blocking rates, reaching up to a 74.13% reduction in the blocking rate. Such insights underscore the critical importance of selecting appropriate crosstalk measurement techniques in optimizing network performance within SDM-EON frameworks.

This thesis also presents a resource allocation solution tailored for core-constrained scenarios within SDM-EON architectures. The proposed ASMC strategy assigns robust modulation formats to the central core, augmenting circuit provision within regions subjected to intense XT impact. Furthermore, the heuristic chooses cores based on the parity of slot numbers for each circuit, aiming to reduce fragmentation. Simulations demonstrate the efficacy of the proposed solution, with a reduction in blocking rates by a minimum of 43.64% when compared to existing solutions in the literature.

Furthermore, this thesis introduces a defragmentation methodology tailored for SLC-enabled SDM-EON architectures. The proposed heuristic applies two techniques, namely push-pull and fast-switching, to execute defragmentation operations, reaching a substantial decrease in defragmentation latency.

Finally, this thesis introduces the Sparse Core Switching paradigm as an intermediary between the core-constrained and the SLC-enabled paradigms. The sparse core switching deploys SSS equipment throughout the network, focusing on nodes where they offer more benefits. Consequently, network nodes exhibit varying degrees of core-switching capacity. The efficacy of this approach becomes apparent as the blocking rate reduces as the available budget increases. The sparse solution demonstrates performance comparable to SLC-enabled scenarios with just a fraction of the budget if the heuristic solution distributes resources efficiently. An efficient implementation of SCS may even outperform SLC-enabled setups, highlighting its potential for enhancing network performance.

8.1 Research challenges

This Thesis highlights a series of challenges inherent in SDM-EON scenarios, emphasizing their status as potential research efforts. Here, we delineate some of these challenges as a starting point for future investigations.

- The development of suitable equipment to switch the optical circuit in the SDM-EON. Papers found in the literature refer to hypothetical architectures, capable of switching the signal between different cores (in some cases). The performed evaluations of viable architectures [5], [63] cite as a solution the adoption of devices (switches, amplifiers, and multiplexers) found in other types of networks.
- A challenge found in SDM-EON is the mitigation of the *crosstalk* effect. This interference of the physical layer is responsible for the unavailability of spectral resources, which are idle when crosstalk is high enough (XT above $-25dB$ [5]), and turns inadequate the circuit allocation. Some types of fiber are proposed to reduce the crosstalk effect (such as Trench-Assisted MCF), under a distance threshold defined by the manufacturer.
- The production of equipment with a low financial cost, leading to low cost for SDM-EON implementation. Besides, the performance achieved by a n core MCF should be similar to the performance obtained by n coupled single-core fibers, which reinforces the development of fibers with higher immunity to crosstalk interference.
- We demonstrate in this thesis that the value of n in the crosstalk equation can be used statically or dynamically and also can analyze the crosstalk impact from the new circuit to already established circuits. An in-depth investigation of the impact of different crosstalk scenarios can also be done in the future to outline the scenario closest to the crosstalk occurrence in a real network.

- The elaboration of a high efficiency (RMSCA) solution is also necessary. Nowadays, the papers found in the literature that propose RMSCA solutions compare their performance with classical literature algorithms such as the Dijkstra algorithm for routing and the First Fit strategy for spectrum allocation. Besides, different traffic profiles should be considered as some RMSCA solutions get better performance in specific traffic configurations.
- Design of more flexible switching architectures to improve the network performance, provide more options to the resource allocation solution, and reduce impact in terms of cost and physical interference.

References

[1] Xiang Liu. Enabling optical network technologies for 5g and beyond. *Journal of Lightwave Technology*, 40(2):358–367, 2022. vii, 1

[2] Alessio Ferrari, Antonio Napoli, Johannes K. Fischer, Nelson Costa, Andrea D'Amico, João Pedro, Wladek Forysiak, Erwan Pincemin, Andrew Lord, Alexandros Stavdas, Juan Pedro F.-P. Gimenez, Gunther Roelkens, Nicola Calabretta, Silvio Abrate, Bernd Sommerkorn-Krombholz, and Vittorio Curri. Assessment on the achievable throughput of multi-band itu-t g.652.d fiber transmission systems. *Journal of Lightwave Technology*, 38(16):4279–4291, 2020. vii, 1

[3] Agbotiname Lucky Imoize, Oluwadara Adedeji, Nistha Tandiya, and Sachin Shetty. 6g enabled smart infrastructure for sustainable society: Opportunities, challenges, and research roadmap. *Sensors*, 21(5), 2021. vii, 1

[4] M. Jinno, H. Takara, B. Kozicki, Y. Tsukishima, Y. Sone, and S. Matsuoka. Spectrum-efficient and scalable elastic optical path network: architecture, benefits, and enabling technologies. *IEEE Communications Magazine*, 47(11):66–73, November 2009. vii, 1, 8

[5] DJ Richardson, JM Fini, and LE Nelson. Space-division multiplexing in optical fibres. *Nature Photonics*, 7(5):354–362, 2013. viii, xiii, 1, 9, 10, 23, 27, 35, 36, 40, 85

[6] Saurabh Jain, Carlos Castro, Yongmin Jung, John Hayes, Reza Sandoghchi, Takayuki Mizuno, Yusuke Sasaki, Yoshimichi Amma, Yutaka Miyamoto, Marc Bohn, Klaus Pulverer, Md. Nooruzzaman, Toshio Morioka, Shaiful Alam, and David J. Richardson. 32-core erbium/ytterbium-doped multicore fiber amplifier for next generation space-division multiplexed transmission system. *Opt. Express*, 25(26):32887–32896, Dec 2017. viii, 2

[7] Kazi S. Abedin, Man F. Yan, Thierry F. Taunay, Benyuan Zhu, Eric M. Monberg, and David J. DiGiovanni. State-of-the-art multicore fiber amplifiers for space division multiplexing. *Optical Fiber Technology*, 35:64–71, 2017. Next Generation Multiplexing Schemes in Fiber-based Systems. viii

[8] Amado M Velázquez-Benítez, J Enrique Antonio-López, Juan C Alvarado-Zacarías, Nicolas K Fontaine, Roland Ryf, Haoshuo Chen, Juan Hernández-Cordero, Pierre Sillard, Chigo Okonkwo, Sergio G Leon-Saval, et al. Scaling photonic lanterns for space-division multiplexing. *Scientific reports*, 8(1):8897, 2018. viii, 2

[9] Ruijie Zhu, Yongli Zhao, Hui Yang, Haoran Chen, Jie Zhang, and Jason P. Jue. Crosstalk-aware rcsa for spatial division multiplexing enabled elastic optical networks with multi-core fibers. *Chin. Opt. Lett.*, 14(10):100604, Oct 2016. ix, 31, 32, 34, 35, 40, 53

[10] Hideki Tode and Yusuke Hirota. Routing, spectrum and core assignment on sdm optical networks (invited). In *2016 Optical Fiber Communications Conference and Exhibition (OFC)*, pages 1–3, 2016. ix, 53

[11] J. M. Fini, B. Zhu, T. F. Taunay, M. F. Yan, and K. S. Abedin. Crosstalk in multicore optical fibres. In *2011 37th European Conference and Exhibition on Optical Communication*, pages 1–3, Sept 2011. xiii, 10, 21, 22, 40

[12] N. K. Fontaine. Photonic lantern spatial multiplexers in space-division multiplexing. In *2013 IEEE Photonics Society Summer Topical Meeting Series*, pages 97–98, July 2013. xiii, 37

[13] Mingcong Yang, Chenxiao Zhang, Qian Wu, Weichang Zheng, and Yongbing Zhang. Comparison of switching policies in terms of switching cost and network performance in static SDM-EONs. *Optical Switching and Networking*, 38(May), 2020. xv, 37, 70, 75

[14] Dao Thanh Hai. Optical-computing-enabled network: An avant-garde architecture to sustain traffic growth. *Results in Optics*, 13:100504, 2023. 1

[15] Weichang Zheng, Mingcong Yang, Chenxiao Zhang, Yu Zheng, and Yongbing Zhang. Evaluation of optical transport unit line-card integration in spatially and spectrally flexible optical networks in terms of device cost and network performance. *Journal of Lightwave Technology*, 40:6319–6330, 10 2022. 2, 8, 69

[16] A. Muhammad, G. Zervas, and R. Forchheimer. Resource allocation for space-division multiplexing: Optical white box versus optical black box networking. *Journal of Lightwave Technology*, 33(23):4928–4941, Dec 2015. 2, 8, 15, 29, 32, 34, 35, 40, 43, 44, 48, 52

[17] T. Hayashi, T. Taru, O. Shimakawa, T. Sasaki, and E. Sasaoka. Characterization of crosstalk in ultra-low-crosstalk multi-core fiber. *Journal of Lightwave Technology*, 30(4):583–589, Feb 2012. 2, 21, 22, 35, 40

[18] R. Zhu, S. Li, P. Wang, Y. Tan, and J. Yuan. Gradual migration of co-existing fixed/flexible optical networks for cloud-fog computing. *IEEE Access*, 8:50637–50647, 2020. 8

[19] J. Yuan, R. Zhu, Y. Zhao, Q. Zhang, X. Li, D. Zhang, and A. Samuel. A spectrum assignment algorithm in elastic optical network with minimum sum of weighted resource reductions in all associated paths. *Journal of Lightwave Technology*, 37(21):5583–5592, 2019. 8

[20] Ruijie Zhu, Shihu Li, Peisen Wang, and Junling Yuan. Time and spectrum fragmentation-aware virtual optical network embedding in elastic optical networks. *Optical Fiber Technology*, 54:102117, 2020. 8

[21] Junling Yuan, Yunyang Fu, Ruijie Zhu, Xuhong Li, Qikun Zhang, Jing Zhang, and Aretor Samuel. A constrained-lower-indexed-block spectrum assignment policy in elastic optical networks. *Optical Switching and Networking*, 33:25–33, 2019. 8

[22] Bijoy Chand Chatterjee, Nityananda Sarma, and Eiji Oki. Routing and spectrum allocation in elastic optical networks: A tutorial. *IEEE Communications Surveys & Tutorials*, 17(3):1776–1800, 2015. 8

[23] K. Walkowiak, M. Klinkowski, and P. Lechowicz. Dynamic routing in spectrally spatially flexible optical networks with back-to-back regeneration. *IEEE/OSA Journal of Optical Communications and Networking*, 10(5):523–534, May 2018. 8, 33, 35, 40

[24] H. Tode and Y. Hirota. Routing, spectrum and core assignment for space division multiplexing elastic optical networks. In *2014 16th International Telecommunications Network Strategy and Planning Symposium (Networks)*, pages 1–7, Sept 2014. 8, 29

[25] Ítalo Brasileiro, Lucas Costa, and André Drummond. A survey on challenges of Spatial Division Multiplexing enabled elastic optical networks. *Optical Switching and Networking*, 38:100584, 2020. 8

[26] Mingcong Yang, Qian Wu, Maiko Shigeno, and Yongbing Zhang. Hierarchical routing and resource assignment in spatial channel networks (scns): Oriented toward the massive sdm era. *Journal of Lightwave Technology*, 39(5):1255–1270, 2021. 9, 48

[27] A. Jørgensen, Deming Kong, M. Henriksen, Frederik Klejs, Z. Ye, Ò Helgason, Henrik Hansen, Hao Hu, Metodi Yankov, Søren Forchhammer, P. Andrekson, A. Larsson, M. Karlsson, J. Schröder, Yusuke Sasaki, Kazuhiko Aikawa, J. Thomsen, Toshio Morioka, Michael Galili, and L.K. Oxenlowe. Petabit-per-second data transmission using a chip-scale microcomb ring resonator source. *Nature Photonics*, 16:1–5, 10 2022. 9

[28] N. Amaya, M. Irfan, G. Zervas, R. Nejabati, D. Simeonidou, J. Sakaguchi, W. Klaus, B.J. Puttnam, T. Miyazawa, Y. Awaji, N. Wada, and I. Henning. Fully-elastic multi-granular network with space/frequency/time switching using multi-core fibres and programmable optical nodes. *Opt. Express*, 21(7):8865–8872, Apr 2013. 9, 27, 40

[29] Shan Yin, Sicong Ding, Zhenhao Wang, Wenchao Zhang, and Shanguo Huang. Flexibility and fragmentation aware routing, core and spectrum allocation for hybrid aod nodes in sdm-eons. *Opt. Express*, 30(15):27623–27644, Jul 2022. 9, 69, 70

[30] Tetsuya Hayashi. Multi-core fiber technology from design to deployment. In *2022 European Conference on Optical Communication (ECOC)*, pages 1–4, 2022. 9

[31] George M. Saridis, Dimitris Alexandropoulos, Georgios Zervas, and Dimitra Simeonidou. Survey and evaluation of space division multiplexing: From technologies to optical networks. *IEEE Communications Surveys Tutorials*, 17(4):2136–2156, 2015. 9, 10, 27, 35, 40, 69

[32] Georg Rademacher, Ruben S. Luís, Benjamin J. Puttnam, Yoshinari Awaji, and Naoya Wada. Crosstalk dynamics in multi-core fibers. *Opt. Express*, 25(10):12020–12028, May 2017. 10

[33] Katsuhiro Takenaga, Yoko Arakawa, Yusuke Sasaki, Shoji Tanigawa, Shoichiro Matsuo, Kunimasa Saitoh, and Masanori Koshiba. A large effective area multi-core fiber with an optimized cladding thickness. *Opt. Express*, 19(26):B543–B550, Dec 2011. 10, 22, 40

[34] K. Takenaga, Y. Arakawa, S. Tanigawa, N. Guan, S. Matsuo, K. Saitoh, and M. Koshiba. Reduction of crosstalk by trench-assisted multi-core fiber. In *2011 Optical Fiber Communication Conference and Exposition and the National Fiber Optic Engineers Conference*, pages 1–3, March 2011. 10, 21, 22, 35, 40

[35] S. Fujii, Y. Hirota, H. Tode, and K. Murakami. On-demand spectrum and core allocation for reducing crosstalk in multicore fibers in elastic optical networks. *IEEE/OSA Journal of Optical Communications and Networking*, 6(12):1059–1071, Dec 2014. 10, 21, 28, 29, 32, 35, 40

[36] G. Savva, G. Ellinas, B. Shariati, and I. Tomkos. Physical layer-aware routing, spectrum, and core allocation in spectrally-spatially flexible optical networks with multicore fibers. In *2018 IEEE International Conference on Communications (ICC)*, pages 1–6, May 2018. 10, 32, 35, 40

[37] Masahiko Jinno and Yutaka Mori. Unified architecture of an integrated sdm-wss employing a plc-based spatial beam transformer array for various types of sdm fibers. *Journal of Optical Communications and Networking*, 9(2):A198–A206, 2017. 11, 67

[38] Yiran Ma, Luke Stewart, Julian Armstrong, Ian G. Clarke, and Glenn Baxter. Recent progress of wavelength selective switch. *Journal of Lightwave Technology*, 39(4):896–903, 2021. 12

[39] Raül Muñoz, Ramon Casellas, Ricardo Martínez, and Ricard Vilalta. Pce: What is it, how does it work and what are its limitations? *Journal of Lightwave Technology*, 32(4):528–543, 2014. 12

[40] A. Muhammad, G. Zervas, D. Simeonidou, and R. Forchheimer. Routing, spectrum and core allocation in flexgrid sdm networks with multi-core fibers. In *2014 International Conference on Optical Network Design and Modeling*, pages 192–197, May 2014. 13, 28, 32, 35, 40

[41] P. S. Khodashenas, J. M. Rivas-Moscoso, D. Siracusa, F. Pederzolli, B. Shariati, D. Klonidis, E. Salvadori, and I. Tomkos. Comparison of spectral and spatial superchannel allocation schemes for sdm networks. *Journal of Lightwave Technology*, 34(11):2710–2716, June 2016. 13, 27, 34, 35, 40

[42] S. Sugihara, Y. Hirota, S. Fujii, H. Tode, and T. Watanabe. Dynamic resource allocation for immediate and advance reservation in space-division-multiplexing-based elastic optical networks. *IEEE/OSA Journal of Optical Communications and Networking*, 9(3):183–197, March 2017. 13, 14, 31, 33, 35, 40

[43] Waddah S. Saif, Maged A. Esmail, Amr M. Ragheb, Tariq A. Alshawi, and Saleh A. Alshebeili. Machine learning techniques for optical performance monitoring and modulation format identification: A survey. *IEEE Communications Surveys & Tutorials*, 22(4):2839–2882, 2020. 14

[44] L. R. Costa and A. C. Drummond. New distance-adaptive modulation scheme for elastic optical networks. *IEEE Communications Letters*, 21(2):282–285, Feb 2017. 14, 43

[45] Hamzeh Beyranvand and Jawad A Salehi. A quality-of-transmission aware dynamic routing and spectrum assignment scheme for future elastic optical networks. *Journal of Lightwave Technology*, 31(18):3043–3054, 2013. 15

[46] Lucas R. Costa, Ítalo B. Brasileiro, and André C. Drummond. Energy efficiency in sliceable-transponder enabled elastic optical networks. *IEEE Transactions on Green Communications and Networking*, 5(2):789–802, 2021. 15

[47] Yang Wang, Xiaojun Cao, and Yi Pan. A study of the routing and spectrum allocation in spectrum-sliced Elastic Optical Path networks. *Proceedings - IEEE INFOCOM*, pages 1503–1511, 2011. 18

[48] Rui Wang and Biswanath Mukherjee. Spectrum management in heterogeneous bandwidth optical networks. *Optical Switching and Networking*, 11(Part A):83 – 91, 2014. 19, 57

[49] B. C. Chatterjee, S. Ba, and E. Oki. Fragmentation problems and management approaches in elastic optical networks: A survey. *IEEE Communications Surveys Tutorials*, 20(1):183–210, Firstquarter 2018. 19, 56, 57, 58, 59

[50] Silvana Trindade and Nelson L. S. da Fonseca. Proactive Fragmentation-Aware Routing, Modulation Format, Core, and Spectrum Allocation in EON-SDM. *ICC 2019 - 2019 IEEE International Conference on Communications (ICC)*, pages 1–6, 2019. 19, 31, 33, 35, 40

[51] Piotr Lechowicz, Massimo Tornatore, Adam Wlodarczyk, and Krzysztof Walkowiak. Fragmentation metrics and fragmentation-Aware algorithm for spectrally/spatially flexible optical networks. *Journal of Optical Communications and Networking*, 12(5):133–145, 2020. 19, 20, 27, 33, 35, 40

[52] André K. Horota, Gustavo B. Figueiredo, and Nelson L. S. da Fonseca. Algoritmo de roteamento e atribuição de espectro com minimização de fragmentação em redes ópticas elásticas. *Simpósio Brasileiro de Redes de Computadores e Sistemas Distribuídos*, 32:895–908, 2014. 19

[53] Jurandir C. Lacerda Jr., Aline G. Morais, Adolfo V. T. Cartaxo, and André C. B. Soares. A new algorithm to mitigate fragmentation and crosstalk in multi-core elastic optical networks. *Photonics*, 11(6), 2024. 21

[54] John A Jay. An overview of macrobending and microbending of optical fibers. *White paper of Corning*, pages 1–21, 2010. 22

[55] Tetsuya Hayashi, Toshiki Taru, Osamu Shimakawa, Takashi Sasaki, and Eisuke Sasaoka. Uncoupled multi-core fiber enhancing signal-to-noise ratio. *Opt. Express*, 20(26):B94–B103, Dec 2012. 22, 40

[56] Miroslaw Klinkowski, Piotr Lechowicz, and Krzysztof Walkowiak. A Study on the Impact of Inter-Core Crosstalk on SDM Network Performance. *2018 International Conference on Computing, Networking and Communications, ICNC 2018*, pages 404–408, 2018. 22, 40

[57] Yanbo Chen, Nan Feng, Yue Zhou, Danping Ren, and Jijun Zhao. Crosstalk classification based on synthetically consider crosstalk and fragmentation rmcsa in multi-core fiber-based eons. *Photonics*, 10:340, 3 2023. 22, 28, 70

[58] Tetsuya Hayashi, Takuji Nagashima, Osamu Shimakawa, Takashi Sasaki, and Eisuke Sasaoka. Crosstalk variation of multi-core fibre due to fibre bend. In *36th European Conference and Exhibition on Optical Communication*, pages 1–3, 2010. 23

[59] Masanori Koshiba, Kunimasa Saitoh, Katsuhiro Takenaga, and Shoichiro Matsuo. Multi-core fiber design and analysis: coupled-mode theory and coupled-power theory. *Optics Express*, 19(26):B102, 2011. 23, 40

[60] Kotaro Hashino, Yusuke Hirota, Yosuke Tanigawa, and Hideki Tode. A Strict and Less Computational Crosstalk-Aware Spectrum and Core Allocation Method with Crosstalk-Prohibited Frequency Slots in SDM-EONs. *2018 Photonics in Switching and Computing (PSC)*, pages 1–3, 2019. 23, 32, 35, 40

[61] Yuanlong Tan, Ruijie Zhu, Hui Yang, Yongli Zhao, Jie Zhang, Zhu Liu, Qinghai Qu, and Ziguan Zhou. Crosstalk-aware provisioning strategy with dedicated path protection for elastic multi-core fiber networks. In *2016 15th International Conference on Optical Communications and Networks (ICOCN)*, pages 1–3, Sept 2016. 23, 30, 32, 35, 40

[62] Rui Tian, Yongli Zhao, J. Zhang, X. Yu, Yajie Li, Chenbei Yu, J. Zhang, Chuan Liu, and Gang Zhang. Dynamic traffic grooming based on auxiliary graph in spatial division multiplexing enabled elastic optical networks. In *2016 15th International Conference on Optical Communications and Networks (ICOCN)*, pages 1–3, Sept 2016. 27, 35, 40

[63] Dan M. Marom, Paul D. Colbourne, Antonio D'Errico, Nicolas K. Fontaine, Yuichiro Ikuma, Roberto Proietti, Liangjia Zong, José M. Rivas-Moscoso, and Ioannis Tomkos. Survey of Photonic Switching Architectures and Technologies in Support of Spatially and Spectrally Flexible Optical Networking [Invited]. *Journal of Optical Communications and Networking*, 9(1):26, 2017. 27, 35, 36, 40, 85

[64] Fengxian Tang, Sanjay K. Bose, Mirosław Klinkowski, and Gangxiang Shen. Minimizing inter-core crosstalk jointly in spatial, frequency, and time domains for scheduled lightpath demands in a multi-core fiber optical network. *Optics InfoBase Conference Papers*, Part F138-(c), 2019. 27

[65] Miroslaw Klinkowski and Grzegorz Zalewski. Dynamic crosstalk-aware lightpath provisioning in spectrally-spatially flexible optical networks. *Journal of Optical Communications and Networking*, 11:213–225, 2019. 28, 32, 34, 35, 40, 46

[66] H. Tode and Y. Hirota. Routing, spectrum, and core and/or mode assignment on space-division multiplexing optical networks [invited]. *IEEE/OSA Journal of Optical Communications and Networking*, 9(1):A99–A113, Jan 2017. 28, 30, 33, 34, 35, 40

[67] Qingcheng Zhu, Lulu Lv, Lei Zhu, Ting Wang, Lihang Gao, Yu Lei, Bowen Chen, and Qianwu Zhang. Service-Classified Routing, Core, and Spectrum Assignment in Spatial Division Multiplexing Elastic Optical Networks with Multicore Fiber. *Asia Communications and Photonics Conference, ACP*, 2018-Octob:1–3, 2018. 28, 30, 32, 35, 40

[68] L. Zhang, N. Ansari, and A. Khreishah. Anycast planning in space division multiplexing elastic optical networks with multi-core fibers. *IEEE Communications Letters*, 20(10):1983–1986, Oct 2016. 29, 32, 35, 40

[69] Elham Ehsani Moghaddam, Hamzeh Beyranvand, and Jawad A. Salehi. Crosstalk-aware Routing, Modulation Level, Core and Spectrum Assignment, and Scheduling in SDM-based Elastic Optical Networks. *9th International Symposium on Telecommunication: With Emphasis on Information and Communication Technology, IST 2018*, pages 160–165, 2019. 29, 32, 35, 40

[70] Qiuyan Yao, Hui Yang, Ao Yu, and Jie Zhang. Transductive transfer learning-based spectrum optimization for resource reservation in seven-core elastic optical networks. *Journal of Lightwave Technology*, 37:4164–4172, 2019. 29, 33, 35, 40

[71] S. Fujii, Y. Hirota, and H. Tode. Dynamic resource allocation with virtual grid for space division multiplexed elastic optical network. In *39th European Conference and Exhibition on Optical Communication (ECOC 2013)*, pages 1–3, Sept 2013. 29, 32, 35, 40

[72] H. M. Nunes da Silva Oliveira and N. L. Saldanha da Fonseca. The minimum interference p-cycle algorithm for protection of space division multiplexing elastic optical networks. *IEEE Latin America Transactions*, 15(7):1342–1348, 2017. 29, 30, 33, 35, 40

[73] Kotaro Hashino, Yusuke Hirota, Yosuke Tanigawa, and Hideki Tode. Crosstalk-aware spectrum and core allocation with crosstalk-prohibited frequency slot in space-division multiplexing elastic optical networks. In *Advanced Photonics 2017 (IPR, NOMA, Sensors, Networks, SPPCom, PS)*, page PM3D.2. Optical Society of America, 2017. 30, 32, 35, 40

[74] Yu Lei, Bowen Chen, Mingyi Gao, Lian Xiang, and Qianwu Zhang. Dynamic Routing, Core, and Spectrum Assignment with Minimized Crosstalk in Spatial Division Multiplexing Elastic Optical Networks. *Asia Communications and Photonics Conference, ACP*, 2018-Octob:1–3, 2018. 30, 32, 35, 40

[75] Kosuke Kubota, Yosuke Tanigawa, Hideki Tode, and Yusuke Hirota. Spectrum Allocation Considering Crosstalk Impacts at both Fibers and Nodes in Space-Division Multiplexing Elastic Optical Networks. *2019 24th OptoElectronics and Communications Conference (OECC) and 2019 International Conference on Photonics in Switching and Computing (PSC)*, pages 1–3, 2019. 30, 32, 35, 40

[76] H. M. N. S. Oliveira and N. L. S. da Fonseca. Algorithm for protection of space division multiplexing elastic optical networks. In *2016 IEEE Global Communications Conference (GLOBECOM)*, pages 1–6, Dec 2016. 30, 33, 35

[77] H. M. N. S. Oliveira and N. L. S. da Fonseca. Algorithm for shared path for protection of space division multiplexing elastic optical networks. In *2017 IEEE International Conference on Communications (ICC)*, pages 1–6, May 2017. 30, 33, 35, 40

[78] Helder M. N. S. Oliveira and Nelson L. S. da Fonseca. P-cycle Protected Multipath Routing, Spectrum and Core Allocation in SDM Elastic Optical Networks. *ICC 2019 - 2019 IEEE International Conference on Communications (ICC)*, pages 1–6, 2019. 30, 33, 35, 40

[79] Helder M. N. S. Oliveira and Nelson L. S. da Fonseca. Protection, Routing, Spectrum and Core Allocation in EONs-SDM for Efficient Spectrum Utilization. *ICC 2019 - 2019 IEEE International Conference on Communications (ICC)*, pages 1–6, 2019. 30, 33, 35, 40

[80] S Iyer. On the cost minimization in space division multiplexing based elastic optical networks. *Journal of Optical Communications*, 2018. 31, 33, 35, 40

[81] R. Zhu, Yongli Zhao, Hui Yang, X. Yu, Yuanlong Tan, Jie Zhang, N. Wang, and J. P. Jue. Multi-dimensional resource assignment in spatial division multiplexing enabled elastic optical networks with multi-core fibers. In *2016 15th International Conference on Optical Communications and Networks (ICOCN)*, pages 1–3, Sep. 2016. 31, 33, 35, 40

[82] G. Meloni, F. Fresi, M. Imran, F. Paolucci, F. Cugini, A. D'Errico, L. Giorgi, T. Sasaki, P. Castoldi, and L. Pot. Software-defined defragmentation in space-division multiplexing with quasi-hitless fast core switching. *Journal of Lightwave Technology*, 34(8):1956–1962, April 2016. 31, 40

[83] M. Imran, F. Paolucci, F. Cugini, A. D'Errico, L. Giorgi, T. Sasaki, P. Castoldi, and L. Poti. Quasi-hitless software-defined defragmentation in space division multiplexing (sdm). In *2015 European Conference on Optical Communication (ECOC)*, pages 1–3, Sep. 2015. 31, 40, 59, 65

[84] Yongli Zhao, Liyazhou Hu, Ruijie Zhu, Xiaosong Yu, Xinbo Wang, and Jie Zhang. Crosstalk-Aware Spectrum Defragmentation Based on Spectrum Compactness in Space Division Multiplexing Enabled Elastic Optical Networks with Multicore Fiber. *IEEE Access*, 6(4):15346–15355, 2018. 31, 35, 40, 60

[85] Yongli Zhao, Liyazhou Hu, Ruijie Zhu, Xiaosong Yu, Yajie Li, Wei Wang, and Jie Zhang. Crosstalk-aware spectrum defragmentation by re-provisioning advance reservation requests in space division multiplexing enabled elastic optical networks with multi-core fiber. *Opt. Express*, 27(4):5014–5032, Feb 2019. 31, 40

[86] Y. Zhao and J. Zhang. Crosstalk-aware cross-core virtual concatenation in spatial division multiplexing elastic optical networks. *Electronics Letters*, 52(20):1701–1703, 2016. 31, 32, 35, 40

[87] M. Yang, Y. Zhang, and Q. Wu. Routing, spectrum, and core assignment in sdm-eons with mcf: node-arc ilp/milp methods and an efficient xt-aware heuristic algorithm. *IEEE/OSA Journal of Optical Communications and Networking*, 10(3):195–208, March 2018. 32, 35, 40

[88] M. Yaghubi-Namaad, A. G. Rahbar, and B. Alizadeh. Adaptive modulation and flexible resource allocation in space-division- multiplexed elastic optical networks. *IEEE/OSA Journal of Optical Communications and Networking*, 10(3):240–251, March 2018. 32, 35, 40

[89] F. Tang, Y. Li, G. Shen, and G. Rouskas. Minimizing inter-core crosstalk jointly in spatial, frequency, and time domains for scheduled lightpath demands in multi-core fiber-based elastic optical network. *Journal of Lightwave Technology*, pages 1–1, 2020. 32, 35, 40

[90] Q. Yao, H. Yang, R. Zhu, A. Yu, W. Bai, Y. Tan, J. Zhang, and H. Xiao. Core, mode, and spectrum assignment based on machine learning in space division multiplexing elastic optical networks. *IEEE Access*, 6:15898–15907, 2018. 32, 35, 40

[91] Krzysztof Walkowiak, Adam Wlodarczyk, and Miroslaw Klinkowski. Effective worst-case crosstalk estimation for dynamic translucent sdm elastic optical networks. In *ICC 2019 - 2019 IEEE International Conference on Communications (ICC)*, pages 1–7, 2019. 32, 34, 35, 40

[92] H. M. N. S. Oliveira and N. L. S. da Fonseca. Sharing spectrum and straddling p-cycle fipp for protection against two simultaneous failures in sdm elastic optical networks. In *2017 IEEE 9th Latin-American Conference on Communications (LATINCOM)*, pages 1–6, Nov 2017. 33, 35, 40

[93] H. M. N. S. Oliveira and N. L. S. da Fonseca. Routing, spectrum, core and modulation level assignment algorithm for protected sdm optical networks. In *GLOBECOM 2017 - 2017 IEEE Global Communications Conference*, pages 1–6, Dec 2017. 33, 35, 40

[94] S. Fujii, Y. Hirota, H. Tode, and T. Watanabe. On-demand routing and spectrum allocation for energy-efficient aod nodes in sdm-eons. *IEEE/OSA Journal of Optical Communications and Networking*, 9(11):960–973, Nov 2017. 33, 35, 40

[95] H. M. N. S. Oliveira and N. L. S. Da Fonseca. Protection, routing, modulation, core, and spectrum allocation in sdm elastic optical networks. *IEEE Communications Letters*, 22(9):1806–1809, Sep. 2018. 33, 35, 40

[96] Sridhar Iyer and Shree Prakash Singh. A novel protection strategy for elastic optical networks based on space division multiplexing. *SPCOM 2018 - 12th International Conference on Signal Processing and Communications*, pages 41–45, 2018. 33, 35, 40

[97] K. Imamura, K. Mukasa, and T. Yagi. Investigation on multi-core fibers with large aeff and low micro bending loss. In *2010 Conference on Optical Fiber Communication (OFC/NFOEC), collocated National Fiber Optic Engineers Conference*, pages 1–3, March 2010. 35, 40

[98] K. Imamura, H. Inaba, K. Mukasa, and R. Sugizaki. 19-core multi core fiber to realize high density space division multiplexing transmission. In *2012 IEEE Photonics Society Summer Topical Meeting Series*, pages 208–209, July 2012. 35, 40

[99] Y. Cao, Y. Zhao, X. Yu, Q. Ou, Z. Liu, X. Liao, and J. Zhang. Mode conversion-based crosstalk-aware routing, spectrum and mode assignment in space-division multiplexing elastic optical networks. In *2017 16th International Conference on Optical Communications and Networks (ICOCN)*, pages 1–3, Aug 2017. 35, 40

[100] J. Zhu and Z. Zhu. Physical-layer security in mcf-based sdm-eons: Would crosstalk-aware service provisioning be good enough? *Journal of Lightwave Technology*, 35(22):4826–4837, Nov 2017. 35, 40

[101] Dablu Kumar and Rakesh Ranjan. Optimal design for crosstalk analysis in 12-core 5-lp mode homogeneous multicore fiber for different lattice structure. *Optical Fiber Technology*, 41:95 – 103, 2018. 35, 40

[102] R. Proietti, L. Liu, R. P. Scott, B. Guan, C. Qin, T. Su, F. Giannone, and S. J. B. Yoo. 3d elastic optical networking in the temporal, spectral, and spatial domains. *IEEE Communications Magazine*, 53(2):79–87, Feb 2015. 34, 35, 40

[103] Mattia Cantono and Vittorio Curri. Coupled vs. uncoupled sdm solutions: A physical layer aware networking comparison. *2018 20th International Conference on Transparent Optical Networks (ICTON)*, pages 1–4, 2018. 35

[104] Y. Zhao, L. Hu, C. Wang, R. Zhu, X. Yu, and J. Zhang. Multi-core virtual concatenation scheme considering inter-core crosstalk in spatial division multiplexing enabled elastic optical networks. *China Communications*, 14(10):108–117, Oct 2017. 35, 40

[105] K. Takenaga, S. Tanigawa, N. Guan, S. Matsuo, K. Saitoh, and M. Koshiba. Reduction of crosstalk by quasi-homogeneous solid multi-core fiber. In *2010 Conference on Optical Fiber Communication (OFC/NFOEC), collocated National Fiber Optic Engineers Conference*, pages 1–3, March 2010. 35

[106] Tetsuya Hayashi, Toshiki Taru, Osamu Shimakawa, Takashi Sasaki, and Eisuke Sasaoka. Design and fabrication of ultra-low crosstalk and low-loss multi-core fiber. *Opt. Express*, 19(17):16576–16592, Aug 2011. 35, 40

[107] Katsuhiro TAKENAGA, Yoko ARAKAWA, Shoji TANIGAWA, Ning GUAN, Shoichiro MATSUO, Kunimasa SAITOH, and Masanori KOSHIBA. An investigation on crosstalk in multi-core fibers by introducing random fluctuation along longitudinal direction. *IEICE Transactions on Communications*, E94.B(2):409–416, 2011. 35, 40

[108] M. Klinkowski, G. Zalewski, and K. Walkowiak. Optimization of spectrally and spatially flexible optical networks with spatial mode conversion. In *2018 International Conference on Optical Network Design and Modeling (ONDM)*, pages 148–153, May 2018. 35, 40

[109] Mingcong Yang, Qian Wu, Kai Guo, and Yongbing Zhang. Evaluation of device cost, power consumption, and network performance in spatially and spectrally flexible sdm optical networks. *Journal of Lightwave Technology*, 37:5259–5272, 2019. 36, 37, 38

[110] Qian Wu, Jiading Wang, and Maiko Shigeno. A novel channel-based model for the problem of routing, space, and spectrum assignment. *Optical Switching and Networking*, 43:100636, 2022. 37

[111] Jiading Wang, Sibo Chen, Qian Wu, Yiliu Tan, and Maiko Shigeno. Solving the static resource-allocation problem in sdm-eons via a node-type ilp model. *Sensors*, 22(24), 2022. 37

[112] Kunimasa Saitoh, Masanori Koshiba, Katsuhiro Takenaga, and Shoichiro Matsuo. Crosstalk and core density in uncoupled multicore fibers. *IEEE Photonics Technology Letters*, 24(21):1898–1901, 2012. 39

[113] Helder M.N.S. Oliveira and Nelson L.S. Da Fonseca. Spectrum overlap and traffic grooming in P-Cycle algorithm protected SDM optical networks. *IEEE International Conference on Communications*, 2018-May:1–6, 2018. 40

[114] Helder M.N.S. Oliveira and Nelson L.S. da Fonseca. Routing, spectrum and core assignment algorithms for protection of space division multiplexing elastic optical networks. *Journal of Network and Computer Applications*, 128:78–89, 2019. 40

[115] Piotr Lechowicz, Krzysztof Walkowiak, and Mirosław Klinkowski. Greedy randomized adaptive search procedure for joint optimization of unicast and anycast traffic in spectrally-spatially flexible optical networks. *Computer Networks*, 146:167–182, 2018. 40

[116] Shohei Fujii, Yusuke Hirota, Hideki Tode, and Koso Murakami. On-Demand Spectrum and Core Allocation for Multi-Core Fibers in Elastic Optical Network. *Optical Fiber Communication Conference/National Fiber Optic Engineers Conference 2013*, 6(12):OTh4B.4, 2013. 40

[117] Krzysztof Walkowiak, Miroslaw Klinkowski, and Piotr Lechowicz. Scalability Analysis of Spectrally-Spatially Flexible Optical Networks with Back-to-Back Regeneration. *International Conference on Transparent Optical Networks*, 2018-July:18–21, 2018. 40

[118] C. Politi, V. Anagnostopoulos, C. Matrakidis, A. Stavdas, A. Lord, V. López, and J. P. Fernández-Palacios. Dynamic operation of flexi-grid ofdm-based networks. In *OFC/NFOEC*, pages 1–3, 2012. 43

[119] Lucas R. Costa, Léia S. de Sousa, Felipe R. de Oliveira, Kaio A. da Silva, Paulo J. S. Júnior, and André C. Drummond. ONS: Simulador de Eventos Discretos para Redes Ópticas WDM/EON. In *SBRC 2016 - Salao de Ferramentas*, may 2016. 43

[120] Í. Brasileiro, J. Valdemir, and A. Soares. Regenerator assignment with circuit invigorating. *Optical Switching and Networking*, 34, 2019. 49

[121] Edsger W Dijkstra. A note on two problems in connexion with graphs. *Numerische mathematik*, 1(1):269–271, 1959. 50, 52

[122] G. Zhang, M. De Leenheer, A. Morea, and B. Mukherjee. A survey on ofdm-based elastic core optical networking. *IEEE Communications Surveys Tutorials*, 15(1):65–87, First 2013. 56, 57

[123] Gianluca Meloni, Francesco Fresi, Muhammad Imran, Francesco Paolucci, Filippo Cugini, Antonio D'Errico, Luca Giorgi, Takashi Sasaki, Piero Castoldi, and Luca Pot. Software-defined defragmentation in space-division multiplexing with quasi-hitless fast core switching. *Journal of Lightwave Technology*, 34(8):1956–1962, 2016. 56, 57, 59, 60, 65

[124] I. Tomkos, S. Azodolmolky, J. Solé-Pareta, D. Careglio, and E. Palkopoulou. A tutorial on the flexible optical networking paradigm: State of the art, trends, and research challenges. *Proceedings of the IEEE*, 102(9):1317–1337, Sep. 2014. 56, 57

[125] Ankitkumar N. Patel, Philip N. Ji, Jason P. Jue, and Ting Wang. Defragmentation of transparent flexible optical wdm (fwdm) networks. In *2011 Optical Fiber Communication Conference and Exposition and the National Fiber Optic Engineers Conference*, pages 1–3, 2011. 58

[126] Tatsumi Takagi, Hiroshi Hasegawa, Ken-ichi Sato, Yoshiaki Sone, Akira Hirano, and Masahiko Jinno. Disruption minimized spectrum defragmentation in elastic optical path networks that adopt distance adaptive modulation. In *2011 37th European Conference and Exhibition on Optical Communication*, pages 1–3, 2011. 58

[127] F. Cugini, F. Paolucci, G. Meloni, G. Berrettini, M. Secondini, F. Fresi, N. Sambo, L. Poti, and P. Castoldi. Push-pull defragmentation without traffic disruption in flexible grid optical networks. *Journal of Lightwave Technology*, 31(1):125–133, 2013. 58, 59

[128] Roberto Proietti, Chuan Qin, Binbin Guan, Yawei Yin, Ryan P. Scott, Runxiang Yu, and S. J. B. Yoo. Rapid and complete hitless defragmentation method using a coherent rx lo with fast wavelength tracking in elastic optical networks. *Opt. Express*, 20(24):26958–26968, Nov 2012. 58

[129] R. Proietti, R. Yu, K. Wen, Yawei Yin, and S. J. B. Yoo. Quasi-hitless defragmentation technique in elastic optical networks by a coherent rx lo with fast tx wavelength tracking. In *2012 International Conference on Photonics in Switching (PS)*, pages 1–3, Sep. 2012. 58

[130] Ferhat Dikbiyik, Laxman Sahasrabuddhe, Massimo Tornatore, and Biswanath Mukherjee. Exploiting excess capacity to improve robustness of wdm mesh networks. *IEEE/ACM Transactions on Networking*, 20(1):114–124, 2012. 64

[131] Rubén Rumipamba-Zambrano, Francisco-Javier Moreno-Muro, Jordi Perelló, Pablo Pavón-Mariño, and Salvatore Spadaro. Space continuity constraint in dynamic flexgrid/sdm optical core networks: An evaluation with spatial and spectral superchannels. *Computer Communications*, 126:38–49, 2018. 67, 70

[132] Ítalo Barbosa Brasileiro, André Castelo Branco Soares, and José Valdemir dos Reis. Planning and evaluation of translucent elastic optical networks in terms of cost-benefit. In *2017 19th International Conference on Transparent Optical Networks (ICTON)*, pages 1–4, 2017. 79

[133] Jose Maranhao, Helio Waldman, Andre Soares, and William Giozza. Wavelength conversion architectures in obs networks. In *NOMS 2008 - 2008 IEEE Network Operations and Management Symposium*, pages 939–942, 2008. 79